Human and plant proteins as reservoirs of host defence peptides

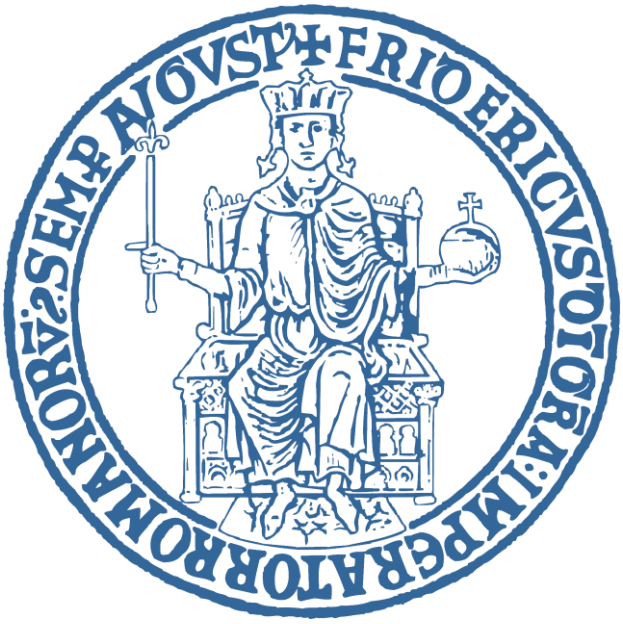

University of Naples Federico II

PhD in Biology

Tutor: Elio Pizzo

Candidate: Andrea Bosso

Human and plant proteins as reservoirs of host defence peptides

Andrea Bosso

TABLE OF CONTENTS

ABSTRACT

Antimicrobial peptides (AMPs), known also as host defense peptides, are fundamental evolutionarily conserved components of innate immunity. Constitutively or inducibly expressed in response to invasion by pathogens, they operate synergistically with other defence molecules to combat infections. Despite differences in their size and sequence, many of them share a net positive charge at neutral pH, and fold into amphipathic structures, often after contact with bacterial surfaces. HDPs are attractive alternative candidates for antibiotic treatment, because they offer several advantages over the currently used drugs. They combat pathogens by targeting bacterial membranes, thus impairing essential membrane-related functions, and, in some cases, also target intracellular components. Due to their peculiar mechanism, the resistance towards these peptides would be difficult for the bacteria to develop. Several proteins, including proteins apparently not involved in immunity, can behave as sources of HDPs hidden in their primary structures and released by the action of host and/or bacterial proteases. Recently it has been developed a bioinformatic tool allowing to identify such "cryptic HDPs". Analyzing a library of 4000 proteins, we have identified and studied several novel cryptic HDPs from human and plant. Among these, three human peptides (GVF27, ApoBS and ApoBL) show pharmacologically relevant properties like significant antimicrobial activity on a broad spectrum of bacteria (including some clinical isolates), very promising antibiofilm properties (both on pre-formed and attached biofilm), strong affinity for endotoxins as LPS and LTA and immunomodulatory properties on LPS induced murine macrophages, while two peptides from plant (IKY31 and IKY23) are strong anti-biofilm agents and not toxic against eukaryotic cells. Overall our data suggest that these new cryptic HDPs, could serve as leads for the design of innovative antimicrobials with immunostimulating and immunomodulatory properties.

Riassunto

I peptidi antimicrobici sono molecole naturali multifunzionali prodotte in vari organismi. La maggior parte di queste molecole sono cationiche e per questo anche note come *cationic Host Defence Peptides* (cHDPs), effettori del sistema immunitario innato che contribuiscono alla rapida eliminazione di agenti patogeni come batteri o funghi. In aggiunta alla loro attività antimicrobica e antifungina, i cHDPs sono anche in grado di modulare la risposta immunitaria. Questi peptidi possono agire direttamente o indirettamente, inducendo in modo selettivo la produzione di chemochine in cellule del sistema immunitario e il reclutamento di altre cellule immunitarie al sito di infezione. Questa particolare combinazione di attività farmacologicamente interessanti e lo sviluppo sempre più frequente del fenomeno di resistenza agli antibiotici tra i batteri patogeni, rendono i cHDPs un'alternativa molto valida agli antibiotici convenzionali. Alcuni cHDPs sono già in fase II / III di *trial* clinico. Il mio progetto di dottorato è stato incentrato sull'identificazione e caratterizzazione di nuovi cHDPs, ponendo particolare attenzione sia alla loro attività antimicrobica sia alla verifica della loro potenziale capacità di bloccare l'eccessivo effetto pro-infiammatorio di endotossine come l'LPS dei batteri Gram negativi o l'LTA dei Gram positivi. Recentemente, è stato sviluppato un sistema bioinformatico atto all'identificazione di proteine (cHDPs -*Releasing Proteins*) che possono contenere, ed eventualmente liberare, potenziali peptidi antimicrobici nascosti nella loro struttura primaria. Tale metodo si basa sul calcolo della carica netta, idrofobicità e lunghezza del peptide e permette una previsione semi-quantitativa della sua attività antimicrobica. Utilizzando tale metodo e consultando banche dati di proteine sia umane sia vegetali, diversi nuovi cHDPs criptici sono stati identificati e alcuni di questi sono stati oggetto di studio durante il dottorato.

GVF27, ad esempio, è un cHDP identificato nella proteina HSD-3 umana**.** Tale proteina appartiene a una famiglia di deidrogenasi che agisce in maniera NADP- dipendente. L'analisi dell'attività antimicrobica di GVF27, ottenuta analizzando un ampio pannello di ceppi batterici sia Gram negativi sia Gram positivi e confrontata a quella della catelicidina da pollo CATH-2, ha confermato che questo peptide è un forte agente antimicrobico. Il potere antimicrobico di GVF27 è stato analizzato anche in presenza di concentrazioni fisiologiche di cationi bivalenti ottenendo con ciò un risultato piuttosto interessante se si considera che tali condizioni in genere sono inattivanti per la maggior parte dei peptidi antimicrobici. Allo scopo di investigare più approfonditamente l'attività antimicrobica di GVF27, è stato allestito inoltre un saggio in grado di valutare il livello di ATP extracellulare di due colture batteriche (*Escherichia coli* ATCC 25922 e *Staphylococcus aureus* multiresistente WKZ-2). I risultati ottenuti da tale saggio indicano chiaramente che GVF27 ha un meccanismo di azione di tipo litico. Ulteriori analisi hanno evidenziato che GVF27 possiede anche proprietà antibiofilm. Infatti è stato osservato che GVF27 è in grado sia di inibire la formazione del biofilm sia di destrutturare biofilm preformati. In entrambi i casi analizzati inoltre va sottolineato che GVF27 conserva il suo potere citotossico nei confronti dei batteri incapsulati nella matrice del biofilm. Generalmente i peptidi antimicrobici cationici posseggono un particolare vantaggio che è quello della selettività di membrana per cui, essendo carichi positivamente, interagiscono preferenzialmente con le membrane cariche negativamente dei batteri piuttosto che con quelle eucariotiche (per lo più zwitterioniche). A tal riguardo sono stati allestiti esperimenti per verificare la potenziale tossicità di GVF27 su diverse linee cellulari e murine. I risultati ottenuti

evidenziano che GVF27, nonostante la sua spiccata tossicità per le cellule microbiche, non presenta alcun effetto tossico (anche a dosi superiori alle MIC) sulle cellule eucariotiche analizzate. Sono stati inoltre effettuati anche saggi di emolisi somministrando GVF27 a eritrociti di topo. Anche in questo caso è stata verificata l'assoluta non tossicità del peptide. Come descritto in precedenza, molti peptidi antimicrobici ricoprono anche un ruolo immunomodulante. Molti di questi infatti appartengono al sistema del complemento che permette il riconoscimento dei batteri patogeni dalle cellule del sistema immunitario. Altri invece attenuano risposte immunitarie eccessive che potrebbero portare a *shock* settici. In tale contesto, è risultato quindi opportuno investigare le eventuali proprietà immunomodulatorie di GVF27 attraverso esperimenti di ELISA e saggi di Griess condotti su macrofagi murini pre-trattati con LPS (endotossina specifica dei Gram negativi) e successivamente trattati con GVF27 oppure su macrofagi trattati con una miscela LPS/peptide hanno permesso di rilevare che il peptide in tutte le condizioni analizzate è in grado di attenuare significativamente sia la secrezione di Interleuchina-6 sia la produzione di ossido nitrico (NO), entrambi mediatori dell'infiammazione. Questi dati supportano l'idea che GVF27 possa interagire e bloccare l'LPS. Tuttavia sono stati condotti anche ulteriori esperimenti in cui le cellule era prima trattate con GVF27 e poi con LPS. Sorprendentemente, anche in questo caso il GVF27 è riuscito ad attenuare l'infiammazione indotta dall'LPS, in maniera indipendente dall'interazione diretta con questa molecola. Ulteriori evidenze, riguardo le proprietà immunomodulatorie di GVF27, sono state recentemente raccolte. I macrofagi sono cellule specializzate nella fagocitosi di agenti patogeni e nella loro digestione intracellulare. Tuttavia sono noti alcuni patogeni intracellulari che sono in grado di eludere i processi di digestione nei fagolisosomi. In questo caso è necessario che il potenziale antibatterico del macrofago venga incrementato e tale processo, può essere indotto grazie a segnali extracellulari, primo tra tutti l'IFN-γ. Questo meccanismo prende il nome di attivazione del macrofago e risulta difficoltosa in pazienti con carenza di IFN-γ o del suo recettore. Pertanto, oltre alle sopracitate attività anti-infiammatorie di GVF27, si è voluto anche indagare se il peptide presentasse la capacità di aumentare l'attività di macrofagi murini in seguito alla fagocitosi di un batterio. A tal riguardo è stato allestito un esperimento nel quale macrofagi murini pre-trattati con GVF27 sono stati successivamente incubati con il batterio *Salmonella enterica* serovar *Thypimurium* ATCC 14028. Al termine dell'incubazione, dopo aver eliminato mediante antibiotici tutti i batteri extracellulari, i macrofagi sono stati lisati ed è stata valutata la crescita dei batteri ancora vitali. In tal modo è stato possibile valutare il contributo di GVF27 all'uccisione intracellulare dei batteri fagocitati. Da tale esperimento è emerso che GVF27 è in grado di incrementare l'attività microbicida dei macrofagi in maniera dose dipendente. Inoltre, da dati pregressi in letteratura e da predizioni *in silico* emerge che anche le apolipoproteine umane sono fonte di peptidi bioattivi. L'apolipoproteina B è l'apolipoproteina principale dei chilomicroni, delle particelle VLDL, IDL e LDL ed è responsabile del trasporto di molecole di grasso, compreso il colesterolo, intorno al corpo (all'interno delle cellule esterne dell'acqua) a tutte le cellule di tutti i tessuti. Utilizzando il metodo bioinformatico sopra citato, sono stati identificati due nuovi HDP criptici nell'Apolipoproteina B (residui 887-922): chiamati ApoBL e ApoBS, rispettivamente di 38 e 26 residui amminoacidici. È stato dimostrato che entrambi gli HDP sono dotati di un'attività antimicrobica ad ampio spettro e al contempo non mostrano né effetti tossici né emolitici verso le cellule eucariotiche. Oltre all'attività citotossica su cellule planctoniche, è interessante notare che per entrambi gli HDP è stata evidenziata anche un'importante attività anti-biofilm. I due peptidi infatti, quando sono stati saggiati sul biofilm formato da *E. coli ATCC* 25922, *S. aureus* MRSA

WKZ-2, *P. aeruginosa* ATCC 27853 e *P. aeruginosa* PAO1 presentano attività sia nei confronti del biofilm preformato sia durante la sua formazione, conservando in tutti i casi le proprietà puramente antibatteriche. Allo scopo di potenziare l'efficacia antimicrobica dei peptidi identificati da ApoB, nella prospettiva di un loro eventuale utilizzo terapeutico, si è deciso di allestire analisi denominate di terapia combinata, coadiuvando simultaneamente peptidi anti batterici e antibiotici in diverse combinazioni. Uno dei test più noti per valutare il sinergismo tra due composti è il cosiddetto esperimento "*chequerboard*" in cui viene utilizzata una serie bidimensionale di concentrazioni seriali di composti di prova come base per il calcolo di un indice di concentrazione inibitoria frazionaria (FIC) per dimostrare che combinazioni accoppiate di agenti possono esercitare effetti inibitori che non derivano semplicemente dalla somma degli effetti dei singoli componenti. Tutte le combinazioni testate si sono dimostrate efficaci, sia con effetti addizionali sia sinergici tra peptidi e antibiotici. Sui medesimi peptidi sono state condotte anche analisi di dicroismo circolare. Entrambi i peptidi tendono ad acquisire una conformazione specifica in presenza di SDS, TFE e LPS, mentre in acqua risultano destrutturati. Tale dato suggerisce che questi cHDPs, a contatto con le cellule batteriche, potrebbero adattarsi in prossimità delle membrane prima di agire su di essa, sia nel caso di un'azione destrutturante sia per essere trasportati all'interno della cellula. Va sottolineato inoltre che, in maniera analoga a GVF27, entrambi i peptidi derivanti da ApoB sono in grado di mitigare la produzione di interleuchina-6 e di ossido nitrico nei macrofagi murini indotti da LPS. Infine, risultati preliminari ottenuti su cheratinociti umani, indicano che i peptidi identificati in ApoB presentano interessanti proprietà di *wound healing* (in particolare ApoBL). Complessivamente i dati raccolti su questi nuovi cHDPs, compreso il sopracitato GVF27, aprono prospettive interessanti su un loro uso terapeutico.

Inoltre, già durante il mio primo anno di dottorato è stato identificato per frammentazione in bromuro di cianogeno e caratterizzato il primo peptide antimicrobico criptico nascosto in PD-L4, una proteina inattivante il ribosoma di tipo 1 (RIP) dalle foglie di *Phytolacca dioica L*. Le proteine RIP sono degli enzimi identificati in piante, funghi, alghe e batteri. Essi sono dotati di attività di N-glicosilasica, che determina la scissione di un residuo adenino-specifico in un sito conservato del rRNA 28S, con conseguente inibizione della sintesi proteica. Grazie all'approccio bioinformatico precedentemente citato, sono stati identificati, nel dominio N-terminale di PD-L1 / 2, un ulteriore membro del pool di proteine RIP di tipo 1 di *P. dioica*, due nuovi HDP criptici. Questi due peptidi, qui denominati IKY31 e IKY23, non presentano tossicità per le cellule eucariotiche ma presentano al contempo un'attività antibatterica ad ampio spettro. Oltre all'azione antimicrobica, è stato anche verificato che entrambi i peptidi posseggono significative proprietà antibiofilm. Infatti sia IKY23 che IKY31 sono in grado di destrutturare il biofilm prodotto da due ceppi Gram-negativi: *Klebsiella pneumoniae* e *Pseudomonas aeruginosa*. È stato verificato che i peptidi derivati da PD-L1/2 sono in grado di indurre una forte riduzione, dose dipendente, della biomassa del biofilm, di influenzare lo spessore del biofilm e, nel caso di IKY31, di interferire sull'adesione cellula/cellula, probabilmente interagendo componenti strutturali del biofilm. Inoltre, mediante analisi CD, è stato anche rilevato che entrambi i peptidi derivati da PD-L1/2 sono in grado di assumere conformazioni stabili sia in presenza di agenti che mimano la struttura della membrana (TFE e SDS) sia di componenti di parete batteriche extracellulari, come LPS e alginato. Nel complesso, i dati raccolti su questi due peptidi danno un'ulteriore rilevanza all'importanza dei peptidi criptici derivanti da proteine RIP nell'interazione ospite/patogeno, in particolare nelle condizioni indotte da batteri che formano biofilm.

Chapter 1

Human and plant proteins as reservoirs of host defence peptides: an introduction

1. Introduction

1.1 The plague of the antimicrobial resistance

Since Dr. Fleming discovered in 1928 the first antibiotic from the fungus *Penicillium chrysogenum*, several other antimicrobial agents have been discovered and much progress has been made in the host defence field. From this first evidence, there was a widespread research of other new antibiotics with different targets: specific for one or few bacterial species or with a wide spectrum activity; intracellular activity directed on nucleic acids (quinolone, rifampicin), protein synthesis (tetracyclines, chloramphenicol) interfering with bacterial metabolism (sulfonamides, dapsone); directed on the cell wall (bacitracin, cephalosporins) or membrane (polymixins), specific or not for Gram negative (aminoglycoside) and positive (vancomycin) bacteria (**figure 1**). Their discovery should be considered, as well as the development of vaccines, one of the most influent reasons of the growth in human welfare [1].

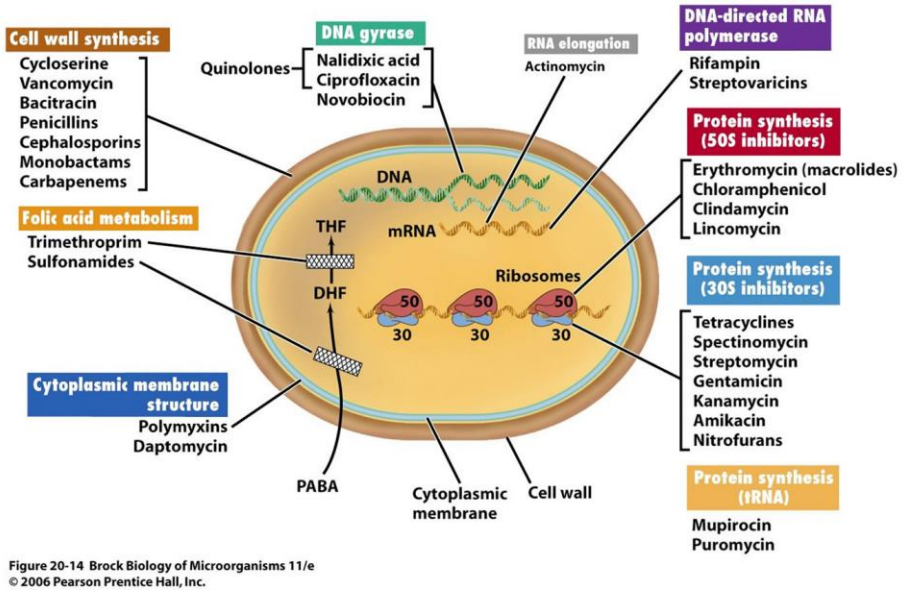

Figure 1. Mode of action of antibiotics (image adopted from [2])

However, even antibiotics have been shown their limits in their own properties. Nowadays, when common infections occur, antibiotics could easily eradicate them, but the healthy microbiota is seldom preserved, because of their multiplicity of target. This is a great disadvantage considering the positive role a healthy microbiota has on human health [3]. Moreover, antibiotics may cause side effects such as allergic reactions due to individual sensitivity to one or more components, toxicity to various organs or intolerance caused by interaction with other drugs. The abuse of drugs can lead to death.

Among these, major problems could be carried by the antibiotic resistance.

Antibiotic resistance was reported to occur when a drug loses its ability to inhibit bacterial growth effectively so that those bacteria become 'resistant' and continue to multiply in the presence of therapeutic levels of the antibiotics [4]. Generally, antibiotic resistance can occur as a natural selection process where nature empowers all bacteria with some degree of low-level resistance and

that is the reason why non-judicial use of antibiotic, in both biomedical and agricultural fields, is responsible for making microbes resistant [5]. The Center for Disease Control and Prevention (CDC) reported that 1.7 million people were nosocomially infected in hospitals in 2002 and 99,000 deaths were occurring annually in the United States due to drug-resistant microbes [6].

Antibiotics fight to eliminate bacteria. But, bacteria tend to have a natural process that encourages resistance due to the exposure to antibiotics themselves. The resistance process can occur via gene level mutations. Antibiotics induce selective pressure and the genes act in association with selective pressure to favour bacteria that have gained the resistance, which results in a selective advantage. For example, β-lactam antimicrobial agents is the most common treatment for bacterial infections and continues, paradoxically, to be the prominent cause of resistance to β-lactam antibiotics among Gram-negative bacteria worldwide. The persistent exposure of bacterial strains to a multitude of β-lactams has induced dynamic and continuous production and mutation of β-lactamase genes in these bacteria, expanding their activity even against the newly developed β-lactam antibiotics [7]. Moreover, bacteria possess the ability to directly transfer genetic material between each other by transferring plasmids, this behaviour signifies that natural selection is not the only mechanism by which resistance evolves, but their mutual transformation could be a process of resistance amplification. Development of resistance may also likely occur if users fail to take their full course of prescribed antibiotic treatment. Bacteria subsequently remain untouched gaining more strength against the antibiotics. In this way, bacteria may collect multiple resistance traits over time and can become resistant to multiple classes of antibiotics [8]. Obviously, bacterial genetical resistance is translated in a protein-mediated system to avoid the mechanism of action: modifying their targets, enzymatically inactivating or eliminating antibiotics by efflux pumps. Different mechanisms of the common drug resistance are shown in **Table 1** [4].

Antibiotic class	Example(s)	Mode(s) of resistance
P-Lactams	Penicillins, Cephalosporins, Penems, Monobactams	Hydrolysis, efflux, altered target
Aminoglycosides	Gentamicin, Streptomycin, Spectinomycin	Phosphorylation, acetylation, nucleotidylation, efflux, altered target
Glycopeptides	Vancomycin, Teicoplanin	Reprogramming peptidoglycan biosynthesis
Tetracyclines	Minocycline, Tigecycline	Monooxygenation, efflux, altered target
Macrolides	Erythromycin, azithromycin	Hydrolysis, glycosylation, phosphorylation, efflux, altered target
Lincosamides	Clindamycin	Nucleotidylation, efflux, altered target
Streptogramins	Synercid	Carbon-Oxygen lyase, acetylation, efflux, altered target
Oxazolidinones	Linezolid	Efflux, altered target
Phenicols	Chloramphenicol	Acetylation, efflux, altered target
Quinolones	Ciprofloxacin	Acetylation, efflux, altered target
Pyrimidines	Trimethoprim	Efflux, altered target
Sulfonamides	Sulfamethoxazole	Efflux, altered target
Rifamycins	Rifampin	ADP-ribosylation, efflux, altered target
Lipopeptides	Daptomycin	Altered target
Cationic peptides	Colistin	Altered target, efflux

Table 1. Table representing the mechanism of drug resistance of common antibiotics (image adopted from [4].

Unfortunately, resistance has increasingly become a problem in recent years because the pace at which we novel antibiotics are discovered has slowed drastically now, while antibiotic use is rising. And it is not just a problem confined to bacteria, but all microbes, including parasites, fungi and viruses, that have the potential to mutate and render our drugs ineffective [9]. According to the prevision of deaths attributable to antimicrobial resistance every year compared to other major causes of death in 2050, victims of the ineffectiveness of antibiotics will be more numerous than those of cancer as shown in **figure 2** [10].

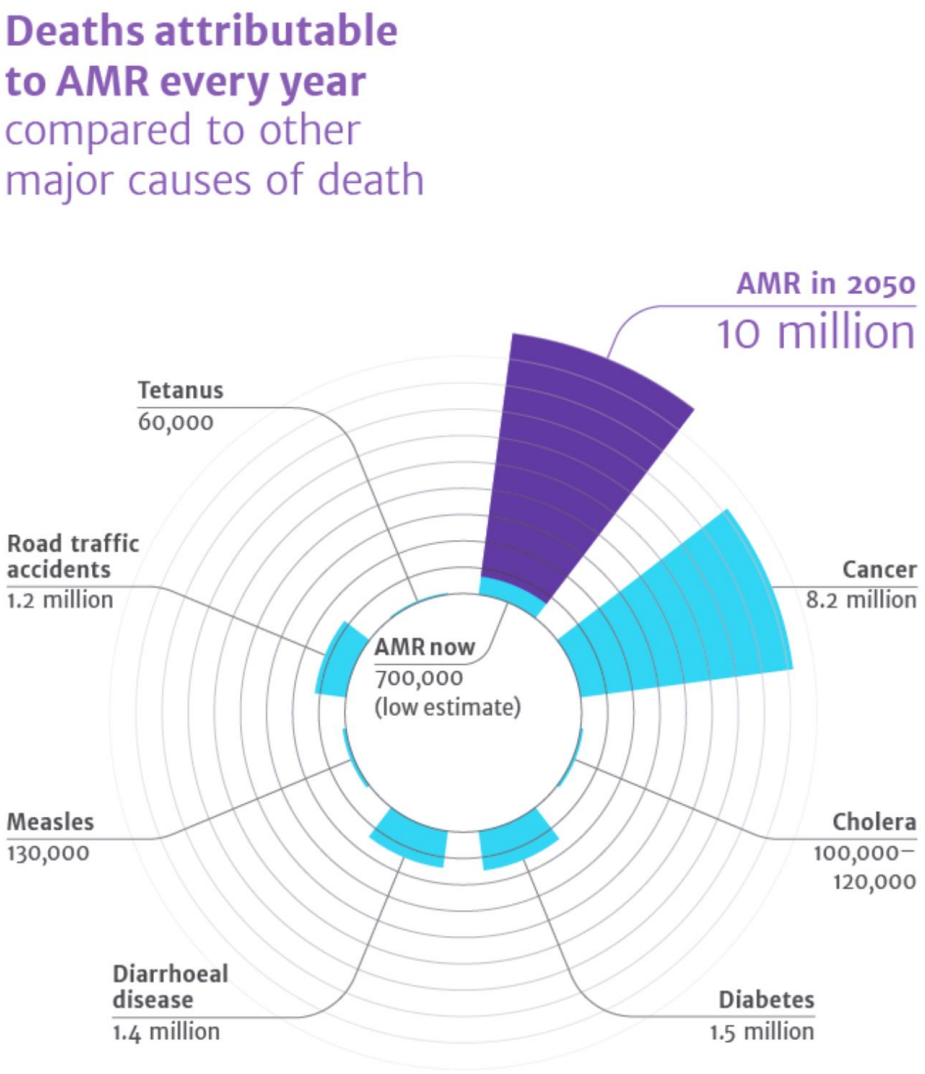

Figure 2. Death due to **AMR (A**nti**M**icrobial **R**esistance) estimate in 2050 compared to mortalities caused by other major illnesses [10].

All these considerations have shown how mandatory the development of new antimicrobial molecules is and the importance of a constant renovation which had lead the scientific community to point their interest on alternative and new molecules e.g. antimicrobial peptides (AMPs) which are considered as an alternative to conventional drugs [11].

1.2 From antimicrobial peptides to host defence peptides (HDPs)

Antimicrobial Peptides (AMPs), are small molecules consisting of 12-50 amino acids with a positive net charge widely diffused in most living organisms. Peptides with biological activity have been isolated from a high number of organisms belonging to both plant and animal kingdoms such as bacteria, plants, insects, amphibians and mammals. The skin of numerous species of amphibians, for example, has proved to be a rich source of peptides (bombesin, magainin, temporin, etc.), products and secretions from granular glands in response to a variety of stimuli [12]. In humans and in other mammals (like mouse, rat or rabbit), antimicrobial peptides belonging to the defensin family are stored as granules in neutrophils (blood cells specializing in phagocytosis), while polymorphonucleated leukocytes of bovine animals are rich in peptides belonging to the family of cathelicidins that demonstrated significant antimicrobial activity *in vitro* and *in vivo*.

AMPs play a very important role in so-called innate or natural immunity, consisting of a series of non-specific defense mechanisms, that is, directed towards a wide spectrum of microorganisms and present in an individual since birth. These are pre-existing to exposure to foreign substance (antigen) and represent the first true defense barrier of the organism from the pathogens [13]. It has been shown that some peptides exhibit strong antimicrobial activity against both Gram-positive and Gram-negative bacteria, *fungi* and are also capable to inhibit the replication of some viruses [14]. The mechanism of action of most AMPs is due to the alteration of cell membranes following interaction between the peptide and membrane structures. The effects that can be achieved in this interaction are: disorganization of membrane structure, alteration of permeability, leakage of cytoplasmic components and lysis of the cell. Some peptides, such as buforin interact directly with intracellular targets (DNA and / or RNA) by inhibiting vital cell functions. Moreover, other AMPs (e.g. peptides derived from cathelicidins and defensins) act as demonstrated in recent years with a mechanism independent from direct microbial killing; in fact, in the presence of pathogenic agents they can act inhibiting the host's proinflammatory response and / or stimulate immune defense reactions, for this reason they are better named *host defense peptides (HDP)* [15]. Biological features of these molecules justify the interest in the scientific community as innovative and alternative therapeutic agents, especially in infections sustained by antibiotic-resistant microorganisms.

1.3 Features of host defense peptides

HDPs are usually produced as pre-pro-peptides of about 60-170 amino acids. When they are released they are cut into their mature form due to the action of specific proteases. HDPs vary considerably in size and secondary structure, but they have common characteristics including that most of these peptides are cationic and amphipatic. The specificity of HDPs for bacterial membranes is based on the differences in charge and lipid composition between membranes of prokaryotic and eukaryotic cells. The membrane of eukaryotic cells is rich in zwitterionic lipids, while that of prokaryotic cells is rich in negative charged lipids that can interact with cationic HDPs [16]. Cationic HDPs are divided into four subgroups on the basis of their amino acid composition and structure: (i) α-helical peptides, linear peptides enriched for specific amino acids (e.g. proline and arginine), (ii) peptides prone to form stable β-sheets stabilized by one or more disulfide bridges,

(iii) loop peptides with a single disulfide bridge; and (iv) peptides without a well-defined structure [17]. Cationic HDPs generally are small and contain 12–50 amino acids, with 2–9 positively charged lysine or arginine residues, and up to 50% hydrophobic amino acids. For these reasons, they tend to form amphipathic structures in the hydrophobic environment, characteristics that allow peptides, in contrast to conventional antibiotics, to interact with microbial membranes through not only electrostatic but also hydrophobic interactions [18]. In this manner, they can destroy bacterial membrane normal functions by forming ion channels or pores, dissolving the membrane as if they were detergents, or causing damages in the membrane itself.

1.4 Mechanisms of action

In the following paragraph some of the major mechanisms of action are described of host defense peptides:

a. **Direct bacterial killing**
b. **LPS neutralization**
c. **Intracellular targets**
d. **Opsonization and intracellular killing**

Direct bacterial killing

As already mentioned, HDPs have been also named host defense peptides for their involvement into immune system regulation and immune response modulation [15]. However, some peptides act, simply and directly, killing the target. This kind of peptides could be clustered in two big groups: peptides that have their target on the surface of bacteria or in their cytoplasm. Most of the peptides that act on the surface of bacteria form pores on this surface. Several models that particularly address the actions of defensins and linear amphiphilic cationic peptides propose formation of channels through and/or disruption of bacterial membranes [19].

Killing of bacteria via pore formation in the bacterial membrane requires three principal steps: binding to the bacterial membrane, aggregation within the membrane, and formation of channels. The channel formation leads to leakage of internal cell contents, e.g. ATP molecules, and cell death [20].

An HDP must cross the negatively charged outer wall of Gram-negative bacteria, which contains lipopolysaccharides (LPS), or the outer cell wall of Gram-positive bacteria, which contains acidic polysaccharides. The three well-established models for pore formation are the barrel-stave pore, the toroidal pore, and the carpet model (**figure 3**):

1) **Barrel stave model**: multimers of HDP cross the cell membrane so that the hydrophobic part is facing the lipid bilayer and the hydrophilic part is facing the lumen of the pore. The assembled peptides form barrel-like channels resembling staves;
2) **Toroidal pore**: the HDP form a monolayer by connecting the outer and inner lipid layers in the pore;

3) **Carpet model**: in this model peptides first cover the outer surface of the membrane like a carpet and then act like detergents, disrupting the membrane bilayer after reaching a threshold concentration. The pores are formed from micelle-like units.

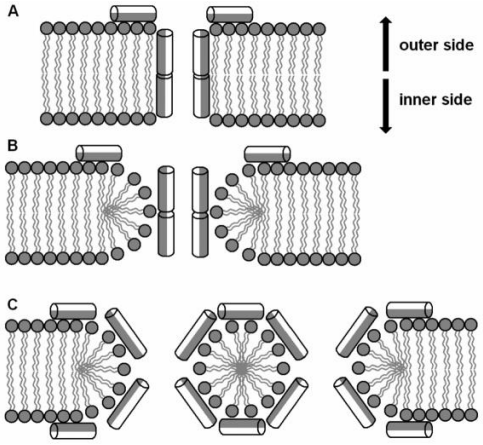

Figure 3. A. the barrel-stave pore; B. the thoroidal pore; C. the carpet model. (the image is by [19])

Intracellular targets

There is increasing evidence for intracellular targeting of microbes as both alternative and synergistic pathways to membrane rupture and cell lysis [23]. The HDP buforin II, possessing a linear proline hinge and containing an amphipathic α-helical peptide, has been proven to translocate across the cell membrane without loss of the transmembrane potential and with intracellular contents intact even at five times the MIC. Cellular function of *Escherichia coli* is inhibited by accumulation of buforin II in the cytoplasm and via binding to DNA and RNA [24]. Some HDPs such as indolicidin have been demonstrated to penetrate bacterial cell membranes rendering them relatively undamaged but with antibacterial activity achieved by inhibition of RNA, DNA and protein synthesis [25]. Other hypotheses for intracellular action include stimulation of the autolytic enzyme cascade. Cationic HDPs, for example lactoferrin and lysozyme, may mimic the action of β-lactam antibiotics and activate autolytic cell wall enzymes such as muramidases causing bacteriolysis [26]. Intracellular targeting of protein synthesis by degradation of proteins required for DNA replication has been shown to be a primary mechanism of action for indolicidin and the pig intestinal peptide PR-39. Further, apidaecin and oncocin inhibit protein translation in bacteria by binding to and inactivating the 70S ribosome and Bac7(1-35) accumulates within *Escherichia coli* to high concentrations and inhibits protein synthesis by binding to the ribosome [27].

LPS neutralization

LPS is one of the most studied targets of HDPs for their ability to neutralize or modulate the aggregation of this endotoxin. LPS is a major component of the outer leaflet of the outer membrane in Gram-negative bacteria. LPSs consist of an O-specific chain that is highly variable in different bacterial strains, a core oligosaccharide, and lipid A. LPSs are essential for

bacterial growth and viability, but macrophages stimulated by LPS induce the release of pro-inflammatory cytokines (TNF-α, IL-1 and IL-6) into the blood, resulting in septic shock [21]. Accordingly, LPSs are excellent target for HDPs because they have the potential to both directly inhibit the growth of multidrug-resistant bacteria and to neutralize the action of released LPS due to its stimulation of immune cells. HDPs generally bind to LPS through electrostatic interactions between their cationic amino acids (Lysine and Arginine) and head groups of LPS, and this complex is stabilized through hydrophobic interactions between the hydrophobic amino acids of the peptide and fatty acyl chains of LPS [22].

Opsonization and intracellular killing

The first line of defense of the organism by pathogens is represented by the epithelial barrier. Damages of this barrier facilitate host invasion by pathogens and the initiation of an infection process to which the body responds to the inflammatory state through immune system cells. Resolving inflammation requires the cooperation of many cellular components of the immune system, such as lymphocytes, T helper cells, neutrophils, natural killer cells (NK) or macrophages [28]. Macrophages are immune system cells specializing in the phagocytosis of infected, dead or tumorous eukaryotic cells, as well as pathogens such as viruses, parasites, or bacteria. Many of the HDPs are secreted as inactive pro-peptides from neutrophils, macrophages or epithelial cells and enzymatically activated to release the active form that is able to interact with the pathogen membrane. This interaction could promote the recognition of bacteria by the macrophages (**opsonization**) encouraging their phagocytosis and the follow eradication of the pathogen. LL37 is the most know human HDPs that is able to act as an opsonins [29].

After the phagocytosis, digestion of pathogens follows mediated by intracellular factors and vesicle acidification into the phagolysosomes. Normally, a macrophage is able to complete phagocytosis and bacterial clearance alone, but some pathogens of clinical relevance can chronically infect the macrophage by inactivating it. In fact, there are various mechanisms developed by bacteria to survive the intracellular environment of macrophages by inhibiting, for example, lysosomal fusion or acidification necessary for the activation of lysosomal proteases, or even invading the cell cytoplasm or further they can change their own outer membrane structure or decrease their negative charge to avoid cationic HDP effectiveness [30]. All these mechanisms can lead the macrophage to death. In order to avoid this process, the immune system developed a known counterfeit such as macrophage activation. This activation is carried out by type 1 T helper cells (TH1), which secrete additional activator signals that increase the antimicrobial capacity of the macrophages by allowing them to destroy intracellular pathogens. Activated macrophages become effective cells with powerful antibacterial activity: they more effectively blend the lysosomes with phagocytes, produce radical forms of oxygen and nitric oxide (NO), but also HDPs and proteases that can attack extracellular and intracellular pathogens. The reason why macrophages are normally in an inactivated state is that activated state requires greater energy consumption and increased macrophage aggression due to nitric oxide, protease or oxygen radicals toxicity. This would cause a danger to the healthy tissue of the host.

Among the signal molecules necessary for the activation of macrophages there are the IFN-γ and the ligand of CD40, a receptor present on the macrophage membrane. Patients with genetic

diseases that determine IFN-γ deficiency, or its receptor, fail to control infections due to intracellular pathogens. Activation of macrophages induces increased CD40 and TNF-α receptors expression and promotes TNF-α production. This autocrine stimulus has a synergistic effect with IFN-γ secreted by TH1 cells in increasing the bactericidal action of the macrophage. All these signals lead to macrophage sensitization increasing their phagocytic activity and inner antimicrobial systems, however, not only these signals are able to activate it. For example, Crotamin is a peptide that has been discovered to stimulate macrophagic phagocytosis [31]. This process can also be triggered by small amounts of LPS or, as recently reported, by HDPs like LL37 alone or complexed with DNA [32]. Since some bacterial strains, like *Salmonella enterica or Staphylococcus aureus* are able to actively invade epithelial cells, intriguingly, has been also reported that HDPs, like temporin B, could defend these cells from invasive bacteria [33]. To note, as it is possible to activate macrophages, they may also be inhibited by anti-inflammatory factors, such as IL-10 secreted by TH2 cells.

1.5 Cryptic host defense peptides and their *in silico* identification

Some bacterial strains have acquired a limited resistance to HDPs by producing specific proteases [34]. To overcome this resistance, multicellular eukaryotes secrete "HDP-Releasing Proteins" (HDP-RPs) which release active peptides only after a partial proteolytic processing operated by bacterial and/or host proteases. Therefore, a bacterial strain producing defense proteases against HDPs "commits suicide" by triggering itself the release of "cryptic" HDPs from their precursors. This mechanism has been indeed demonstrated for Zf-3, a ribonuclease from *Danio rerio* [35]. Several proteins can be considered as HDP-RPs. Lysozyme is a well-known example in this sense as it exerts bactericidal action by hydrolyzing peptidoglycan but, if inactivated by proteolysis, it releases HDPs [36, 37]. Mammalian's lactoferrin, a multifunctional protein, owns bactericidal determinants at the N-terminus. Its proteolysis in infants' stomach leads to the release of peptides, which are more bactericidal than the corresponding native protein on several strains, including antibiotic-resistant strains [38, 39]. Human thrombin, a key enzyme in the coagulation cascade, bears bactericidal determinants in the C-terminal region [40, 41]. Other interesting examples of cryptic HDPs can be seen in several heparin-binding domains [42], growth-factors [43, 44] and chemokines [45].

Fast bioinformatic approaches highlighted the presence of putative antimicrobial regions that could be extremely useful for the discovery of new cryptic host defence peptides. Pane et al. [46] developed an efficient strategy to identify potential HDP-RPs and to locate antimicrobial fragment(s) hidden into their amino acidic sequence. This method also allows a semi-quantitative prediction of the antimicrobial activity and, due to the inclusion of some strain-specific variables, could be fine-tuned to predict efficacy on specific bacterial strains. This method assigns to any given peptide an antimicrobial score, known as "absolute score" (AS), based on net charge, hydrophobicity and length of the peptide and of two bacterial strain-dependent weight factors defining the contribution of charge and hydrophobicity to the antimicrobial activity. To analyse a protein potentially bearing hidden antimicrobial regions, the AS values of all the peptides of the desired length contained in a precursor protein can be plotted as a function of peptide sequence and length, thus obtaining an accurate map of the antimicrobial activity determinants.

This method has been recently used to identify two novel HDPS in the sequences of an archaeal transcription factor [47] two human apolipoproteins [48, 49], a human putative dehydrogenase [50], a type 1 ribosome inactivating protein (RIP) from *Phytolacca dioica* L. [51] and other different proteins, some of which described in this thesis.

1.6 Aim of this thesis

Due to the extreme necessity of new antibiotics, lately HDPs have decisively sparked research interest thanks to their successful properties like the multifunctional role, ductility in formulation and therapeutic application [52].

Aim of this thesis was to report a wide characterization of six new cryptic HDPs from human and plants identified *in silico* by Professor Ennio Notomista [46]. This thesis concerns GVF27 [50], a peptide identified at the C-terminus of four isoforms of human 11-hydroxysteroid dehydrogenase-1 β-like; two peptides from human Apolipoprotein B [49] and three peptides from type 1 ribosome-inactivating proteins (RIPs) from leaves of *Phytolacca dioica* L., one from the protein PD-L4 [51] and two from the protein PD-L1/2.

References

1. Dane Lyddiard, Graham L. Jones, Ben W. Greatrex; Keeping it simple: lessons from the golden era of antibiotic discovery, FEMS Microbiology Letters, Volume 363, Issue 8, 1 April 2016, https://doi.org/10.1093/femsle/fnw084.
2. Bbosa, G., Mwebaza, N., Odda, J., Kyegombe, D. and Ntale, M. (2014) Antibiotics/antibacterial drug use, their marketing and promotion during the post-antibiotic golden age and their role in emergence of bacterial resistance. *Health*, **6**, 410-425. doi: 10.4236/health.2014.65059.
3. Belkaid Y, Hand T. Role of the Microbiota in Immunity and inflammation. *Cell*. 2014;157(1):121-141.; Homeostatic Immunity and the Microbiota Yasmine Belkaid1,2, * and Oliver J. Harrison1; doi:10.1016/j.cell.2014.03.011.
4. Zaman SB, Hussain MA, Nye R, Mehta V, Mamun KT, Hossain N. A Review on Antibiotic Resistance: Alarm Bells are Ringing. Muacevic A, Adler JR, eds. *Cureus*. 2017;9(6):e1403. doi:10.7759/cureus.1403
5. Levy S.B. (1992) From Tragedy the Antibiotic Age is Born. In: The Antibiotic Paradox. Springer, Boston, MA
6. Klevens RM, Edwards JR, Richards CL Jr, Horan TC, Gaynes RP, Pollock DA, Cardo DM, Estimating health care-associated infections and deaths in U.S. hospitals, 2002. Public Health Rep. 2007 Mar-Apr; 122(2):160-6.]
7. Shaikh S, Fatima J, Shakil S, Rizvi SMD, Kamal MA. Antibiotic resistance and extended spectrum beta-lactamases: Types, epidemiology and treatment. *Saudi Journal of Biological Sciences*. 2015;22(1):90-101. doi:10.1016/j.sjbs.2014.08.002.)
8. Avorn J, Barrett JF, Davey PG, et al Antibiotic resistance: Synthesis of recommendations by expert policy.
9. The Review on Antimicrobial Resistance, 2014, Chaired by Jim O'Neill
10. Premanandh J, Samara BS, Mazen AN. Race Against Antimicrobial Resistance Requires Coordinated Action – An Overview. *Frontiers in Microbiology*. 2015;6:1536. doi:10.3389/fmicb.2015.01536.)
11. Lloyd DH. Alternatives to conventional antimicrobial drugs: a review of future prospects. Vet Dermatol 2012; 23: 299–304
12. Enrico König, Olaf R.P. Bininda-Emonds, Evidence for convergent evolution in the antimicrobial peptide system in anuran amphibians, In Peptides, Volume 32, Issue 1, 2011, Pages 20-25, ISSN 0196-9781, https://doi.org/10.1016/j.peptides.2010.10.009
13. Wang G. Human Antimicrobial Peptides and Proteins. *Pharmaceuticals*. 2014;7(5):545-594. doi:10.3390/ph7050545.
14. Jenssen H, Hamill P, Hancock REW. 2006. Peptide antimicrobial agents. Clin Microb Rev 19:491–511. 10.1128/CMR.00056-05.
15. Otvos, L., Jr. Immunomodulatory effects of anti-microbial peptides. *Acta Microbiol. Immunol. Hung.* 2016, *63*, 257–277
16. Lee TH, Hall KN, Aguilar MI. Antimicrobial Peptide Structure and Mechanism of Action: A Focus on the Role of Membrane Structure. Curr Top Med Chem. 2016;16(1):25-39. Review.

17. Zasloff M (2002) Antimicrobial peptides of multicellular organisms. Nature 415(0028–0836 (Print)):389–395.)
18. Huang Y, He L, Li G, Zhai N, Jiang H, Chen Y. Role of helicity of α-helical antimicrobial peptides to improve specificity. Protein Cell. 2014;5(8):631-42. doi: 10.1007/s13238-014-0061-0.)
19. Pálffy R, Gardlík R, Behuliak M, Kadasi L, Turna J, Celec P. On the physiology and pathophysiology of antimicrobial peptides. Mol Med. 2009 Jan-Feb;15(1-2):51-9. doi: 10.2119/molmed.2008.00087
20. Jean-François F, Elezgaray J, Berson P, Vacher P, Dufourc EJ. Pore Formation Induced by an Antimicrobial Peptide: Electrostatic Effects. *Biophysical Journal*. 2008;95(12):5748-5756. doi:10.1529/biophysj.108.136655.)
21. Gutsmann T, Müller M, Carroll SF, MacKenzie RC, Wiese A, Seydel U.Dual role of lipopolysaccharide (LPS)-binding protein in neutralization of LPS and enhancement of LPS-induced activation of mononuclear cells. Infect Immun. 2001 Nov;69(11):6942-50.
22. Park S-C, Park Y, Hahm K-S. The Role of Antimicrobial Peptides in Preventing Multidrug-Resistant Bacterial Infections and Biofilm Formation. *International Journal of Molecular Sciences*. 2011;12(9):5971-5992. doi:10.3390/ijms12095971.)
23. Le C-F, Fang C-M, Sekaran SD. Intracellular Targeting Mechanisms by Antimicrobial Peptides. *Antimicrobial Agents and Chemotherapy*. 2017;61(4):e02340-16. doi:10.1128/AAC.02340-16.
24. Xie Y, Fleming E, Chen JL, Elmore DE. Effect of proline position on the antimicrobial mechanism of buforin II. *Peptides*. 2011;32(4):677-682. doi:10.1016/j.peptides.2011.01.010
25. Hsu C-H, Chen C, Jou M-L, et al. Structural and DNA-binding studies on the bovine antimicrobial peptide, indolicidin: evidence for multiple conformations involved in binding to membranes and DNA. *Nucleic Acids Research*. 2005;33(13):4053-4064. doi:10.1093/nar/gki725.)
26. Ginsburg I, van Heerden PV, Koren E. From amino acids polymers, antimicrobial peptides, and histones, to their possible role in the pathogenesis of septic shock: a historical perspective. *Journal of Inflammation Research*. 2017;10:7-15. doi:10.2147/JIR.S126150.
27. Wilson DN, Guichard G, Innis CA. Antimicrobial peptides target ribosomes. *Oncotarget*. 2015;6(19):16826-16827.
28. Clausen ML, Agner T. Antimicrobial Peptides, Infections and the Skin Barrier. Curr Probl Dermatol. 2016;49:38-46. doi: 10.1159/000441543.).
29. Sol et. al. 2013. LL-37 Opsonizes and Inhibits Biofilm Formation of Aggregatibacter actinomycetemcomitans at Sub-bactericidal Concentrations.
30. Susana Matamouros, Samuel I. Miller, S. Typhimurium strategies to resist killing by cationic antimicrobial peptides, Biochimica et Biophysica Acta (BBA) - Biomembranes, Volume 1848, Issue 11, Part B, November 2015, Pages 3021-3025, ISSN 0005-2736, https://doi.org/10.1016/j.bbamem.2015.01.013.
31. Lee KJ, Kim YK, Krupa M, et al. Crotamine stimulates phagocytic activity by inducing nitric oxide and TNF-α via p38 and NFκ-B signaling in RAW 264.7 macrophages. *BMB Reports*. 2016;49(3):185-190. doi:10.5483/BMBRep.2016.49.3.271.)
32. Tang X, Basavarajappa D, Haeggström JZ, Wan M. $P2X_7$ Receptor Regulates Internalization of Antimicrobial Peptide LL-37 by Human Macrophages That Promotes

Intracellular Pathogen Clearance. *The Journal of Immunology Author Choice*. 2015;195(3):1191-1201. doi:10.4049/jimmunol.1402845./ Stephan A, Batinica M, Steiger J, et al. LL37:DNA complexes provide antimicrobial activity against intracellular bacteria in human macrophages. *Immunology*. 2016;148(4):420-432. doi:10.1111/imm.12620.)

33. Di Grazia A, Luca V, Segev-Zarko LT, Shai Y, Mangoni ML. Temporins A and B Stimulate Migration of HaCaT Keratinocytes and Kill Intracellular Staphylococcus aureus. *Antimicrobial Agents and Chemotherapy*. 2014;58(5):2520-2527. doi:10.1128/AAC.02801-13.
34. M. Sieprawska-Lupa, P. Mydel, K. Krawczyk, K. Wojcik, M. Puklo, B. Lupa, P. Suder, J. Silberring, M. Reed, J. Pohl, W. Shafer, F. McAleese, T. Foster, J. Travis, J. Potempa. Degradation of human antimicrobial peptide LL-37 by Staphylococcus aureus-derived proteinases. Antimicrob. Agents Chemother., 48 (2004), pp. 4673-4679
35. Zanfardino, A., Pizzo, E., Di Maro, A., Varcamonti, M. and D'Alessio, G. (2010), The bactericidal action on *Escherichia coli* of ZF-RNase-3 is triggered by the suicidal action of the bacterium OmpT protease. FEBS Journal, 277: 1921–1928. doi:10.1111/j.1742-4658.2010.07614.x
36. H.N. Hunter, W. Jing, D.J. Schibli, T. Trinh, I.Y. Park, S.C. Kim, H.J. Vogel. The interactions of antimicrobial peptides derived from lysozyme with model membrane systems. Biochim Biophys. Acta, 1668 (2005), pp. 175-189
37. H.R. Ibrahim, D. Inazaki, A. Abdou, T. Aoki, M. Kim. Processing of lysozyme at distinct loops by pepsin: a novel action for generating multiple antimicrobial peptide motifs in the newborn stomach. Biochim Biophys. Acta, 1726 (2005), pp. 102-114
38. J.L. Gifford, H.N. Hunter, H.J. Vogel. Lactoferricin: a lactoferrin-derived peptide with antimicrobial, antiviral, antitumor and immunological properties. Cell Mol. Life Sci., 62 (2005), pp. 2588-2598
39. M. Sinha, S. Kaushik, P. Kaur, S. Sharma, T.P. Singh. Antimicrobial lactoferrin peptides: the hidden players in the protective function of a multifunctional protein. Int J. Pept., 2013 (2013), p. 390230
40. G. Kasetty, P. Papareddy, M. Kalle, V. Rydengard, M. Morgelin, B. Albiger, M. Malmsten, A. Schmidtchen. Structure-activity studies and therapeutic potential of host defense peptides of human thrombin. Antimicrob. Agents Chemother., 55 (2011), pp. 2880-2890
41. P. Papareddy, V. Rydengard, M. Pasupuleti, B. Walse, M. Morgelin, A. Chalupka, M. Malmsten, A. Schmidtchen. Proteolysis of human thrombin generates novel host defense peptides. PLoS Pathog., 6 (2010), p. e1000857
42. E. Andersson, V. Rydengard, A. Sonesson, M. Morgelin, L. Bjorck, A. Schmidtchen. Antimicrobial activities of heparin-binding peptides. Eur. J. Biochem., 271 (2004), pp. 1219-1226
43. R.P. Darveau, J. Blake, C.L. Seachord, W.L. Cosand, M.D. Cunningham, L. Cassiano Clough, G. Maloney. Peptides related to the carboxyl terminus of human platelet factor IV with antibacterial activity. J. Clin. Invest., 90 (1992), pp. 447-455;
44. M. Malmsten, M. Davoudi, B. Walse, V. Rydengard, M. Pasupuleti, M. Morgelin, A. Schmidtchen. Antimicrobial peptides derived from growth factors. Growth Factors, 25 (2007), pp. 60-70

45. L.T. Nguyen, H.J. Vogel. Structural perspectives on antimicrobial chemokines. Front Immunol., 3 (2012), p. 384
46. Katia Pane, Lorenzo Durante, Orlando Crescenzi, Valeria Cafaro, Elio Pizzo, Mario Varcamonti, Anna Zanfardino, Viviana Izzo, Alberto Di Donato, Eugenio Notomista, Antimicrobial potency of cationic antimicrobial peptides can be predicted from their amino acid composition: Application to the detection of "cryptic" antimicrobial peptides, Journal of Theoretical Biology, Volume 419, 2017, Pages 254-265, ISSN 0022-5193, http://dx.doi.org/10.1016/j.jtbi.2017.02.012.
47. Notomista E, Falanga A, Fusco S, et al. The identification of a novel *Sulfolobus islandicus* CAMP-like peptide points to archaeal microorganisms as cell factories for the production of antimicrobial molecules. *Microbial Cell Factories*. 2015;14:126. doi:10.1186/s12934-015-0302-9.
48. K. Pane, V. Sgambati, A. Zanfardino, G. Smaldone, V. Cafaro, T. Angrisano, E. Pedone, S. Di Gaetano, D. Capasso, E.F. Haney, V. Izzo, M. Varcamonti, E. Notomista, R.E.W. Hancock, A. Di Donato, E. Pizzo. A new cryptic cationic antimicrobial peptide (amp) from human apolipoprotein E with anti-bacterial activity and immunomodulatory effects on human cells. FEBS J. (2016)
49. Rosa Gaglione, Eliana Dell'Olmo, Andrea Bosso, Marco Chino, Katia Pane, Flora Ascione, Francesco Itri, Sergio Caserta, Angela Amoresano, Angelina Lombardi, Henk P. Haagsman, Renata Piccoli, Elio Pizzo, Edwin J.A. Veldhuizen, Eugenio Notomista, Angela Arciello, Novel human bioactive peptides identified in Apolipoprotein B: Evaluation of their therapeutic potential, In Biochemical Pharmacology, Volume 130, 2017, Pages 34-50, ISSN 0006-2952, https://doi.org/10.1016/j.bcp.2017.01.009.
50. A. Bosso, L. Pirone, R. Gaglione, K. Pane, A. Del Gatto, L. Zaccaro, S. Di Gaetano, D. Diana, R. Fattorusso, E. Pedone, V. Cafaro, H.P. Haagsman, A. van Dijk, M.R. Scheenstra, A. Zanfardino, O. Crescenzi, A. Arciello, M. Varcamonti, E.J.A. Veldhuizen, A. Di Donato, E. Notomista, E. Pizzo, A new cryptic host defense peptide identified in human 11-hydroxysteroid dehydrogenase-1 β-like: from in silico identification to experimental evidence, In Biochimica et Biophysica Acta (BBA) - General Subjects, Volume 1861, Issue 9, 2017, Pages 2342-2353, ISSN 0304-4165, https://doi.org/10.1016/j.bbagen.2017.04.009.
51. Pizzo Elio, Zanfardino Anna, Di Giuseppe Antonella M.A., Bosso Andrea, Landi Nicola, Ragucci Sara, Varcamonti Mario, Notomista Eugenio and Di Maro Antimo (2015), A new active antimicrobial peptide from PD-L4, a type 1 ribosome inactivating protein of*Phytolacca dioica* L.: A new function of RIPs for plant defence?, FEBS Letters, 589, doi: 10.1016/j.febslet.2015.08.018.
52. de Souza Cândido E, e Silva Cardoso MH, Sousa DA, Viana JC, de Oliveira-Júnior NG, Miranda V, Franco OL. The use of versatile plant antimicrobial peptides in agribusiness and human health. Peptides. 2014 May;55:65-78. doi: 10.1016/j.peptides.2014.02.003.

Chapter 2

A new cryptic host defense peptide identified in human 11-hydroxysteroid dehydrogenase-1 β-like: from in silico identification to experimental evidence.

2.1 Introduction

In this chapter the characterization of a cryptic HDP is described. It is a 27 amino acids long peptide, identified in the C' terminal region of the human 11-hydroxysteroid dehydrogenase-1 β-like protein. This sequence has been named GVF27. Human 11-hydroxysteroid dehydrogenase-1 β-like (also known as 11β-HSD3) (UniProtKB: Q7Z5J1, http://www.uniprot.org/uniprot/Q7Z5J1) is an uncharacterized protein, present in eight putative isoforms, whose have been produced experimental evidences just at a transcriptional level. From these data, it seems that transcripts are mainly expressed in brain and lung cells. One of these isoforms has been isolated from a human brain cDNA library and produced in heterologous form in *Escherichia coli.* In this work [1] authors demonstrate that the isoform b has the capability to catalyze the dehydrogenation of cortisol in the presence of NADP(+), but this is the only existing indication in this direction and, moreover, 11β-HSD3 only poorly catalyzes conversion of cortisol to cortisone. To note, it predates the glucocorticoid receptor in evolution [2], presuming a primary function distinct from glucocorticoid biology [3]

This putative enzyme is part of the short-chain dehydrogenase/reductase (SDR) family, that is a very large family of enzymes, most of which are NAD+ or NADP+ dependent oxidoreductases [4]. All the members of the family only have a residue identity level of typically 15–20%, but two motifs are highly conserved [5, 6].

Generally, HSD family members participate in the metabolism of steroids, prostaglandins, retinoids, aliphatic alcohols and xenobiotics. 11β-hydroxysteroid dehydrogenase catalyzes the interconversion of inactive glucocorticoids (cortisone in human, dehydrocorticosterone in rodents) and active glucocorticoids (cortisol in human, corticosterone in rodents). Two major isoenzymes belonging to this subfamily, 11β-HSD1 and 11β- HSD2, have been identified and widely characterized.

11β-HSD1, also called "liver" type 11β-hydroxysteroid dehydrogenase acts mainly as a NADPH-dependent cortisone reductase [7]. The 11β-HSD1 gene is highly expressed in the liver, adipose tissue, bone and the brain [8, 9]. Its main function is activating glucocorticoids, but it is also expressed in the brain, with the highest levels found in the cerebellum, hippocampus, cortex, pituitary and hypothalamus; it plays an important role in human obesity and insulin resistance [7, 10, 11].

11β-HSD2, the "kidney" type 11β-hydroxysteroid dehydrogenase, acts as an NAD+-dependent cortisol dehydrogenase. The 11β-HSD2 gene is highly expressed in classical mineralocorticoid-selective target tissues such as kidney, colon and sweat glands [12, 13, 14, 15]. Moreover, 11β-HSD2 expressed in human fetal brain acts to protect the developing nervous system from the deleterious consequences of glucocorticoid overexposure, but 11β-HSD2 is barely expressed in the human adult brain. Reductase activity of 11β-HSD1 increases local cortisol levels and leads to increased differentiation [16, 17]. The dehydrogenase activity of 11β-HSD2 decreases the availability of active cortisol thereby facilitating proliferation [18]. It was reported that 11β-HSD2 is upregulated in different tumors which suggests that the inhibition of 11β-HSD2 activity can prevent the tumor from growing. These two enzymes have been deeply investigated, while 11-hydroxysteroid dehydrogenase-1 β-like was only recently discovered and never thoroughly studied.

Nevertheless, Huang et al. [1] revealed that the isoform b of 11β-HSD3 is highly expressed in the brain: in the cerebrum, hippocampal neurons, cerebellar glioma and meningioma. These

results suggest that 11β-HSD3 is a “brain type” hydroxysteroid dehydrogenase. 11β-HSD3 was a highly conserved protein during evolution. Its homologs were widely found in different species including animals and plants [19] Furthermore, the expression of 11β-HSD3 in lung cancer cell lines resulted to be upregulated and this effect suggests that the abnormal expression of 11β-HSD3 in the lung maybe related to the development of lung cancer. To note, no evidences have been produced about the involvement of 11β-HSD3 in the host defense.

As described in the **Chapter 1**, recently, the use of bioinformatic approaches has increased the possibility to highlight the presence of putative antimicrobial regions in proteins, thus representing an extremely useful tool for the discovery of new cryptic host defense peptides [20]. Indeed, analyzing a pool of human secreted proteins using the bioinformatic strategy developed by Professor Ennio Notomista [21], a region was identified rich in very high scoring peptides at the C-terminus of four isoforms of human 11-hydroxysteroid dehydrogenase-1 β-like. The region selected, named GVF27, corresponds to this local maximum plus the glycine residue located upstream the 26 residues. The glycine residue was included in the peptide as, according to [22], a glycine at the N-terminus of an HDP is favorable for the activity.

In this chapter, GVF27 has been fully characterized describing its bactericidal properties against planktonic and sessile bacteria, its cytotoxic and anti-inflammatory effects on murine cells and its structural properties in the presence of mimic membrane agents and wall bacterial determinants, such as LPS and LTA.

2.2 Results

2.2.1 Antibacterial activity and mechanism of action of GVF27

The antibacterial effectiveness of synthetic GVF27 was determined by measuring its MIC values on a panel of Gram-negative and Gram-positive strains (**Table 1**). All GVF27 MIC values are comparable to those observed for control peptide chicken cathelicidin CATH-2 both on Gram-negative and Gram-positive strains (**Table 1**).

In order to verify salt resistant properties of GVF27, MIC values were also determined in the presence of physiological amounts of divalent cations as $CaCl_2$ and $MgSO_4$ (0.265 g/L and 0.097 g/L respectively). As shown in **Table 2,** MIC values determined in the presence of divalent cations were only slightly different to those obtained in NB, thus indicating that antimicrobial properties of GVF27 are not affected by the different experimental conditions tested.

Moreover, an experiment was performed to detect GVF27 antimicrobial activity during time until 2 hours towards MRSA WKZ-2 and *E. coli* ATCC 25922. Colonies of the two strains were counted after the incubation with two doses of GVF27. When the killing rate of GVF27 was measured, none of the strains analyzed survived after 2 h at 10 μM peptide doses (**Figure 1**).

GRAM POSITIVE STRAINS	**GVF27**	**CATH-2**	**GRAM NEGATIVE STRAINS**	**GVF27**	**CATH-2**
	MIC values (μM)			**MIC values (μM)**	
MRSA WKZ-2	**5**	**10**	***E. coli* ATCC 25922**	**10**	**10**
***B. globigii* TNO BMO13**	**5**	**5**	***P. aeruginosa* ATCC 27853**	**10**	**10**
***B. licheniformis* ATCC 21424**	**5**	**20**	***P. aeruginosa* PAO1**	**20**	**20**
***S. aureus* ATCC 29213**	**5**	**10**	***S. enteriditis* 706 RIVM**	**10**	**10**

Table 1. Minimum Inhibitory Concentration (MIC, μM) values of GVF27 peptide, compared to those obtained for CATH-2, against a panel of Gram-positive and Gram-negative bacteria. Values were obtained from a minimum of three independent trials.

GRAM POSITIVE STRAINS	0.5X NB	0.5X NB + cations	GRAM NEGATIVE STRAINS	0.5X NB	0.5X NB + cations
	MIC values (μM)			MIC values (μM)	
MRSA WKZ-2	**5**	**10**	***E. coli* ATCC 25922**	**10**	**10**
***B. globigii* TNO BMO13**	**5**	**5**	***S. enteriditis* 706 RIVM**	**10**	**40**

Table 2. Minimum Inhibitory Concentration (MIC, μM) values of GVF27 peptide, tested in different media, against a panel of two Gram-positive and two Gram-negative bacteria. Values were obtained from a minimum of three independent trials.

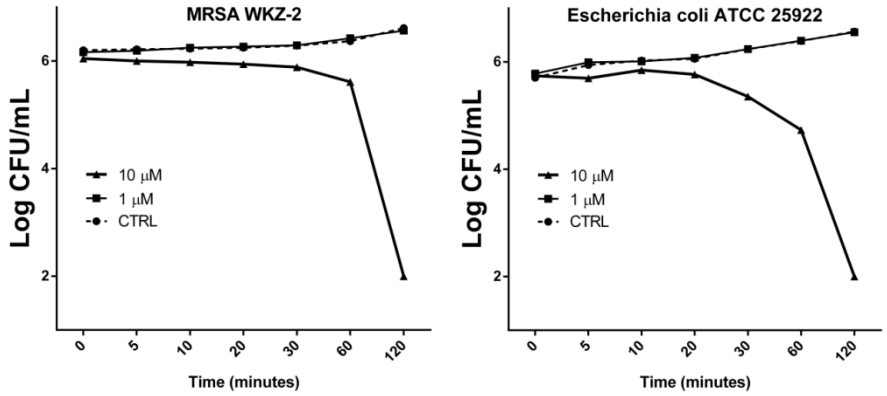

Figure 1: Antibacterial activity rate of GVF27, evaluated by colony count assay, against MRSA WKZ-2 and *Escherichia coli* ATCC 25922.

One of the mechanisms through which HDPs kill bacterial cells is by forming pores into biological membranes, resulting in the leakage of small molecules [23]. We tried to collect data on the mechanism of the antibacterial activity of GVF27 by measuring ATP levels in the media in which bacterial cells are grown in the presence of the peptide. In fact, in bacterial cells intracellular ATP concentration is maintained constant and the release of ATP into the environment can be detected by chemiluminescence, which indicates the disruption of the cell membrane. Thus, we performed an assay to detect ATP leakage using two bacterial strains, *E. coli* and MRSA, treated with two different doses of GVF27 for 20 min. As shown in **Figure 2** (panels A and B), the presence of ATP in the culture media is evident. Thus, we can confidently conclude that GVF27 has a lytic effect both on MRSA WKZ-2 and on *E. coli* cells, with MRSA WKZ-2 cells being particularly sensitive to the peptide. As it is shown in **Figure 2**, GVF27 induced in MRSA WKZ-2 cells a release of 70% ATP at a concentration of 0.5 μM. To obtain the same degree of ATP leakage in *E. coli* cells it was necessary to use a higher concentration of GVF27.

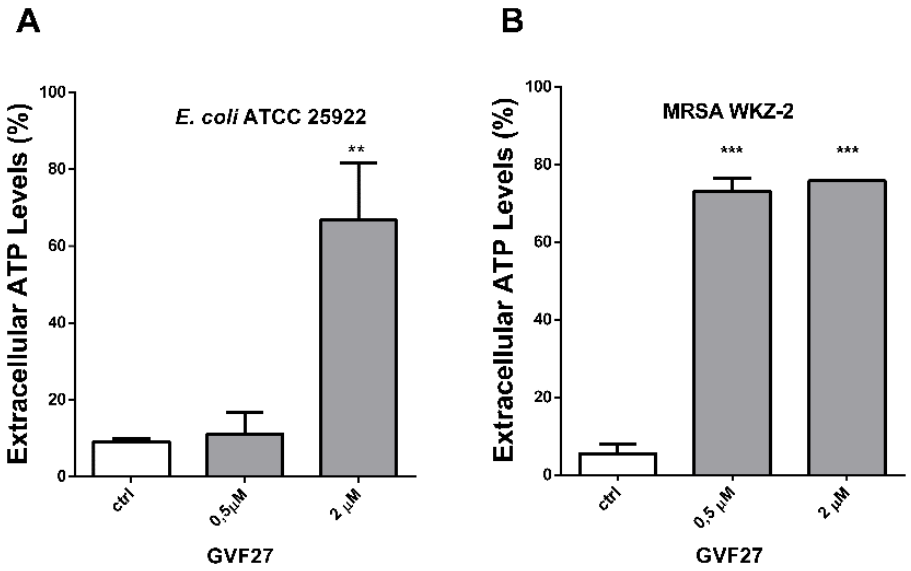

Figure 2: GVF27-induced ATP leakage in MRSA WKZ-2 (**A**) and *Escherichia coli* ATCC 25922 (**B**) after treatment with 0,5 or 2 μM of GVF27. The assays were performed in three independent experiments.

2.2.2 Anti-biofilm properties of GVF27

Bacteria mainly exist as multicellular aggregates embedded within a self-produced extracellular polymeric matrix. In this condition, known as biofilm, growing microbial cells are physiologically distinct from planktonic cells. As natural HDPs have emerged as promising anti biofilm candidates to be used as an alternative to conventional antibiotics, we evaluated if GVF27 is endowed with anti-biofilm activity by performing experiments on *E. coli* ATCC 25922 in BM2 medium. *E. coli* was grown over-night, diluted in BM2 medium containing increasing concentrations of the peptide (from 0,125 to 32 μM), and then incubated for 24 h, at 37˚C to evaluate its effectiveness on the **biofilm formation**. Following incubation, the analysis of biofilm production by crystal violet staining revealed a dose-dependent inhibition of biofilm formation, with about 90% inhibition at the highest concentration of peptide tested (**Figure 3A**). We also collected data that would indicate that GVF27 peptide exerts a significant effect on **biofilm attachment**. To investigate this, we followed the experimental procedure described above with the only exception that bacterial cells were incubated with increasing concentrations of peptide for 4 h, at 37°C. Also in this case, we observed a dose-dependent inhibition of biofilm attachment, with almost total inhibition at 32 μM peptide concentration (**Figure 3A**). Interestingly, GVF27 was found to exert significant effects also on **preformed biofilms**. This was evaluated by incubating preformed biofilm with increasing concentrations of the peptide for 24 h, at 37°C. At the highest peptide concentration tested, we observed a significant (~20%) reduction of the preformed biofilm (**Figure 3A**).

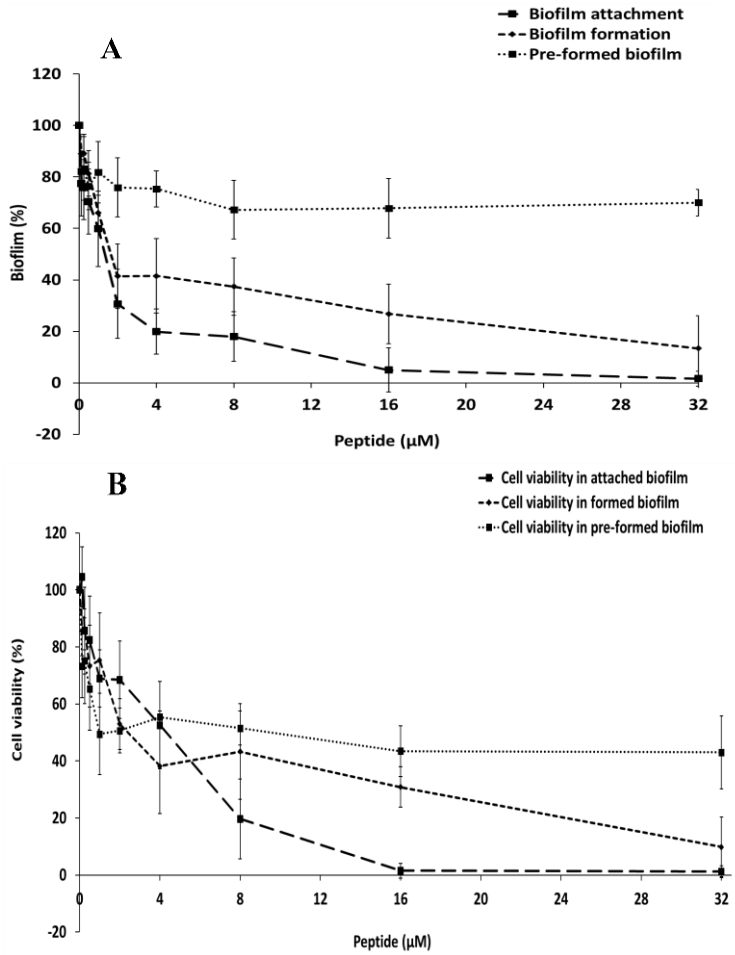

Figure 3: A. Biofilm inhibitory activity of GVF27 against *E. coli* strain in BM2 medium. The effects of increasing concentrations of GVF27 peptide were evaluated either on biofilm formation, biofilm attachment, or on pre-formed biofilm. Biofilm was stained with crystal violet and measured at 630 nm. Shown are mean + SD values of three independent experiments. **B.** Effects of increasing concentrations of GVF27 peptide on the viability of *E. coli* ATCC 25922 bacterial cells inside the biofilm structure. Cell viability was assessed by colony counting assay and expressed as the percentage of viable bacterial cells in treated samples with respect to the control untreated sample. Shown are mean + SD values of three independent experiments.

In all cases, we also evaluated the percentage of viable bacterial cells inside the biofilm by colony counting assay. We found (**Figure 3B**) an almost total reduction of bacterial viability when 32 µM GVF27 was added prior to biofilm attachment, a significant reduction (90%) when it was added prior to biofilm formation and a reduction of about 50% when the peptide was tested on pre-formed biofilm.

2.2.3 Cytotoxicity assays of GVF27 on eukaryotic cells

The promising interest in the use of HDPs stems from their selective action on bacterial cells. We thus studied the cytotoxic effect of GVF27 towards mouse macrophages and erythrocytes. The addition of increasing concentrations (from 0.6 to 40 μM) of GVF27 to mouse macrophages RAW cells 264.7 did not result, at 24 h of incubation time, in any significant reduction in cell viability (**Figure 4A**). The same peptide concentrations were tested also on mouse erythrocytes to detect any hemolytic activity of GVF27. As shown in **Figure 4B**, the peptide did not exert any lytic effect on mouse red blood cells, even at the highest concentration tested.

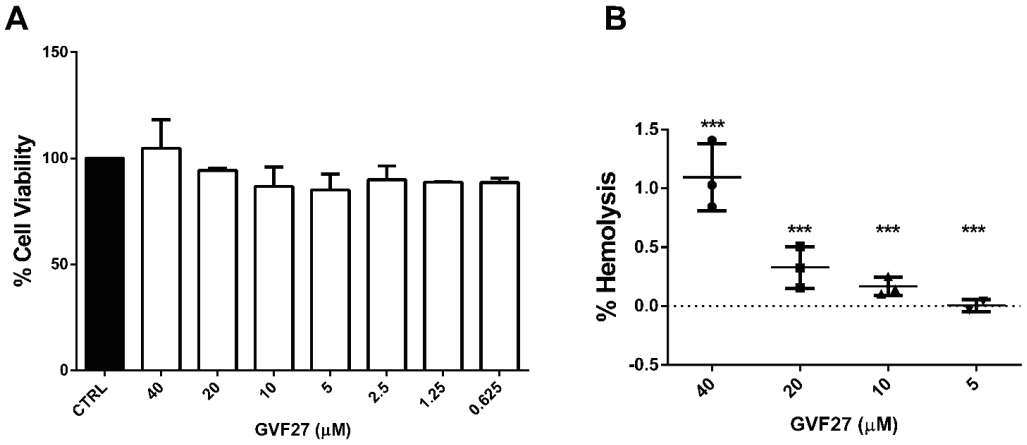

Figure 4: Cytotoxicity of GVF27 on eukaryotic cells. **A**) Effect of GVF27 on the viability of mouse macrophages Raw 264.7. **B**) Hemolytic activity of GVF27 on mouse erythrocytes. In both experiments the mean values ± SD from three independent experiments run in triplicate are shown.

The cytotoxicity of GVF27 was also measured against human keratinocytes (HaCat) and on human cervical cancer cells (HeLa). In all cases, no significant cytotoxicity was ever observed (data not shown). It should be underlined that GVF27 is toxic to bacterial cells at concentrations similar to that used in the cytotoxicity assays described above. This selective behavior is eligible for the perspective of a future in vivo application of GVF27. Moreover, it should be noted that all the experiments mentioned above were carried out after an incubation time of 24 h, since the analysis of GVF27 stability in serum indicated that peptide degradation was almost complete after 24 h (**Table 3**).

Time (hour)	Area %
0	100
1	63
2	41
3	30
24	6

Table 3. Analysis of serum stability of GVF27 by RP-HPLC (see Methods).

2.2.4 Conformational studies of GVF27: Circular Dichroism, Fluorescence and NMR.

Structural analysis by CD spectroscopy provides a qualitative picture of the structural elements that are present in a given peptide. Far-UV CD spectra indicate that GVF27 is largely unstructured both in water and in 10 mM Hepes pH 7.4. On the contrary, it is structured in 40% TFE (**Figure 5**). This behavior can be observed also for other HDPs, all prone to assume a specific conformation when interacting with membrane-mimicking agents like TFE. Moreover, deconvolution data reported in **Table 4**, indicate that structured GVF27 adopts a predominant helical structure (approximately of ≈ 50%).

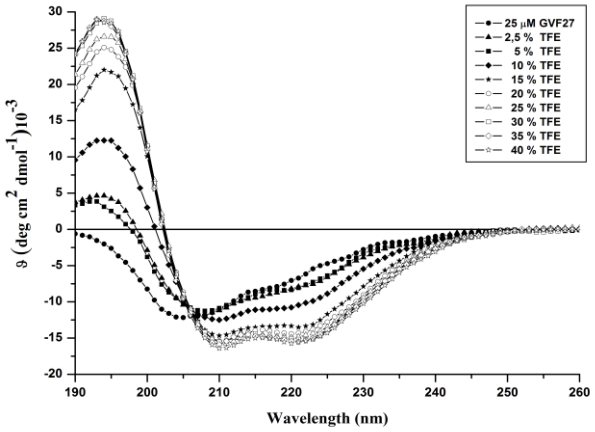

Figure 5: Far UV CD of GVF27 in the presence of increasing concentrations of TFE.

	% α-helical	% β-strand	% coil
GVF27	18.2	24.0	57.8
GVF27 - 40 %TFE	52.6	7.2	40.2
GVF27 - 0,4 mg/mL LPS from *Pseudomonas aeruginosa* strain 10	30.8	18.6	50.6
GVF27 - 0,4 mg/mL LPS from *Pseudomonas aeruginosa* strain KK27	32.1	12.3	55.5
GVF27 - LTA 0,4 mg/mL	33.0	19.5	47.5

Table 4. Secondary structure content of GVF27, calculated by means of CDPRO program.

To further characterize structural properties of GVF27, the interaction with LPS and LTA, the main constituents of the cell wall of Gram negative and positive bacteria, respectively, was analyzed. CD spectra in the presence of LPS isolated from two different *P. aeruginosa* strains (strain 10 and clinical isolate KK27 strain) are shown in **Figure 6** (panels A and B).
GVF27 spectrum in water has a minimum at around 205 nm, indicating that the peptide is in a disordered conformation. Instead, in the presence of LPS (**Fig. 6A-B**), the peptide spectra present two minima centered around 210 and 225 nm, suggesting that in both cases it is able to assume a

helical conformation upon interaction. The deconvolution data (**Table 4**) confirm that both LPSs induce a similar increase in the amount of helical structure (about 31-32%) but with slightly different amounts of beta and coil structure.
CD spectra, acquired in the presence of LTA, (**Figure 6C**), showed a relatively flat shape minimum centered at 215 nm, due to the presence of significant amounts both of alpha and beta structures as shown by deconvolution data (**Table 4**).

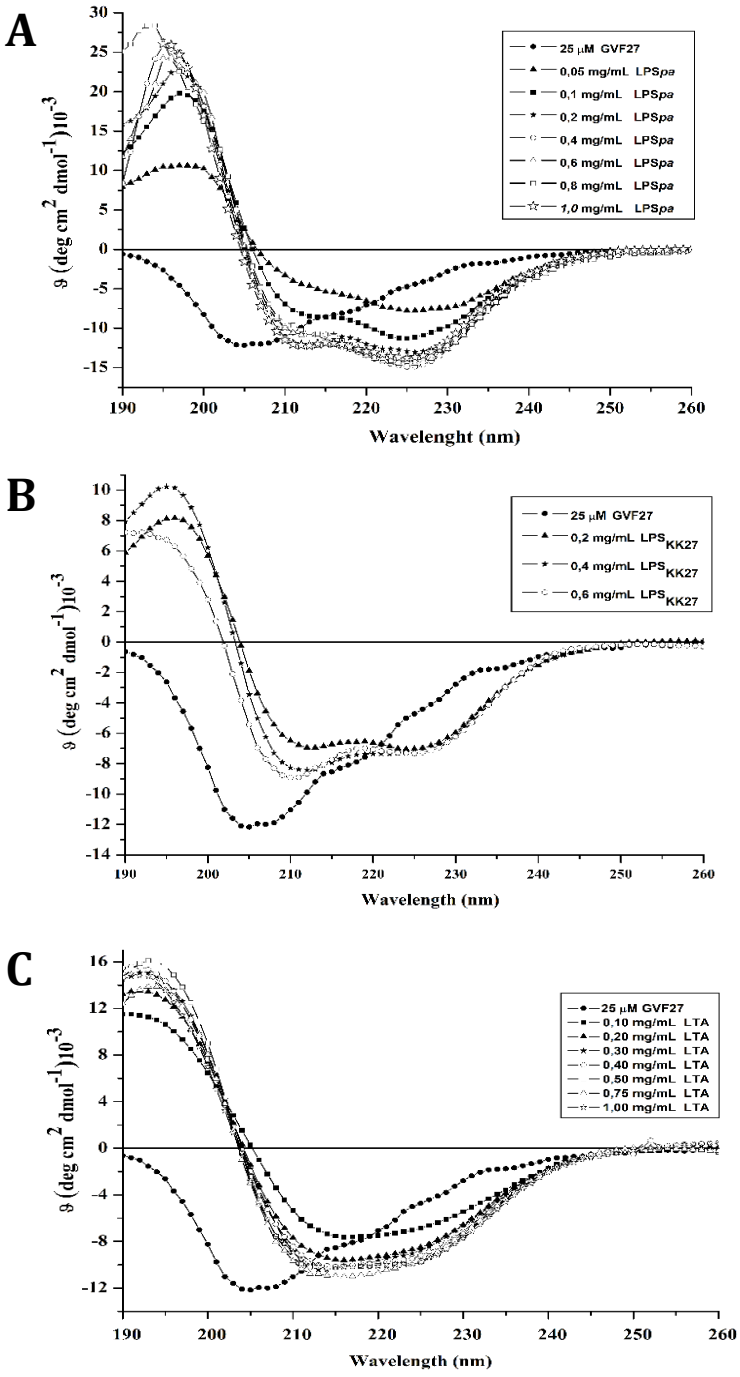

Figure 6: Far UV CD of GVF27 in the presence of increasing concentrations of LPS from *P. aeruginosa* 10 (**A**), from *P. aeruginosa* KK27 (**B**) and of LTA from *Staphylococcus aureus* (**C**).

Spectrofluorimetric data were also collected to investigate if the interaction of GVF27 with LPS and LTA could influence the tertiary structure of the peptide based on the presence in the sequence of three Trp residues (see **Figure 7**). Fluorescence spectra were recorded upon excitation at 280 nm and 295 nm and showed that the interaction of the peptide with LPS, LTA, and TFE results in a blue shift of the wavelength of the maximum of emission, indicating that GVF27 folds upon interaction with LPS or LTA, in agreement with CD data. However, in the presence of TFE a less marked effect was observed.

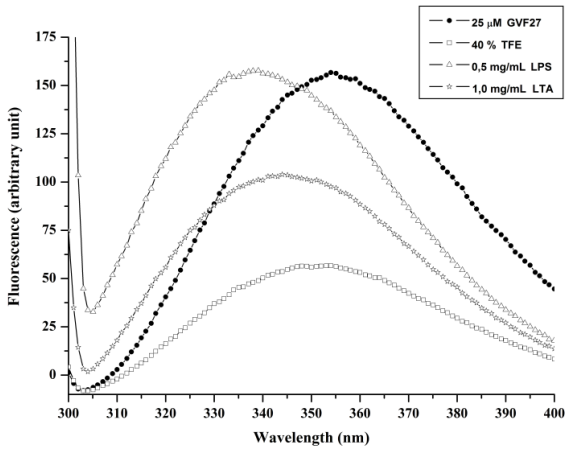

Figure 7: Tryptophan fluorescence spectra for GVF27 in H_2O and in the presence of TFE (40%), LPS (0,5 mg/mL) and LTA (1 mg/mL).

Moreover, a deeper investigation of the conformational preferences of peptide GVF27 was performed by NMR spectroscopy. NMR characterization of GVF27 was performed in TFE-d3/H2O 30:70 (v/v) mixture at 298 K. Through this analysis, GVF27 was confirmed to have a helical conformation like showed in **Figure 8**.

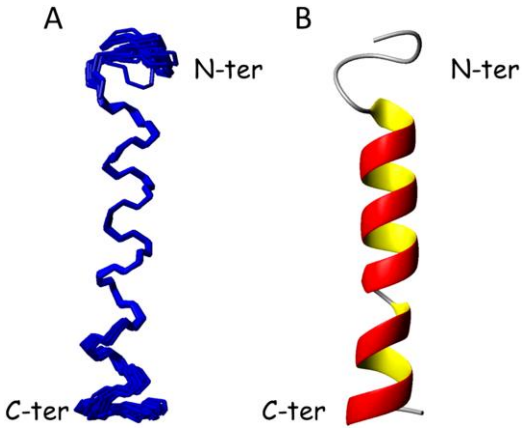

Figure 8: **NMR structures of GVF27 in TFE-d3/H_2O 30:70 mixture at 298 K A**) Backbone superposition of the 20 energy-minimized structures and **B**) Ribbon model of a representative structure.

2.2.5 GVF27 assembles LPS aggregates

Dynamic Light Scattering (DLS) is a well-known technique used to measure Brownian motion (diffusion) and size distribution of particles in solution. For this reason, DLS experiments were used to investigate whether peptide GVF27 may alter the size of micelles of LPS and LTA (above their critical micelle concentration). In both cases GVF27 displayed an associating action, promoting the formation of larger aggregates. In particular, the data indicate that LPS from *Pseudomonas* is poly-dispersed in solution with major size-populations having a hydrodynamic radius centered at about 40 nm (**Figure 9**). Incubation of LPS with GVF27 causes a shift of the average size of LPS micelles to a higher value centered at about 260 nm. On the other hand, when the peptide was incubated with LTA, a mean diameter of 100 nm of the aggregates was observed, indicating a weaker potency of GVF27 in associating LTA aggregates.
It can be hypothesized that this aggregation action, already observed for other HDP [24], may be part of a LPS neutralization mechanism, inhibiting the interaction of LPS with its cell receptors, with the concomitant blocking of cytokine production and release [25].

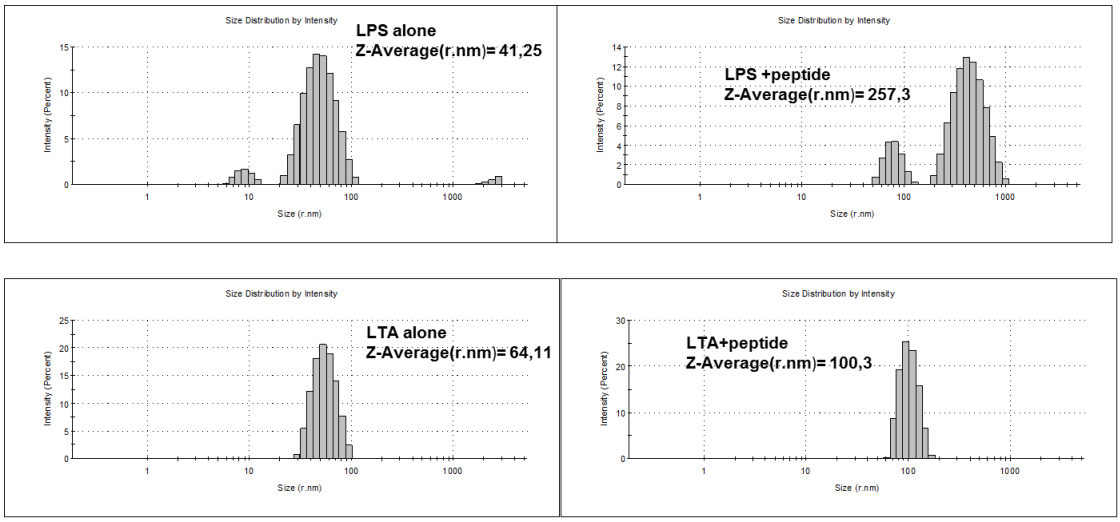

Figure 9: Effect of GVF27 on the structural organization of LPS or LTA micelles. Light scattering of LPS from *P. aeruginosa* 10 (top) or LTA (bottom) before and after incubation with the peptide.

2.2.6 Anti-inflammatory properties of GVF27

Data above would indicate that GVF27 is able to assume specific conformations in the presence of mimic membrane agents, LPS and LTA, as well as to induce aggregation of LPS, and to a lesser extent of LTA. As it has been already reported that several HDPs are able to mitigate up-regulation of LPS-induced pro-inflammatory mediators and cytokines [26], it seemed interesting to verify if GVF27 could possess also putative anti-inflammatory properties. To collect data on possible anti-inflammatory properties of GVF27, nitric oxide production and interleukin Il-6 release in murine macrophages RAW264.7 treated with GVF27 and LPS were analyzed. Nitric oxide (NO) plays diverse roles in biological systems: it is a mediator of vasodilatation, platelet aggregation and neurotransmission, and regulates function, death and survival of various cell types including many of those involved in immunity and inflammation. To study the effect of GVF27 on NO production in LPS induced RAW 264.7 cells, we performed three types of treatments: 1. medium containing

peptide alone (5 or 20 μM) for an initial incubation of 2 h followed by addition of 50 ng/mL LPS from *Salmonella* Minnesota; 2. medium containing 50 ng/mL LPS for an initial incubation of 2h followed by addition of peptide (5 or 20 μM); 3. medium containing a mixture of peptide (5 or 20 μM) and 50 ng/mL LPS. In all the cases, culture supernatants were collected after 24 h. As shown in **Figure 10A**, GVF27 exerts a strong dose-dependent attenuation of the production of NO when co-incubated with 50 ng/ml LPS. Conversely, when we performed a pre-incubation of RAW 264.7 cells with peptide and subsequently we induced LPS infection, the effect of GVF27 on NO production was not significant (**Figure 10A**). Similarly, when RAW 264.7 cells were pre-incubated with LPS and subsequently treated with 5 or 20 μM of GVF27, we revealed a slight dose dependent reduction of NO production (**Figure 10A**).

Cytokines are small proteins (about 25 kDa) released by many cell types, usually after an activation signal, and they induce a response by binding specific receptors. IL-6 is a monomer produced by T cells, macrophages and endothelial cells. It is able to determine growth and differentiation of B and T cells, and the production of acute phase proteins, like C-reactive protein. When we analyzed by ELISA the effect of GVF27 on RAW 264.7 cells, following the same scheme observed in the NO production assay, we revealed a strong inhibitory effect exerted by the peptide on the secretion of IL-6 when the macrophages were co-incubated for 24 h with GVF27 (5 or 20 μM) and 50 ng/ml LPS (see **Figure 10B**). Moreover, we found that GVF27 was able to exert also a significant dose dependent protective effect on cells. Indeed, as shown in **Figure 10B (**on the center**)**, when RAW 264.7 cells were pre-treated for two hours with 5 or 20 μM GVF27 and then incubated for 24 h with 50 ng/ml LPS, it was possible to observe a limited secretion of IL-6. When cells, instead, were pre-incubated with LPS and then subjected to the action of the peptide (see **Figure 10B** – on the right), a slight secretion of IL-6 was revealed. This suggests that, although the incubation time with the endotoxin was too short, the peptide was still able to reduce the secretion of the analyzed interleukin. Collectively, these data indicate that GVF27 is able to exert an intriguing anti-inflammatory effect on LPS treated cells.

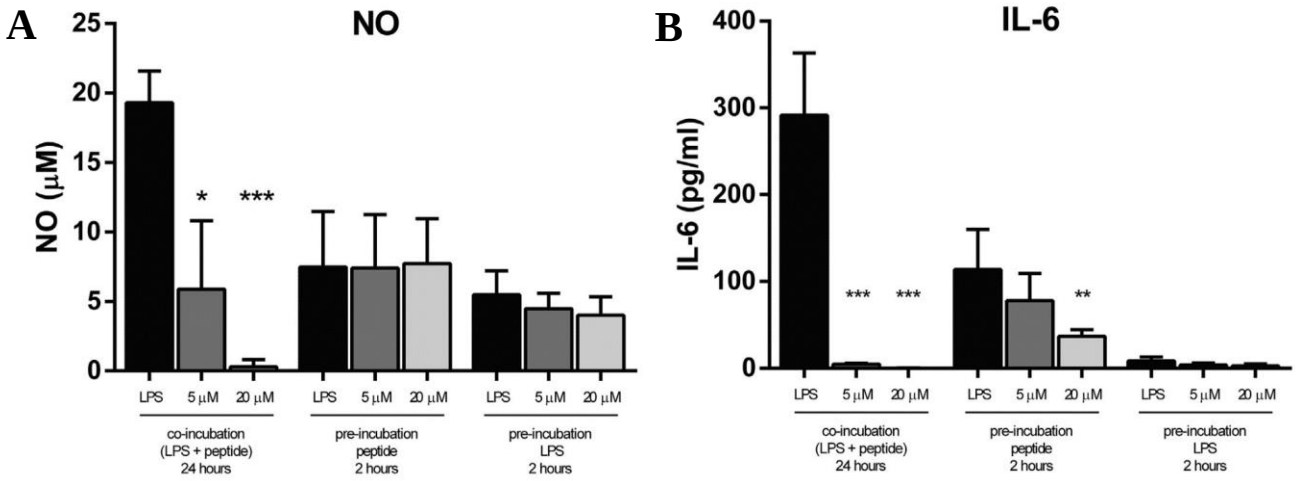

Figure 10: (A) Effect of GVF27 on NO production in LPS induced mouse macrophages RAW 264.1. LPS extracted from *Salmonella minnesota* was assayed at a final concentration of 50 ng/mL. All experiments were carried out for an incubation time of 24 h. **(B) Effect of GVF27 on IL-6 release in LPS induced mouse macrophages RAW 264.1** LPS extracted from *Salmonella minnesota* was assayed at a final concentration of 50 ng/mL. All experiments were carried out for an incubation time of 24 h.

Finally, the ability of GVF27 to bind LPS, was further confirmed by a different approach using the chromogenic LAL (*Limulus amaebocyte* lysate) assay [27]. Three different concentrations of GVF27 (6.25 - 12.5 – 25 μM) were incubated for 30 minutes at 37 °C with LPS from *Escherichia coli* 011:B4 following manufacturer instructions. As shown in **Figure 11**, a concentration of 12.5 μM GVF27 was enough to neutralize about 40% of LPS whereas the presence of 25 μM GVF27 completely neutralized LPS thus supporting the hypothesis that GVF27 might act in a dose-dependent manner as a scavenger of Gram negative's LPS (**Figure 11**).

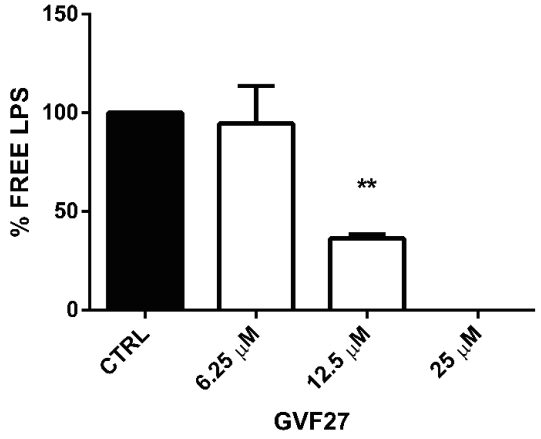

Figure 11: Neutralization LPS in the presence of GVF27. Peptide was incubated with the endotoxin (0.25 units/ml) for 30 min and the amount of free endotoxin quantified by LAL assay (see methods).

2.2.7 Intracellular killing

As already mentioned in the introduction, macrophages are specialized cells in the phagocytosis of pathogens and their intracellular digestion. However, some intracellular pathogens can escape digestion in phagolysosomes [28]. To cope with these pathogens, the antibacterial potential of the macrophage must be increased. This process is named macrophages activation and it can take place through extracellular signals, i.g. with the IFN-γ. Such activation is difficult in patients with a deficiency in IFN-γ or its receptor, however, there are other signals that may trigger the macrophage, such as LPS of Gram negative bacteria. In this experiment, we wanted to investigate whether beyond the immune modulating activities already described for GVF27, there was also the capability to increase the activity of murine macrophages in the intracellular digestion of *Salmonella enterica* serovar *Thypimurium* ATCC 14028, as has been already demonstrated for other HDPs [29]. Raw cells were preliminarily treated with two different doses of GVF27 (1 and 10 μM) for 2 hours. They were then infected with 1 x 10^8 CFU / mL of *Salmonella enterica* for 1 h. Subsequently, with the use of antibiotics for 1h, all the bacterial cells remaining in the extracellular environment were killed. Finally, the macrophages were lysed to release the bacterial cells still alive. These cells were then plated on LB-agar and the next day the intracellular killing percentage was evaluated (**Figure 12**).

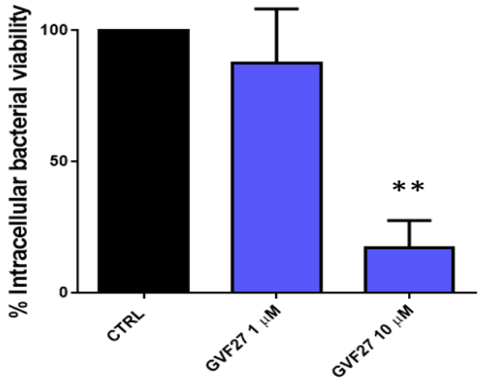

Figure 12: Intracellular clearance of *Salmonella enterica* induced by GVF27 in murine macrophages**.**

From this experiment, carried out 5 times, it was found that the lowest tested dose of the peptide was not sufficient to determine the macrophage activation, however at the concentration of 10 μM of GVF27, this was able to reduce to the number of viable intracellular bacteria more than 50 % with respect to untreated control. Further investigation should explain the mechanism through which GVF27 is able to kill intracellular bacteria in macrophages. Major hypotheses to explain these phenomena are (i) that the peptide could be taken up by the macrophage from the media into the cytoplasm and there exert its antimicrobial activity; otherwise (ii) the peptide could extracellularly activate the macrophage as well as act on other known paracrine signals.

2.3 Conclusions

A number of human proteins, whose primary functions are not necessarily related to host defense, contain HDPs hidden inside their sequence. In 2017, Pane Katia et al. [21] have established a bioinformatic procedure through which it is possible to identify host defense peptides in precursor protein sequences and predict their strain dependent antimicrobial propensities. By using this tool to analyze about 4,000 human secreted proteins, a cryptic peptide has been identified in human 11-hydroxysteroid dehydrogenase-1 β-like (accession number UniProtKB: Q7Z5J1), here named GVF27, with potent antimicrobial activity. The experiments described in this chapter confirm that GVF27 peptide exhibits antibacterial activities, with MIC values comparable to that of a well-studied cathelicidin [30], against a broad spectrum of both Gram-positive and -negative strains. Interestingly, its antibacterial properties are not limited to planktonic cells but are significant also on sessile bacteria forming biofilm. Indeed, here we provide evidences that GVF27 inhibits biofilm formation, as well as it is able to eradicate existing mature biofilm in a dose dependent manner. In addition, GVF27 is also able to induce a strong reduction of viable sessile bacterial cells. This suggests that our peptide presents affinity for biofilm components, presumably extracellular DNA and/or polysaccharides, but also retains its ability to attack bacterial membranes due to its amphipatic properties. This clearly confers to the peptide a relevant potential as an anti-biofilm agent alternative to conventional antibiotics, the latter being almost totally ineffective against microbes encapsulated in biofilm.

A crucial point regarding the development of membranolytic antimicrobial therapeutics is that they must not destroy the membrane of mammalian cells. We showed here that, although endowed with antimicrobial activity, GVF27 displays virtually no hemolytic and cytotoxic activity on an assortment of murine and human cell lines. This implies that GVF27, probably due to its net positive charge composition, has evident high membrane selectivity towards bacterial cells but not mammalian cells.

From a structural point of view, in agreement with the canonical properties of most HDPs, we verified by CD and NMR experiments that GVF27 is unstructured in aqueous buffer whereas it tends to assume a helical conformation in the presence of TFE. Moreover, NMR data clearly indicate that the spatial segregation of polar and apolar amino acids of GVF27 are on opposite faces oriented along the axis of a helical structure. This would indicate that GFV27 is able to assume an optimal conformation to effectively promote strong membrane association. Further tests by CD and light scattering have also allowed to highlight that the peptide is able to interact both with LPS and LTA, albeit in a less effective manner with the latter, thus suggesting that it can bind to the microbial surfaces via these wall determinants.

The ability of GVF27 to interact with LPS has been also confirmed by different approaches, thanks to which it has been possible to show that the peptide is able to inhibit the pro-inflammatory response. Indeed, GVF27 strongly down-regulates the release of NO and the production of IL-6 both in LPS pre-treated murine macrophages cells and upon co-administration of the peptide and the endotoxin. Moreover, it is worth noting that in murine macrophages treated with GVF27 and then subjected to LPS, a decrease of both NO and IL-6 was still detectable, thus suggesting also a protecting action for the peptide. GVF27 also demonstrated that this protecting action could be exerted by enhancing macrophages intracellular antimicrobial systems that act on phagocyted bacteria like *Salmonella enterica*. This opens an interesting scenario because GVF27 is a “hidden” peptide in a protein that, although not yet been characterized, could be constitutively

present under physiological conditions and able to release, by induced proteolysis, a fragment containing GVF27 in response to pathogen invasion. Our hypothesis is substantiated by an *in silico* prediction of peptides obtainable as a result of hydrolysis, which was carried out on the isoforms in which we identified GVF27 by simulating hydrolysis mediated by neutrophil elastase. Indeed, as shown in **Figure 13**, possible peptides released by hydrolysis are virtually superimposable to GVF27 and all have high antimicrobial scores, thus clearly supporting our idea that human proteins may fascinatingly be seen as active reservoirs of HDPs.

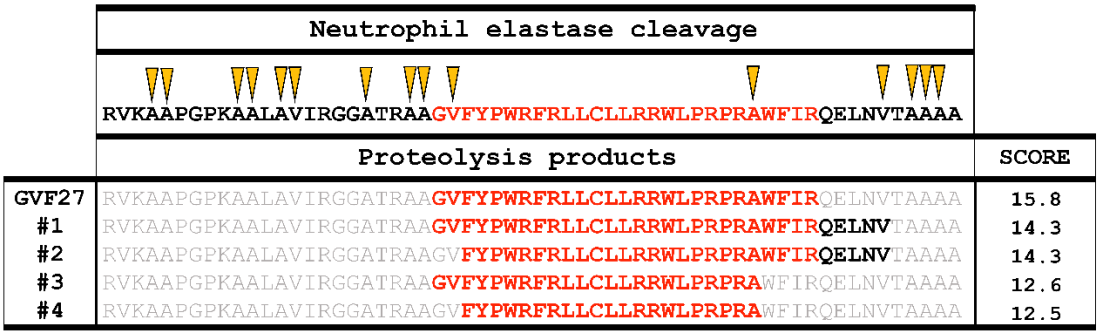

	Proteolysis products	SCORE
GVF27	RVKAAPGPKAALAVIRGGATRAAGVFYPWRFRLLCLLRRWLPRPRAWFIRQELNVTAAAA	15.8
#1	RVKAAPGPKAALAVIRGGATRAAGVFYPWRFRLLCLLRRWLPRPRAWFIRQELNVTAAAA	14.3
#2	RVKAAPGPKAALAVIRGGATRAAGVFYPWRFRLLCLLRRWLPRPRAWFIRQELNVTAAAA	14.3
#3	RVKAAPGPKAALAVIRGGATRAAGVFYPWRFRLLCLLRRWLPRPRAWFIRQELNVTAAAA	12.6
#4	RVKAAPGPKAALAVIRGGATRAAGVFYPWRFRLLCLLRRWLPRPRAWFIRQELNVTAAAA	12.5

Figure 13. *In silico* prediction, on the C-terminal region of the four isoforms in which we have identified GVF27, of hypothetical peptides released by cleavage mediated by human neutrophil elastase.

For each putative peptide (#1, #2, #3 and #4) the antimicrobial score by using the bioinformatic procedure described in Pane et al 2017 [21] has also been calculated. In our opinion at least three mechanisms could be responsible for GVF27 immune-modulatory properties. First, GVF27 might modulate cellular response to pro-inflammatory mediators by acting as an endotoxin scavenger during initial steps of infection. In this case the peptide could bind to and neutralize the endotoxin directly. Second, GVF27 might reduce inflammatory dysfunction during immune response by interacting with membrane receptors, i.e CD14, that then would activate down regulation of different pro-inflammatory pathways. Third, endogenous GVF27, or internalized from paracrine cells, may contribute to attenuation of the inflammatory response by interacting with intracellular targets. Based on these hypotheses and on the evidences described in this chapter, it is indisputable that the existence of cryptic HDPs implies that innate immunity is more complex than usually believed and that the human proteome is an unexplored and essential source of bioactive agents. In conclusion, GVF27 may offer several advantages compared to other antimicrobial agents: (i) it is non-immunogenic given its human origin; (ii) specifically targets bacterial strains, (iii) is not hemolytic and contributes to enhance anti-inflammatory response without altering cell viability. Thus, we confidentially believe that structural, immunomodulatory and antimicrobial data of GVF27 presented in this work, could serve as leads for the design of human-specific therapeutics.

2.4 Experimental procedures

2.4.1 Peptide synthesis

Peptide GVF27 was manually synthesized using the fluorenylmethyloxycarbonyl (Fmoc) solid-phase strategy (0.1 mmol). Synthesis was performed on NovaSyn TGA resin (loading 0.25 mmol/g), using all standard amino acids. The first amino acid was bound to the resin by treatment with Fmoc-Thr(tBu)-OH (5equiv)/MSNT (5 equiv)/MeIm (3.75 equiv) in DCM for 3 h. Fmoc protecting group was removed by reaction with 30% piperidine in DMF (3 × 10 min). The amino acids in 10-fold excess were pre-activated with HBTU (9.8 equiv)/HOBT (9.8 equiv)/DIPEA (10 equiv) in DMF for 5 min and then added to the resin suspended in DMF. The reaction was carried out for 1 h and coupling efficiency was assessed by the Kaiser test. The peptide was cleaved off the resin by treatment with a mixture of trifluoroacetic acid (TFA)/water/triisopropylsilane (95:2.5:2.5 v/v/v) for 3 h at room temperature. Resin was filtered, and crude peptide was precipitated with diethyl ether, dissolved in H_2O/ACN solution, and lyophilized. The product was purified by preparative RP-HPLC on a Shimadzu system equipped with a UV−visible detector SPD10A using a Phenomenex Jupiter Proteo column (21.2 × 250 mm; 4 μm; 90 Å) and a linear gradient of H_2O (0.1% TFA)/ACN (0.1% TFA) from 20%–80% of ACN (0.1%TFA) in 20 min at a flow rate of 20 mL/min. Identity and purity of the compound were assessed by LC/MS using an AGILENT Q-TOF LC/MS instrument equipped with a diode array detector combined with a dual ESI source and an Agilent C18 column (2.1 × 50 mm; 1.8 μm; 300 Å) at a flow rate of 200 μL/min and a linear gradient of H_2O (0.01% TFA)/ACN (0.01% TFA) from 5%–70% of ACN (0.01% TFA) in 15 min.

2.4.2 Antimicrobial activity assays

Antimicrobial activity of GVF27 peptide was tested against *Escherichia coli* ATCC 25922, MRSA WKZ-2 (methicillin-resistant *Staphylococcus aureus*), *Salmonella enteriditis* 706 RIVM, *Bacillus globigii* TNO BM013, *Bacillus licheniformis* ATCC 21424, *Staphylococcus aureus* ATCC 29213, *Pseudomonas aeruginosa* PAO1, and *Pseudomonas aeruginosa* ATCC 27853. Bacteria were grown to mid-logarithmic phase in Muller Hinton broth (MHB) at 37°C. Cells were then diluted to 2 x 10^6 CFU/ml in Difco 0.5X Nutrient Broth (Becton-Dickenson, Franklin Lakes, NJ) containing increasing amounts of GVF27 (0,6-40 μM). Starting from a peptide stock solution, two-fold serial dilutions were sequentially carried out, accordingly to broth microdilution method [31]. Following over-night incubation, MIC_{100} values were determined as the lowest peptide concentration responsible for no visible bacterial growth. Alternative antimicrobial assays to test salt resistant properties of GVF27 have been carried out following the same procedure described above and using 0.5X Nutrient Broth medium containing physiological concentrations of divalent cations as $CaCl_2$ and $MgSO_4$ (0.265 g/L and 0.097 g/L respectively).

2.4.3 Killing kinetics

To assess the time point of bacterial growth inhibition, killing kinetics with GVF27 were performed. Two different peptide concentrations (1 or 10μM GVF27) were incubated with mid-logarithmic (2×10^6 CFU/ml) *E. coli* ATCC 25922 or MRSA WKZ-2. At 1, 5, 10, 20, 30, 60 and 120 min, 100 μl aliquots were taken and immediately plated on TSA. Additionally, 20μl aliquots were diluted 10- to 1,000-fold and again 100μl was plated. After 16h incubation at 37 °C the surviving bacteria were counted.

2.4.4 ATP leakage measurements

MRSA WKZ-2 and *Escherichia coli* ATCC 25922 were grown in Muller Hinton broth (MHB) at 37°C to mid-logarithmic phase. Bacteria were centrifuged, resuspended in 10 mM phosphate buffer pH 7.0 + 1:100 MHB and diluted to 2×10^7 CFU/ml. From each diluted sample, 60 μl of bacterial suspension were incubated with 60 μl peptide solution (0.5 or 2 μM) for 20 min at 37°C. Samples were then centrifuged, the supernatant was stored at 4°C until further use, and the bacterial pellet was suspended in lysis buffer and further incubated at 100°C. Cell lysates were centrifuged and supernatants were kept on ice. Subsequently, both intra- and extracellular ATP levels were determined using the Roche ATP bioluminescence kit HS II (Roche Diagnostics Nederland B.V., Almere, the Netherlands), according to the manufacturer's protocols.

2.4.5 Serum Stability Assays

The proteolytic susceptibility of GVF27 peptide was determined in 50% (v:v) human serum (Lonza, Basel, Switzerland). Human serum was previously activated by cooling at 4°C, centrifugation at 13,000g for 5 min and incubation at 37°C for 10 min in order to eliminate the lipid fraction. Then, 250 μL of serum was added to a 250 μL of an aqueous solution of GVF27 at a concentration of 1 mg/mL. The mixture was incubated at 37°C and, after 1, 2, 3 and 24 h, samples (25 μL) were centrifuged at 13,000g for 5 min and the supernatant was added to 75 μL of H_2O containing 0.1% TFA and further centrifuged. Supernatants were finally analyzed by the analytical Agilent 1200 Series Liquid Chromatograph, equipped with a binary pump delivery system, robotic autosampler, column thermostat and multi-wavelength detector. An ET 250/8/4 Nucleosil 5-C18 column Machery-Nagel column (300 x 4mm, 5μm) and a linear gradient of H_2O (0.1%TFA)/CH_3CN (0.1%TFA) from 5 to 70% of CH_3CN (0.1%TFA) in 30 min at flow rate of 1mL/min were employed. The experiment was run in duplicate.

2.4.6 Anti-biofilm activity assays

Escherichia coli strain ATCC 25922 was grown over-night in Muller Hinton broth (MHB) and then diluted to 1×10^8 CFU/mL in BM2 medium containing increasing peptide concentrations (0.125-32 μM). Incubation with the peptide was carried out either for 4 h, in order to test peptide effects on biofilm attachment, or for 24 h, in order to test peptide effects on biofilm formation. When peptide effects on preformed biofilm were evaluated, bacterial biofilms were

formed for 24 h at 37 °C, and then treated with increasing concentrations of the peptide (0.125-32 μM). In all the cases, at the end of the incubation, the crystal violet assay [32] was performed. To do this, the planktonic culture was removed from the wells, which were washed three times with sterile PBS prior to staining with 0.04% crystal violet for 20 min. The colorant excess was eliminated by three successive washes with sterile PBS. Finally, the crystal violet was solubilized with 33% acetic acid and samples optical absorbance values were determined at 630 nm by using a microtiter plate reader (FLUOstar Omega, BMG LABTECH, Germany). To determine the percentage of viable bacterial cells inside the biofilm structure, upon biofilm disruption with 0,1% Triton X-100, bacterial cells were ten-fold diluted on solid TSA and incubated for 16 h at 37 °C. Once evaluated the number of colony forming units, bacterial cell survival was calculated as follows: ($_{CFUin\ treated\ sample}$/$CFU_{in\ untreated\ sample}$) x 100.

2.4.7 Cytotoxicity Assay

Cytotoxic effects of peptide on Raw 264.7 cells were determined using the cell proliferation reagent WST-1 (Roche Applied Science, Mannheim, Germany), designed to be used for the spectrophotometric quantification of cell proliferation. Briefly 5×10^4 cells were seeded into a 96-well plate and incubated at 37°C with 5% CO_2. Medium was then replaced with 100 μl of fresh media containing peptide solution to a final concentration ranging from 0–40 μM/well. After 24 h of incubation at 37°C, the peptide-containing medium was removed, and 100 μl of fresh medium containing 10% WST-1 reagent was added to each well and incubated for 30 min at 37°C in the dark. Subsequently, the absorbance was measured in a microtiter plate reader (FLUOstar Omega, BMG labtech) at 450 nm, using 650 nm as the reference wavelength.

2.4.8 Hemolytic Assay

EDTA anti-coagulated mouse blood was centrifuged for 10 min at 800 × g (20 °C) to sediment the red blood cells. Pelleted RBCs were washed three times and diluted 200-fold in PBS. In 96-well polypropylene plates, 75 μl of serial peptide dilutions (0–80 μM) were mixed with an equal volume of RBC suspension and incubated for 1 h at 37 °C. PBS served as baseline and a 0.2% (v/v) Triton X-100 solution served as a control for complete lysis. Supernatants, collected after 10 min centrifugation at 1300 × g (20 °C), were transferred into polystyrene 96-wells plates and absorbance was measured at 405 nm. Hemolysis (%) was calculated as follows: ((APeptide −ABlank)/(ATriton − ABlank)) × 100.

2.4.9 Measurement of nitric oxide production

Nitric oxide production was assessed as the accumulation of nitrite (NO_2^-) in cell supernatants as a result of 24 h incubation period. Nitrite concentrations were determined by a colorimetric reaction using the Griess reagent. Briefly, cell culture supernatants were mixed with an equal volume of 1% sulfanilamide (dissolved in 2.5% phosphoric acid) and incubated for 5 min. The same volume of 0.1% N-(1-naphthyl) ethylenediamine dihydrochloride was added and

incubated for 5 min. The absorbance was measured at 520 nm using a 96-well microplate reader (FLUOstar Omega, BMG labtech).

2.4.10 Inhibition of IL-6 production mediated by GVF27

The ability of the peptide to modulate cytokine production in RAW 264.7 cells was measured by ELISA (enzyme-linked immunosorbent assay). Cells (5×10^4 cells) were seeded into 96-wells microtiter plates. Next day culture medium was discarded and replaced with fresh medium containing peptide alone (5 or 20 μM) for an initial incubation of 2h followed by addition of 50 ng/mL LPS from *Salmonella* Minnesota or, alternatively, with 50 ng/mL LPS for an initial incubation of 2h followed by addition of peptide (5 or 20 μM) or of a mixture of peptide (5 or 20 μM) and 50 ng/mL LPS. In all the cases, culture supernatants were collected after 24 h. After each pre-incubation, either with LPS or with peptide, and prior to the subsequent addition of peptide or LPS to murine macrophages, at least three washing steps were performed to remove any residual traces of agents previously used. Expression levels of mouse IL-6 were measured using the commercial available DuoSet ELISA kits (R&D Systems), following the protocols provided by the manufacturer. All samples were centrifuged briefly at 5,000 rpm for 3 min at room temperature to remove cell debris prior to use. Microtiter plates were read at 450 nm using 550 nm as a reference wavelength to correct optical imperfections of the microtiter plate.

2.4.11 LPS binding assay

The ability of GVF27 to neutralize LPS was determined using the commercially available Limulus amebocyte lysate (LAL) assay (Pierce® LAL Chromogenic Endotoxin Quantitation Kit, Thermo Scientific, USA). Briefly, 25 μl of serially diluted peptide (25,12.5, 6.25 μM) was added to 25 μl of 0.5 U/ml *E. coli* O11:B4 LPS for 30 min at 37 °C, followed by incubation with 50 μl of amoebocyte lysate reagent for 10 min. Absorbance at 405 nm was measured 10 min after the addition of 100 μl of the chromogenic substrate, Ac-Ile-Glu-Ala-Arg-p-nitroanilide. The amount of non-bound LPS was extrapolated from a standard curve, and percentage inhibition calculated as: [(amount of free LPS in control samples) − (amount of free LPS in test samples)]×100/amount of free LPS in control samples.

2.4.12 Spectroscopic studies

CD spectra of GVF27 were recorded with a J-810 spectropolarimeter equipped with a Peltier temperature control system (Model PTC- 423-S, Jasco Europe, Cremella, LC, Italy). Far-UV measurements (190–260 nm) were carried out at 20° C using a 0.1 cm optical path length cell and a peptide concentration of 25μM. Baseline was corrected by subtracting the complete buffer spectrum. CD spectra were carried out in the presence of LPS from *Pseudomonas aeruginosa* strain 10 (Sigma, purified by phenol extraction) and from *P. aeruginosa* clinical strain KK27 [29]. Further analyses were carried out in the presence of lipotechoic acid from *Staphylococcus aureus* (LTA, Product Number L 2515, Sigma). All measurements were recorded using different concentration of

each compound (from 0.05 to 1.0 mg/ml). Baseline was corrected by subtracting the spectrum of both LPS and LTA alone at the same concentration. Additional CD spectra were performed using different concentrations of trifluoroethanol (TFE) (0-40%). Deconvolutions of CD spectra were obtained using the web-based program CdPro (http://lamar.colostate.edu/~sreeram/CDPro/). Fluorescence experiments were carried out under the same conditions used for CD analyses. Fluorescence spectra were collected at 20°C using a Varian Cary Eclipse spectrophotometer at λ excitation of 295 and 280 nm, a 1.0 cm path length cell at 5 ε_{em} and 5 ε_{ex}. Emission spectra (300-400 nm) were collected in the presence of 40% TFE, 5 mg/ml LPS or 10 mg/ml LTA.

2.4.13 LPS micelles measurements by using dynamic light scattering (DLS)

To estimate the average size of the LPS particles, the Hydrodynamic Radii (RH) was measured by Dynamic Light Scattering technique (DLS). DLS measurements were carried out using a Zetasizer Nano ZS (Malvern Instruments, Westborough, MA) equipped with a 173° backscatter detector, at 25 °C, using a disposable sizing cuvette. DLS measurements in triplicate were carried out on aqueous LPS and LTA samples at 0.5 mg/mL. Data were analyzed using the Software of OMNISIZE (Viscotek). LPS and LTA size measurements were performed before and after peptide addition (0.5 mg/ml).

2.4.14 Nuclear magnetic resonance spectroscopy

NMR experiments were recorded at 25 °C on a Varian Unity INOVA 600 MHz NMR spectrometer equipped with a cold probe. Two-dimensional (2D) nuclear Overhauser effect spectroscopy (NOESY), total correlation spectroscopy (TOCSY) and 2D double-quantum-filtered correlated spectroscopy (DQFCOSY) experiments were recorded. NOESY mixing times were 200 ms and TOCSY mixing times were 70 ms. These experiments were collected with 512 and 1024 complex points with acquisition times of 64 and 128 ms in the indirectly and directly acquired 1H dimensions, respectively. The DQFCOSY experiment was collected with 1024 and 2048 complex points and acquisition times of 128 and 256 ms in the indirectly and directly acquired 1H dimensions, respectively. In all experiments water suppression was obtained using pre-saturation in order to simultaneously suppress the hydroxyl protons from TFE that are in fast exchange with protons from water. Hydroxyl protons from TFE were seen to attenuate signals in both 1D and 2D datasets in WATERGATE based suppression. 1D spectra were analyzed using ACD/NMR Processor 12.0 (ACD/NMR Processor Freeware, Version 12.01 Advanced Chemistry Development, Inc., Toronto, ON, Canada (2012), www.acdlabs.com). 2D TOCSY and NOESY spectra for 1H chemical shift assignment were analyzed using Neasy, a tool available in CARA (Computer Aided Resonance Assignment) software (Keller, R. L. J. The Computer Aided Resonance Assignment Tutorial. CANTINA Verlag, 2004, downloaded from cara.nmr.ch). Structure calculation was performed with the program CYANA version 2.1 [33]. The NOE cross peak intensities were used to obtain distance constraints. The angle restraints were derived from 3JHNHα coupling constants. Structure calculations were initiated from 100 random conformers; the 20 structures with the lowest CYANA target function ns were analyzed with the programs MOLMOL [34] and PyMOL Molecular Graphics System, Version 1.8 Schrödinger, LLC. (http://www.pymol.org/).

2.4.15 Intracellular bacterial killing assay

$2x10^5$ RAW 264.7 cells were incubated with 1-10 μM at 37°C for 2h and then washed three times with sterile PBS. Cells were incubated with $1x10^8$ CFU/mL of *Salmonella enterica Typhimurium* ATCC 14028 at 37°C in DMEM supplemented with 10% FBS, 2 mM L-glutamine but without any antibiotics. After 1 h of infection, cells were washed three times with PBS to move away un-phagocyted bacteria. To ensure that extracellular environment was free from bacteria, cells were incubated 1h at 37°C with DMEM supplemented with 10% FBS, 2 mM L-glutamine and Pen-Strep as source of antibiotics. Then, cells were washed three times with PBS again. Cells were lysed using 0.1% Triton X-100 in PBS for 5 minutes at room temperature to release intracellular bacteria. Thereafter, the lysates were serially diluted and plated onto agar plates. The following day, viable bacteria were counted (CFU).

2.4.16 Statistics

Results are presented as the mean ± standard error of the mean (SEM) of at least three independent experiments. Statistical significance was assessed with one-way ANOVA in Prism software, version 6.02 (GraphPad Prism, La Jolla, CA, USA). All samples were compared to the negative control. *$p < 0.05$; **$p < 0.01$; ***$p < 0.001$.

References

1. Huang C, Wan B, Gao B, Hexige S, Yu L. Isolation and characterization of novel human short-chain dehydrogenase/reductase SCDR10B which is highly expressed in the brain and acts as hydroxysteroid dehydrogenase. Acta Biochim Pol 56: 279–289, 2009
2. Baker ME. Evolution of 11beta-hydroxysteroid dehydrogenase-type 1 and 11beta-hydroxysteroid dehydrogenase-type 3. FEBS Lett. 2010 Jun 3; 584(11):2279-84
3. Chapman K, Holmes M, Seckl J. 11β-Hydroxysteroid Dehydrogenases: Intracellular Gate-Keepers of Tissue Glucocorticoid Action. *Physiological Reviews*. 2013;93(3):1139-1206. doi:10.1152/physrev.00020.2012.)
4. Kallberg, Y., Oppermann, U., Jörnvall, H. and Persson, B. (2002), Short-chain dehydrogenases/reductases (SDRs). European Journal of Biochemistry, 269: 4409–4417. doi:10.1046/j.1432-1033.2002.03130.x
5. Oppermann, U.C., Filling, C., Berndt, K.D., Persson, B., Benach, J., Ladenstein, R., Jornvall, H. Active site directed mutagenesis of 3 β/17 β-hydroxysteroid dehydrogenase establishes differential effects on short-chain dehydrogenase/reductase reactions. Biochemistry. 1997; 36:34–40.
6. Filling, C., Berndt, K.D., Benach, J., Knapp, S., Prozorovski, T., Nordling, E., Ladenstein, R., Jornvall, H., Oppermann, U. Critical residues for structure and catalysis in short-chain dehydrogenases/reductases. J. Biol. Chem. 2002;277:25677–25684.
7. Bujalska IJ, Kumar S, Hewison M, Stewart PM. Differentiation of adipose stromal cells: the roles of glucocorticoids and 11beta-hydroxysteroid dehydrogenase. Endocrinology 140: 3188–3196, 1999
8. Ricketts ML, Verhaeg JM, Bujalska I, Howie AJ, Rainey WE, Stewart PM. Immunohistochemical localization of type 1 11beta-hydroxysteroid dehydrogenase in human tissues. J Clin Endocrinol Metab 83: 1325–1335, 1998
9. Stewart PM, Boulton A, Kumar S, Clark PM, Shackleton CH (1999) Cortisol metabolism in human obesity: impaired cortisone→cortisol conversion in subjects with central adiposity. J Clin Endocrinol Metab 84: 1022–1027
10. Tomlinson JW, Bujalska I, Stewart PM, Cooper MS. The role of 11 beta-hydroxysteroid dehydrogenase in central obesity and osteoporosis. Endocr Res. 2000 Nov;26(4):711-22.;
11. Wolf G (2002) Glucocorticoids in adipocytes stimulate visceral obesity. Nutr Rev 60: 148–151.
12. Diaz R, Brown RW, Seckl JR (1998) Distinct ontogeny of glucocorticoid and mineralocorticoid receptor and 11β- hydroxysteroid dehydrogenase types I and II mRNAs in the fetal rat brain suggest a complex control of glucocorticoid actions. J Neurosci 18: 2570–2580
13. Brereton PS, van Driel RR, Suhaimi F, Koyama K, Dilley R, Krozowski Z (2001) Light and electron microscopy localization of the 11β-hydroxysteroid dehydrogenase type I enzyme in the rat. Endocrinology 142: 1644–1651.
14. Audige A, Dick B, Frey BM, Frey FJ, Corman B, Vogt B (2002) Glucocorticoids and 11β-hydroxysteroid dehydrogenase type 2 gene expression in the aging kidney. Eur J Clin Invest 32: 411–420.
15. Kataoka S, Kudo A, Hirano H, Kawakami H, Kawano T, Higashihara E, Tanaka H, Delarue F, Sraer JD, Mune T, Krozowski ZS, Yan K (2002) 11β-hydroxysteroid dehydrogenase type 2 is expressed in the human kidney glomerulus. J Clin Endocrinol Metab 87: 877–882.

16. Bujalska IJ, Walker EA, Hewison M, Stewart PM (2002a) A switch in dehydrogenase to reductase activity of 11β- hydroxysteroid dehydrogenase type 1 upon differentiation of human omental adipose stromal cells. J Clin Endocrinol Metab 87: 1205–1210.
17. Bujalska IJ, Walker EA, Tomlinson JW, Hewison M, Stewart PM (2002b) 11β-hydroxysteroid dehydrogenase type 1 in differentiating omental human preadipocytes: from de-activation to generation of cortisol. Endocr Res 28: 449–461.
18. Rabbitt EH, Gittoes NJ, Stewart PM, Hewison M (2003) 11β-hydroxysteroid dehydrogenases, cell proliferation and malignancy. J Steroid Biochem Mol Biol 85: 415–421.
19. Baker ME (2004) Evolutionary analysis of 11β-hydroxysteroid dehydrogenase-type 1, -type 2, -type 3 and 17betahydroxysteroid dehydrogenase-type 2 in fish. FEBS Lett 574: 167–170
20. P. Wang, L. Hu, G. Liu, N. Jiang, X. Chen, J. Xu, W. Zheng, L. Li, M. Tan, Z. Chen, H. Song, Y.D. Cai, K.C. Chou, Prediction of antimicrobial peptides based on sequence alignment and feature selection methods, PLoS One. Apr 13;6(4) (2011) e18476
21. K. Pane, L. Durante, O. Crescenzi, V. Cafaro, E. Pizzo, M. Varcamonti, A. Zanfardino, V. Izzo, A. Di Donato, E. Notomista, Antimicrobial potency of cationic antimicrobial peptides can be predicted from their amino acid composition: Application to the detection of "cryptic" antimicrobial peptides. J Theor Biol. 2017 Feb 17;419:254-265
22. Y. Xiao, H. Dai, Y.R. Bommineni, J.L. Soulages, Y.X. Gong, O. Prakash, G. Zhang, Structure-activity relationships of fowlicidin-1, a cathelicidin antimicrobial peptide in chicken, FEBS J. Jun;273(12) (2006) 2581-93
23. E.J. Veldhuizen, V.A. Schneider, H. Agustiandari, A. van Dijk, J.L. Tjeerdsma-van Bokhoven, F.J. Bikker, H.P. Haagsman, Antimicrobial and immunomodulatory activities of PR-39 derived peptides, PLoS One. 9(4) (2014) e95939
24. E. Notomista, A. Falanga, S. Fusco, L. Pirone, A. Zanfardino, S. Galdiero, M. Varcamonti, E. Pedone, P. Contursi, The identification of a novel Sulfolobus islandicus CAMP-like peptide points to archaeal microorganisms as cell factories for the production of antimicrobial molecules, Microb Cell Fact. 14 (2015) 126
25. K. Pane, V. Sgambati, A. Zanfardino, G. Smaldone, V. Cafaro, T. Angrisano, E. Pedone, S. Di Gaetano, D. Capasso, E.F. Haney, V. Izzo, M. Varcamonti, E. Notomista, R.E. Hancock, A. Di Donato, E. Pizzo, A new cryptic cationic antimicrobial peptide from human apolipoprotein E with antibacterial activity and immunomodulatory effects on human cells, FEBS J. 283(11) (2016) 2115-31
26. G. Diamond, N. Beckloff, A. Weinberg, K.O. Kisich, (2009) The roles of antimicrobial peptides in innate host defense, Curr Pharm Des. 15(21) (2009) 2377-92
27. L. Heinbockel, L. Palacios-Chaves, C. Alexander, E. Rietschel, J. Behrends, W. Correa, S. Fukuoka, T. Gutsmann, A.J. Ulmer, K. Brandenburg, Mechanism of Hbγ-35-induced an increase in the activation of the human immune system by endotoxins, Innate Immun. Apr;21(3) (2015) 305-13
28. Terence A. et al., *Salmonella* effectors: important players modulating host cell function during infection. Cellular Microbiology (2011) 13(12), 1858–1869
29. Gon Sup KIM et al. Biological and Antibacterial Activities of the Natural Herb *Houttuynia cordata* Water Extract against the Intracellular Bacterial Pathogen *Salmonella* within the RAW 264.7 Macrophage *Biol. Pharm. Bull.* 31(11) 2012—2017 (2008), Vol. 31, No. 11

30. A. van Dijk, M.H. Tersteeg-Zijderveld, J.L. Tjeerdsma-van Bokhoven, A.J. Jansman, E.J. Veldhuizen, H.P. Haagsman. Chicken heterophils are recruited to the site of Salmonella infection and release antibacterial mature Cathelicidin-2 upon stimulation with LPS. Mol Immunol 46 (2009) 1517-1526.
31. I. Wiegand, K. Hilpert, R.E. Hancock, Agar and broth dilution methods to determine the minimal inhibitory concentration (MIC) of antimicrobial substances, Nat Protoc. 3(2) (2008) 163-75.
32. Y. Xiao, H. Dai, Y.R. Bommineni, J.L. Soulages, Y.X. Gong, O. Prakash, G. Zhang, Structure-activity relationships of fowlicidin-1, a cathelicidin antimicrobial peptide in chicken, FEBS J. Jun;273(12) (2006) 2581-93.
33. S. Correale, C. Esposito, L. Pirone, L. Vitagliano, S. Di Gaetano, E. Pedone, A biophysical characterization of the folded domains of KCTD12: insights into interaction with the GABAB2 receptor. J Mol Recognit.;26(10) (2013) 488-95.
34. M. Leone, P. Di Lello, O. Ohlenschläger, E.M. Pedone, S. Bartolucci, M. Rossi, B. Di Blasio, C. Pedone, M. Saviano, C. Isernia, R. Fattorusso, Solution structure and backbone dynamics of the K18G/R82E Alicyclobacillus acidocaldarius thioredoxin mutant: a molecular analysis of its reduced thermal stability, Biochemistry. 43(20) (2004) 6043-58.

Chapter 3

Novel human bioactive peptides identified in Apolipoprotein B: Evaluation of their therapeutic potential.

3.1 Introduction

Apolipoproteins are the main protein components of plasma lipoproteins and, intriguingly, a source of bioactive peptides. Reports have shown that peptides derived from the cationic receptor binding region of Apolipoprotein E (ApoE141-149) are endowed with broad anti-infective activity [1]. Apolipoprotein B (ApoB) also contains two LDL (low-density lipoprotein) receptor binding domains, namely region A (ApoB3147-3157) and region B (ApoB3359-3367). Region B, more uniformly conserved across species and primarily involved in receptor binding, has been found to be endowed with a significant antiviral activity. Moreover, peptides derived from ApoB have been already used in vaccine preparations [2]. As mentioned in **Chapter 1**, recently, Pane K. et al. developed an *in silico* method [3] to identify HDPs in protein precursors and to predict quantitatively their antibacterial activity. This method allows the identification of novel HDPs within the sequence of known proteins ("cryptic" HDPs), as demonstrated by the identification of a novel cationic HDP endowed with antibacterial and immunomodulatory activities in human ApoE [4].

Further, this method has been applied to the human Apolipoprotein B (ApoB) isoform, and two putative cryptic HDP have been predicted and named ApoBS and ApoBL. The sequence of peptide ApoBL is PHVALKPGKLKFIIPSPKRPVKLLSGGNTLHLVSTTKT, while that of peptide ApoBS is PHVALKPGKLKFIIPSPKRPVKLLSG. To evaluate the therapeutic potential of these peptides, we analysed their structure, antimicrobial and anti-biofilm activities, the ability to act in synergy with conventional antibiotics, their anti-inflammatory and wound healing properties, and their possible toxic effects on eukaryotic cells.

3.2 Results

3.2.1 Antimicrobial activity of $ApoB_L$ and $ApoB_S$ peptides

The antibacterial activity of ApoB derived peptides was determined by measuring their MIC_{100} values on a panel of Gram-negative and Gram-positive bacterial strains (**Table 1**). A significant antimicrobial activity of $ApoB_L$ and $ApoB_S$ peptides was detected towards four out of eight strains tested, *i.e. E. coli* ATCC 25922, *P. aeruginosa* PAO1, *B. globigii* TNO BM013, and *B. licheniformis* 21424, for which almost identical MIC_{100} values were calculated for both ApoB derived peptides. Notably, MIC_{100} values were found to be identical, or even significantly lower than those determined when cathelidin-2 (CATH-2) peptide, a known HDP from chicken [5], was tested as a positive control on the above mentioned strains.

Hence, it can be concluded that $ApoB_L$ and $ApoB_S$ peptides are endowed with a broad-range antimicrobial activity, being effective on both Gram-negative and Gram-positive bacterial strains. On the other hand, ApoB derived peptides were found to be ineffective towards *P. aeruginosa* ATCC 27853, methicillin-resistant *S. aureus* (MRSA WKZ-2), and *S. aureus* 29213, while, in the case of *S. enteriditis* 706 RIVM, a significant antibacterial effect was exerted only by $ApoB_L$ peptide.

GRAM POSITIVE STRAINS	MIC_{100} (μM)			GRAM NEGATIVE STRAINS	MIC_{100} (μM)		
	Apo BL	Apo BS	CATH-2		Apo BL	Apo BS	CATH-2
Staphylococcus aureus MRSA WKZ-2	>40	>40	10	*Escherichia coli* ATCC 25922	10	10	10
Bacillus globigii TNO BM013	5	2,5	5	*Pseudomonas aeruginosa* ATCC 27853	>40	>40	10
Bacillus licheniformis ATCC 21424	1,25	1,25	20	*Pseudomonas aeruginosa* PAO1	20	20	20
Staphylococcus aureus ATCC29213	>40	>40	10	*Salmonella enteriditis* 706 RIVM	10	>40	10

Table 1. Minimum Inhibitory Concentration (MIC, μM) values determined for $ApoB_L$ and $ApoB_S$ peptides tested on a panel of Gram-positive and Gram-negative bacterial strains. Chicken CATH-2 peptide was used as a positive control. Values were obtained from a minimum of three independent experiments.

3.2.2 Combination therapy analyses

To potentiate the antimicrobial efficacy of ApoB derived peptides for therapeutic purposes, especially against *P. aeruginosa* and *S. aureus* strains, we carried out combination therapy analyses by concomitantly administrating peptides and antibiotics in different combinations to bacteria. One of the best known test to evaluate synergism between two compounds is the so called “chequerboard” experiment in which a two-dimensional array of serial concentrations of test compounds is used as the basis for calculation of a fractional inhibitory concentration (FIC) index

to demonstrate that paired combinations of agents can exert inhibitory effects that are more than the sum of their effects alone. It is generally accepted that FIC indexes ≤ 0.5 are indicative of "synergy"; FIC indexes comprised between > 0.5 and – 4.0 are, instead, associated to "additive" or "no interaction" effects, whereas FIC indexes > 4.0 are indicative of "antagonism" [6].

As reported in **Table 2**, all the combinations tested were found to be effective, either with additive or synergistic effects between peptides and antibiotics. Notably, no FIC indexes higher than 2 were measured. The most potent combinations were obtained in the presence of EDTA, which was selected for its ability to affect bacterial outer membrane permeability, thus sensitizing bacteria to a number of antibiotics [7]. Very pronounced synergistic effects were observed for both ApoB derived peptides in combination with EDTA on *S. aureus* MRSA WKZ-2 and both *P. aeuroginosa* strains. We also found that both $ApoB_L$ and $ApoB_S$ showed synergism with the systemic antibiotic ciprofloxacin against all the strains tested. Similarly, we observed synergistic effects between both ApoB derived peptides and colistin against all the strains tested, except for *S. aureus* ATTC 29213. Synergistic effects were also observed in combination with vancomycin against *S. aureus* MRSA WKZ-2, *P. aeruginosa* strains and *E. coli* ATTC 25922. In the presence of erythromycin, synergistic effects were observed only against *P. aeruginosa* ATCC 27853, with a FIC index of 0.38 and 0.17 for $ApoB_L$ and $ApoB_S$ peptides, respectively.

In the case of kanamycin, a different response was obtained depending on the peptide and the specific bacterial strain. In fact, $ApoB_L$ was found to act synergistically with this antibiotic prevalently on Gram-negative bacteria, particularly on the *P. aeruginosa* strains. $ApoB_S$ peptide, instead, was found to be very active against both *S. aureus* strains as well as against *P. aeruginosa* PAO1 strain (FIC indexes < 0.4).

It should be emphasized that combinations of ApoB derived peptides with antibiotics and EDTA were found to have a strong antimicrobial activity also towards strains on which the peptides alone were found to be ineffective, such as both *S. aureus* strains and *P. aeruginosa* ATCC 27853 (**Table 2**). Notably, we did not observe any antagonistic interactions between the peptides and the antimicrobials under test.

Bacterial strains	Antibiotic	$ApoB_L$	$ApoB_S$
Methicillin resistant *S. aureus MRSA WKZ-2*	Ciprofloxacin	0,328	0,365
	Colistin	0,340	0,350
	Erythromycin	1,094	1,375
	Vancomycin	0,425	0,316
	Kanamycin	2,000	0,387
	EDTA	0,278	0,360
***S. aureus* ATTC 29213**	Ciprofloxacin	0,340	0,413
	Colistin	1,049	1,024
	Erythromycin	1,049	1,146
	Vancomycin	1,049	1,097
	Kanamycin	1,049	0,352
	EDTA	1,049	0,351
***P. aeruginosa* ATCC 27853**	Ciprofloxacin	0,347	0,328
	Colistin	0,267	0,255
	Erythromycin	0,389	0,170
	Vancomycin	0,379	0,306
	Kanamycin	0,479	1,030
	EDTA	0,333	0,089
***P. aeruginosa* PAO1**	Ciprofloxacin	0,396	0,444
	Colistin	0,144	0,266
	Erythromycin	0,569	0,556
	Vancomycin	0,500	0,486
	Kanamycin	0,507	0,389
	EDTA	0,396	0,438
***E. coli* ATCC 25922**	Ciprofloxacin	0,363	0,442
	Colistin	0,438	0,292
	Erythromycin	1,243	1,292
	Vancomycin	0,428	0,426
	Kanamycin	0,603	0,572
	EDTA	0,729	0,750

Table 2. Fractional inhibitory concentration (FIC) indexes determined for $ApoB_L$ and $ApoB_S$ peptides tested in combination with antibiotics or EDTA on Gram-positive and Gram-negative bacterial strains. Indexes were obtained from a minimum of three independent experiments, each one carried out with triplicate determinations.

3.2.3 Anti-biofilm activity of $ApoB_L$ and $ApoB_S$ peptides

Anti-biofilm peptides represent a very promising approach to treat biofilm-related infections and have an extraordinary ability to interfere with various stages of the biofilm growth mode [8]. To test whether ApoB derived peptides are endowed with anti-biofilm activity, we performed experiments on different bacterial strains, such as *E. coli* ATCC 25922, *Pseudomonas aeruginosa* PAO1, *Pseudomonas aeruginosa* ATCC 27853, and methicillin-resistant *Staphylococcus aureus* MRSA WKZ-2 in BM2 medium. As a control, the same experiments were performed using CATH-2 and LL-37 peptides. LL-37 is a human HDP known to have a significant anti-biofilm activity against multidrug-resistant bacterial strains [9].

At first, we evaluated the peptide effects on biofilm attachment. To do this, the bacterial culture, following over-night growth, was diluted in BM2 medium containing increasing concentrations of the peptide under test (0-1 μM), and incubated for 4 h at 37 ˚C. Following incubation, biofilm analysis by crystal violet staining revealed a significant dose-dependent inhibition of biofilm attachment in the case of *E. coli* ATCC 25922 (**Fig. 1a**) and *S. aureus* MRSA WKZ-2 (**Fig. 1d**) strains treated with $ApoB_L$ (continuous line in **Fig. 1a, d**) or $ApoB_S$ (smaller dashed line in **Fig. 1a, d**) peptides. Similar results were obtained on these two strains in the case of control peptides, such as CATH-2 (larger dashed line in **Fig. 1a, d**) and LL-37 (dotted line in **Fig. 1a, d**). Strong effects were also exerted by ApoB derived peptides on biofilm attachment in the case of *P. aeruginosa* PAO1 strain. A less pronounced effect of ApoB derived peptides (about 20% inhibition) was observed, instead, on *P. aeruginosa* ATCC 27853 biofilm attachment.

We also demonstrated that ApoB derived peptides have a strong effect on biofilm formation. To investigate this phenomenon, we followed the experimental procedure described above with the only exception that bacterial cells were incubated with increasing concentrations of peptides for 24 h at 37 °C. Also in this case, we observed a significant dose-dependent inhibition of biofilm formation in the case of *E. coli* ATCC 25922 (**Fig. 1b**) and *S. aureus* MRSA WKZ-2 (**Fig. 1e**) strains treated with $ApoB_L$ (continuous line in **Fig. 1b, e**) or $ApoB_S$ (smaller dashed line in **Fig. 1b, e**) peptides. Similar effects on biofilm formation were also obtained in the case of control peptides CATH-2 (larger dashed line in **Fig. 1b, e**) and LL-37 (dotted line in **Fig. 1b, e**). ApoB derived peptides strongly affected also *P. aeruginosa* PAO1biofilm formation. In the case of *P. aeruginosa* ATCC 27853, instead, a less pronounced effect (about 20% biofilm formation inhibition) was observed for all the peptides under test.

Even more interestingly, ApoB derived peptides were also found to strongly affect the preformed biofilm. In fact, by incubating *E. coli* ATCC 25922 (**Fig. 1c**) and *S. aureus* MRSA WKZ-2 (**Fig. 1f**) strains preformed biofilm with increasing concentrations of $ApoB_L$ (continuous line in **Fig. 1c, f**) or $ApoB_S$ (smaller dashed line in **Fig. 1c, f**) peptide, we found a significant inhibition (about 50%), even stronger than that observed in the case of CATH-2 control peptide (larger dashed line in **Fig. 1c, f**). Similar results were also observed in the case of *P. aeruginosa* PAO1 strain. When peptides were tested, instead, on *P. aeruginosa* ATCC 27853 preformed biofilm, a slight effect (about 20% inhibition) was observed for all the peptides except for CATH-2, which was found to exert a strong effect (about 50% inhibition,). We also evaluated the percentage of viable bacterial cells inside the biofilm structure by colony counting assay. We found that, even at the highest ApoB derived peptides concentrations tested, a significant portion of bacterial cells appeared to be still alive (continuous and smaller dashed lines in **Fig. 2 and Table 3**). Similar results were also observed in the case of LL-37 control peptide (dotted lines in **Fig. 2**). In the case of CATH-2 peptide, instead, a strong effect on cell viability was observed in the case of *E. coli* ATCC 25922 and *S. aureus* MRSA WKZ-2 strains (larger dashed lines in **Fig. 2**).

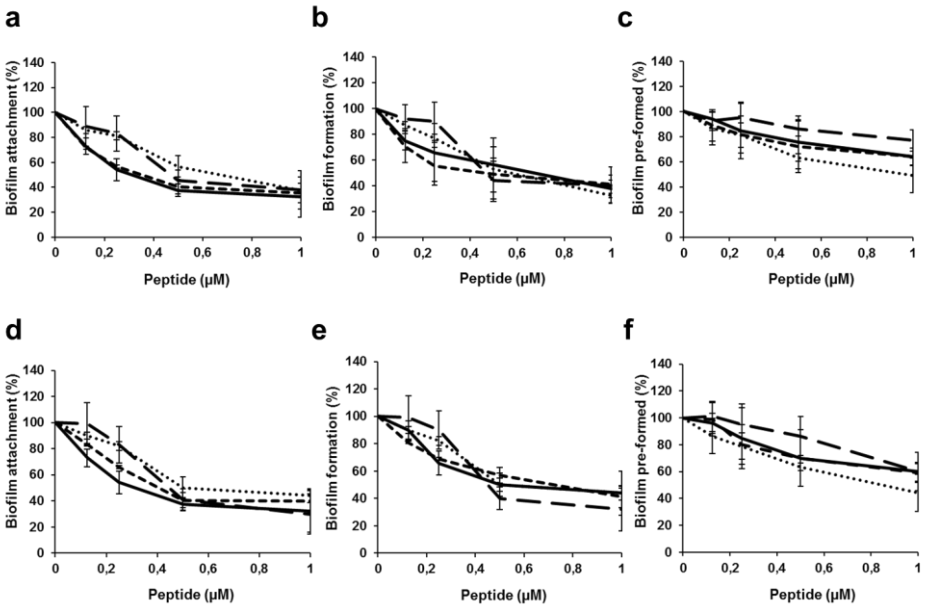

Figure 1. Anti-biofilm activity of $ApoB_L$ (–), $ApoB_S$ (- - -), CATH-2 (– – –), and LL-37 (•••) peptides on *E. coli* ATCC 25922 (**a, b, c**) and *S. aureus* MRSA WKZ-2 (**d, e, f**) strains in BM2 medium. The effects of increasing concentrations of peptides were evaluated either on biofilm attachment (**a, d**), biofilm formation (**b, e**), or on pre-formed (**c, f**) biofilm. Biofilm was stained with crystal violet and measured at 630 nm. Data represent the mean (± standard deviation, SD) of at least three independent experiments, each one carried out with triplicate determinations.

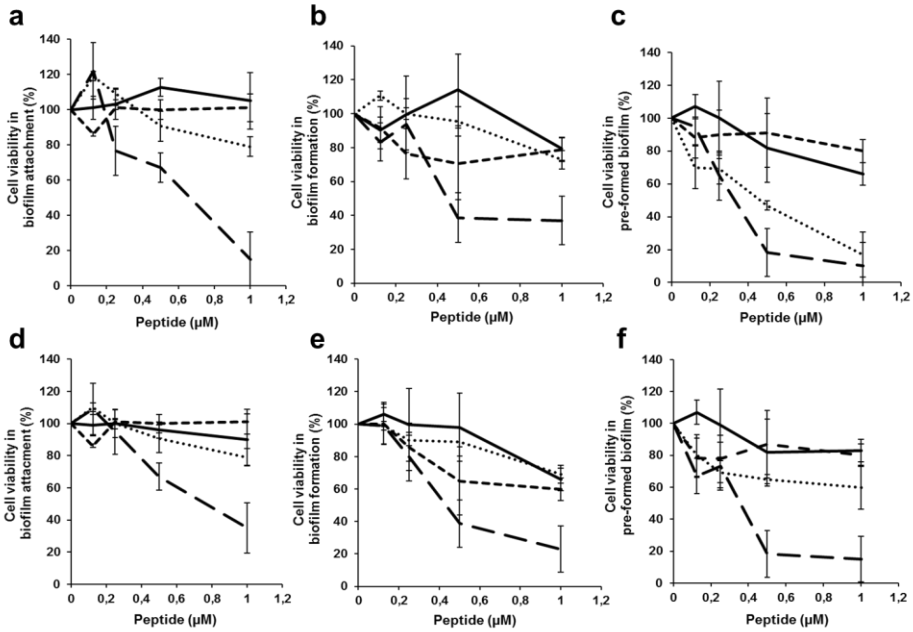

Figure 2. Effects of increasing concentrations of $ApoB_L$ (–), $ApoB_S$ (- - -), CATH-2 (– – –), and LL-37 (•••) peptides on the viability of *E. coli* ATCC 25922 (**a, b, c**) and *S. aureus* MRSA WKZ-2 (**d, e, f**) cells inside the biofilm structure. Cell viability was assessed by colony counting assay, and expressed as the percentage of viable bacterial cells in treated samples with respect to the control untreated sample. Data represent the mean (± standard deviation, SD) of at least three independent experiments, each one carried out with triplicate determinations.

	BIOFILM											
	Attachment (%)				Formation (%)				Eradication (%)			
	$ApoB_L$	$ApoB_S$	CATH-2	LL-37	$ApoB_L$	$ApoB_S$	CATH-2	LL-37	$ApoB_L$	$ApoB_S$	CATH-2	LL-37
Pseudomonas aeruginosa ATCC 27853	79±9	84±8	75±5	80±7	80±9	86±5	74±5	85±3	75±5	80±6	58±9	82±5
Pseudomonas aeruginosa PAO1	62±14	63±11	44±11	56±4	44±16	53±5	47±8	34±12	49±14	54±17	63±11	54±11
	CELL VIABILITY											
	In biofilm attachment (%)				In biofilm formation (%)				In biofilm eradication (%)			
	$ApoB_L$	$ApoB_S$	CATH-2	LL-37	$ApoB_L$	$ApoB_S$	CATH-2	LL-37	$ApoB_L$	$ApoB_S$	CATH-2	LL-37
Pseudomonas aeruginosa ATCC 27853	76±11	68±10	91±5	60±13	66±13	64±14	96±16	77±15	70±15	59±9	59±12	69±5
Pseudomonas aeruginosa PAO1	52±12	77±15	45±7	47±7	56±14	57±14	36±16	25±14	44±15	86±6	50±10	58±9

Table 3. Effect of $ApoB_L$, $ApoB_S$, CATH-2, and LL-37 peptides (1 μM) on biofilm attachment, formation, and eradication. To determine the percentage of viable bacterial cells inside the biofilm structure, biofilm was lysed with Triton X-100 (0,1%), bacterial cells were ten-fold diluted, and colonies were counted after an incubation of 16 h at 37 °C. Data are expressed as percentage with respect to control untreated samples, and represent the mean (± standard deviation, SD) of at least three independent experiments, each one carried out with triplicate determinations.

3.2.4 Biocompatibility of $ApoB_L$ and $ApoB_S$ peptides

The development of HDPs as therapeutic agents is strictly related to their selective toxicity towards bacterial cells [10]. The presence of zwitterionic phospholipids and cholesterol on the outer leaflet of eukaryotic cell membranes largely accounts for the preference of HDPs for bacterial membranes over eukaryotic membranes [11].

To deepen on the therapeutic potential of ApoB derived peptides, we analysed their cytotoxic effects towards a panel of mouse and human eukaryotic cells. The addition of increasing concentrations (from 0.625 to 20 μM) of ApoB derived peptides to mouse macrophages Raw 264.7 cells for 24 h did not result in any significant reduction in cell viability (**Fig. 3a and b**). A slight toxicity was detected only at the highest peptide concentrations tested (10 and 20 μM). Moreover, no significant toxic effects were detected when ApoB derived peptides were assayed on human cervical cancer HeLa cells (data not shown), while a slight toxicity (~20%) was observed in the case of human keratinocytes (HaCaT cells) at the highest peptide concentration tested (20 μM). ApoB derived peptides were also tested on murine red blood cells (RBCs) to exclude hemolytic affects. As shown in **Fig. 4**, both peptides did not exert any lytic effect on mouse RBCs, even at the highest concentration tested (20 μM). It should also be underlined that the antibacterial activity of ApoB derived peptides was detected at peptide concentrations comparable (**Table 1**) to those used in the cytotoxicity assays described above.

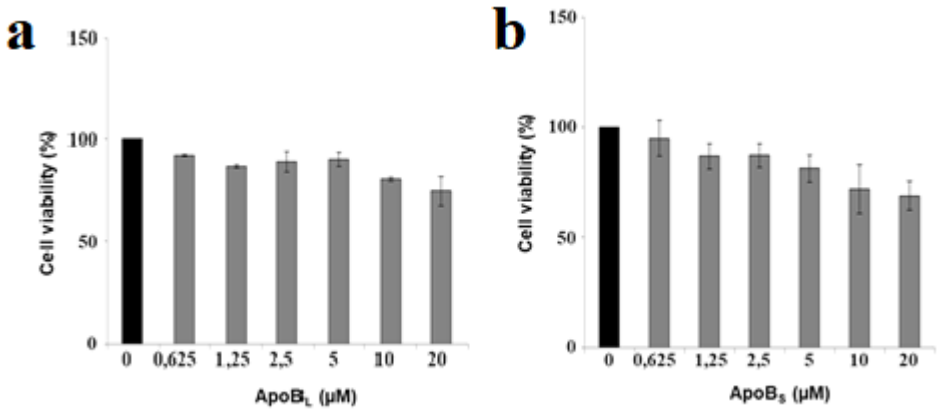

Figure 3. Effects of ApoB$_L$ (**a**) and ApoB$_S$ (**b**) peptides on the viability of RAW 264.7 cells. Cell viability was assessed by WST-1 assay, and expressed as the percentage of viable cells with respect to controls (untreated cells). Error bars indicate standard deviations obtained from at least three independent experiments, each one carried out with triplicate determinations.

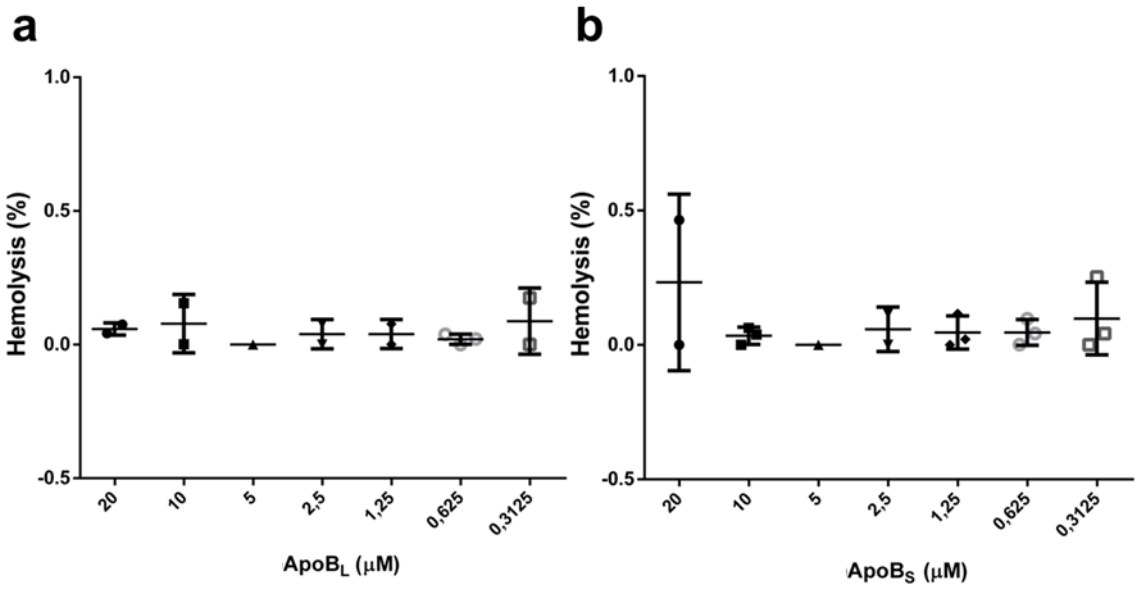

Figure 4. Hemolytic activity of ApoB$_L$ (**a**) and ApoB$_S$ (**b**) peptides towards murine red blood cells (RBCs) after 1 h of incubation at 37 °C. Data represent the mean (± standard deviation, SD) of at least three independent experiments, each one carried out with triplicate determinations.

3.2.5 Analysis of the immunomodulatory activity of ApoB$_L$ and ApoB$_S$ peptides

Since it is widely reported that HDPs are able to mitigate the pro-inflammatory effects induced by endotoxins [12], such as LPS, we tested the anti-inflammatory properties of ApoB derived peptides by monitoring their effects on LPS induced interleukin-6 (IL-6), as well as on nitric oxide (NO) release in murine macrophages (RAW 264.7 cell line). In fact, it is known that, upon activation by internal and external stimuli, macrophages produce and secrete various

endogenous inflammatory mediators, such as nitric oxide (NO) and pro-inflammatory cytokines, including interleukin-6 [13]. An excess of NO, produced by inducible nitric oxide synthase (iNOS) during inflammation, activates the synthesis of inflammatory mediators, which can in turn cause tissue damage, genetic mutations, and nerve injury [14].

To test the effects of ApoB derived peptides on the release of IL-6, ELISA assays were performed on LPS stimulated RAW 264.7 cells. As shown in **Fig. 5a and b**, a significant release of IL-6 was observed in control cells incubated with LPS from *Salmonella Minnesota* (50 ng/mL). When murine macrophages were incubated with LPS (50 ng/mL) in the presence of either $ApoB_L$ (**Fig. 5a**) or $ApoB_S$ **(Fig. 5b**) peptides, at 5 and 20 μM peptide concentration, a strong decrease of IL-6 release was observed with respect to control cells stimulated with LPS in the absence of peptides. Moreover, we found that peptides have a significant protective effect on LPS stimulated RAW 264.7 cells. In fact, when macrophages were pre-treated for 2 h with either $ApoB_L$ or $ApoB_S$ peptide and then incubated for further 24 h with LPS, a significant decrease of IL-6 release was observed (**Fig. 5a and b**). Similar results were observed when the effects of peptides were tested on NO release (**Fig. 5c and d**). Also in this case, following co-incubation of cells with LPS from *Salmonella Minnesota* and either $ApoB_L$ or $ApoB_S$ peptide, a significant attenuation of NO release with respect to control cells was detected (**Fig. 5c and d**). However, in this case, it has to be noticed that a significant effect of peptides on NO release was observed only at the highest peptide concentration tested (20 μM), while at 5 μM concentration both peptides were found to be almost ineffective (**Fig. 5c and d**). However, when RAW 264.7 cells were pre-treated for two h with 5 or 20 μM of $ApoB_L$ or $ApoB_S$ peptides and subsequently stimulated for 24 h with LPS (50 ng/mL), a significant reduction of NO release was observed even at 5 μM peptide concentration (**Fig. 5c and d**), thus confirming a significant protective effect of both peptides on LPS stimulated RAW 264.7 cells.

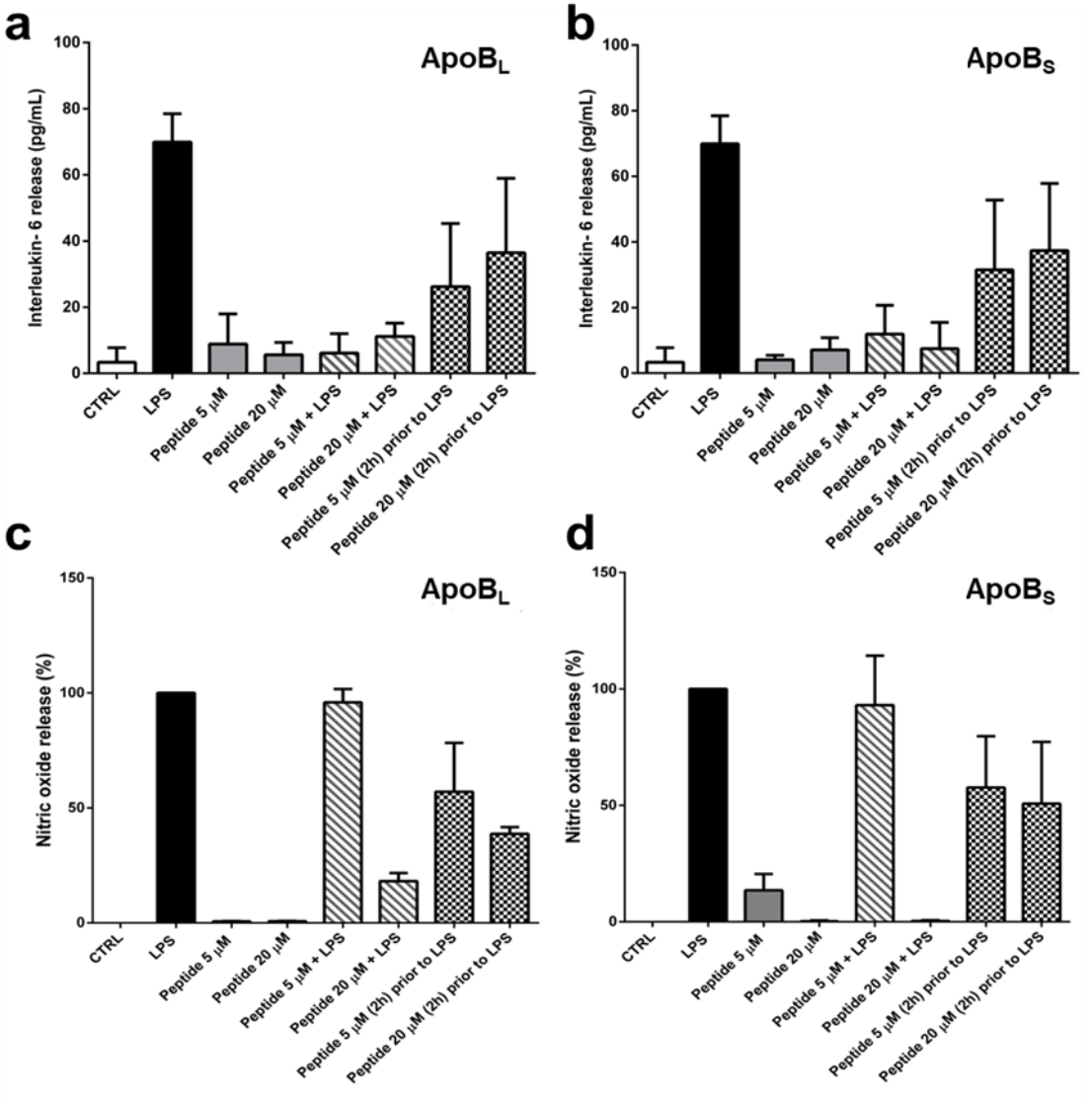

Figure 5. Effects of ApoB derived peptides on the release of IL-6 (**a, b**) and NO (**c, d**) in mouse macrophages RAW 264.7 stimulated with LPS (50 ng/mL) from *Salmonella Minnesota*. The effects of $ApoB_L$ (**a, c**) and $ApoB_S$ (**b, d**) peptides were evaluated either co-incubating cells with peptides (5 or 20 μM) and LPS (oblique grey lanes) or by treating cells with peptides (5 or 20 μM) for 2 h at 37 °C prior to incubation with LPS (chessboard bars). Results were compared to those obtained in the case of control untreated cells (white bars), cells stimulated with the LPS alone (black bars), or cells incubated with two different concentrations (5 or 20 μM) of peptide (grey bars). Data represent the mean (± standard deviation, SD) of at least three independent experiments, each one carried out with triplicate determinations.

3.2.6 Wound healing activity of $ApoB_L$ peptide

Numerous studies support the hypothesis that human HDPs promote wound healing in skin, by modulating cytokine production, cell migration, proliferation and, in some cases, angiogenesis [15]. Based on this, we performed experiments to evaluate if $ApoB_L$ peptide is able to stimulate "wound" re-epithelialization by human keratinocytes (HaCaT cell line). To this purpose, we performed a classical wound healing assay to evaluate peptide effects on cell migration. Hence,

HaCaT cell monolayers were pre-treated with 3 μM mitomycin C for 30 minutes, in order to inhibit cell proliferation, and then wounded with a pipette tip to remove cells from a specific region of the monolayer. Cells were then washed with PBS and incubated with increasing concentrations of $ApoB_L$ (0.5, 10, and 20 μM). It is well known that the spreading of cells in the wound area is due to two mechanisms, *i.e.* cell motility and cell proliferation [16]. Pre-treatment with mitomycin C allowed us to exclude any influence of cell proliferation on the wound healing process. In **Fig. 6a**, we reported the images acquired during a wound healing experiment for control cells, and cells treated with 20 μM $ApoB_L$ peptide at three time points, *i.e.* t=0 h, t=3 h after the lag time (tL), and t=5 h the after tL. By comparing the images obtained for each time point, the cells treated with 20 μM peptide appear to close the wound faster than the control cells.

In order to quantify the wound closure, we used an automated image analysis software, that allowed us to measure the size of the cell-free area (A) for each time point. Obtained values were normalized with respect to the value measured at time 0 (A_0) for each field of view, and plotted as a function of time (**Fig. 6b**). In Fig. **6a**, A/A_0 values were found to be 0.20, and 0.07 for the control sample, and for the cells treated with 20 μM peptide, respectively, at t=5 h after t_L. This evidence further confirms the ability of 20 μM $ApoB_L$ peptide to significantly stimulate wound re-epithelialization by human keratinocytes. As an example, we reported in **Fig. 6b** A/A_0 values, obtained in the case of a control sample, as a function of time. It emerges that, after an initial lag phase, the wound area decreases with a constant velocity. The initial lag phase, corresponding to a transient time period (t_L) before the linear decrease of the wound area, has been observed for all the analysed samples, and has been found to range between 3 and 5 h independently from peptide concentrations under test (**Fig. 6c**).

Following the lag phase, A/A_0 values were always found to linearly decrease over time. The slope (α) of the line represents the measure of the "wound" closure velocity. For each sample, this value (α) was normalized with respect to the value obtained in the case of the control sample (α_{contr}), and plotted as a function of peptide concentration (**Fig. 6d**). It appears that the cells treated with the peptide are characterized by an increase in the "wound" closure velocity with respect to the control cells ($\alpha/\alpha_{contr}>1$).

Overall, our results indicate that $ApoB_L$ peptide is able to promote the migration and the consequent wound healing in HaCaT keratinocyte monolayers when tested at concentration values ranging between 0.5 and 20 μM.

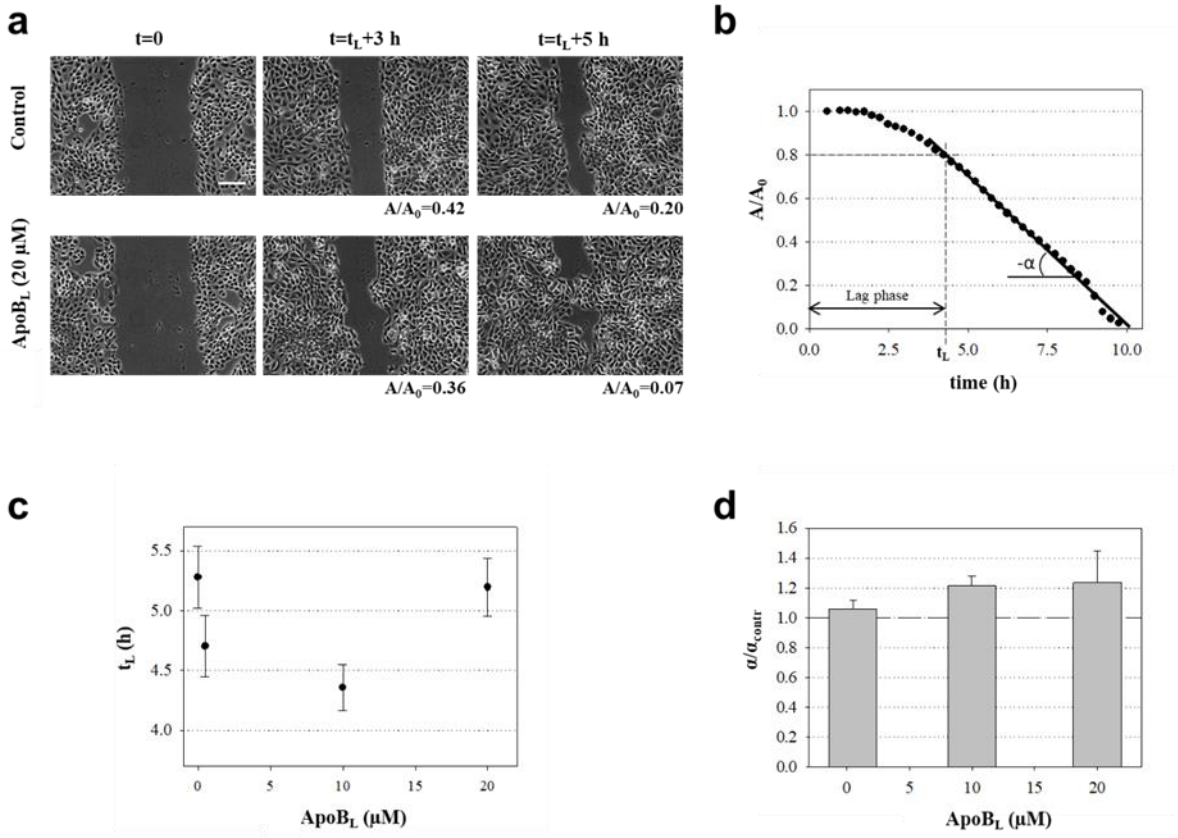

Figure 6: Wound healing activity of $ApoB_L$ peptide on HaCaT cells monolayer. Cells were pre-treated for 30 min with 3 µM mitomycin C, and then wounded prior to incubation with $ApoB_L$ peptide (10 – 20 µM) for 12 h at 37 °C. Images were acquired for untreated HaCaT cells and for cells treated with 20 µM peptide (**a**). The lag phase time (t_L) corresponds to the time interval before the linear decrease of the wound area. Images were acquired at time t=0 (**a, on the left**), 3 h after t_L (**a, in the middle**) and 5 h after t_L (**a, on the right**). For each sample, A/A_0 values are reported, where A is the wound area after a specific incubation time and A_0 is the wound area at time 0. Scale bar = 150 µm. In **b**, evolution in time of the wound area (A), normalized with respect to A_0, is reported for a control sample. A homemade automated image analysis software was used to measure the size of the cell-free area (A) for each time point. For A/A_0 values <0.8, a linear correlation with the incubation time was found. The slope -α of the linear fit, reported as a continuous line, represents a measure of the wound closure velocity. In **c**, determined t_L values are reported as a function of peptide concentration (0.5 - 10 - 20 µM). In d, wound closure velocity (α), normalized with respect to control sample (α_{contr}), is reported as a function of peptide concentration (0.5 - 10 - 20 µM). The dashed line corresponds to α/α_{contr} =1. In **c** and **d**, each data point represents the mean (± standard error) of three independent experiments.

3.3 Conclusions

Here, we focused our attention on the two identified ApoB derived HDPs, here named $ApoB_L$ and $ApoB_S$, 38- and 26-residue long, respectively. Both peptides were found to exhibit antibacterial activities against both Gram-positive and Gram-negative strains, including the pathogenic strains *P. aeruginosa* PAO1 and *B. globigii* TNO BM013, while having negligible cytotoxic effects on a panel of human and murine cell lines. It has to be underlined that ApoB derived peptides were found to be ineffective towards *P. aeruginosa* ATCC 27853, methicillin-resistant *S. aureus* (MRSA WKZ-2), and *S. aureus* ATTC 29213 strains, while, in the case of *S. enteriditis* 706 RIVM strain, a significant antibacterial effect was exerted only by $ApoB_L$ peptide. This observation is in agreement with previous findings indicating that most natural cationic HDPs do not appear to be highly optimized for direct antimicrobial activity, since it is likely that multiple modestly active peptides with concomitant immunomodulatory activities work effectively in combination and/or when induced or delivered to sites of infection [17].

Indeed, considering this, we performed combination therapy analyses and found that both ApoB derived peptides are able to synergistically act with either commonly used antibiotics or EDTA, which was selected for its ability to affect bacterial outer membrane permeability, thus sensitizing bacteria to a number of antibiotics [18]. Intriguingly, this application allows the reduction of therapeutic doses with a consequent mitigation of toxic effects, and possibility to target a broad spectrum of pathogens. In addition, certain combination therapies have prevented the development of drug-resistance in bacteria. A membranolytic action of HDP is expected to produce synergetic effects when administered in combination with conventional antibiotics, and several studies have reported such findings. Cirioni et al. [19] compared the synergies of magainin II and cecropin A administered with or without rifampicin against MDR *Pseudomonas aeruginosa* strains both in vivo and in vitro and found significant reductions in bacterial multiplication, LPS and TNF-α secretion in plasma and mortality. This finding suggested that the membrane-permeabilizing activity of peptides allows rifampicin to gain access to its intracellular target.

In this work, when combined with conventional antibiotics or EDTA, both ApoB derived peptides showed synergist activity towards most of the strains under test, including methicillin-resistant *S. aureus* MRSA WKZ-2 on which peptides alone were found to be ineffective even at high concentrations (40 μM). Interestingly, both $ApoB_L$ and $ApoB_S$ peptides showed synergism with systemic antibiotic ciprofloxacin against all the strains under test (FIC indexes ranging from 0.3 to 0.44). ApoB derived peptides also showed synergistic effects with colistin against all the strains under test, except for *S. aureus* ATTC 29213, and with vancomycin against *S. aureus* MRSA WKZ-2, both *P. aeruginosa* strains and *E. coli* ATTC 25922 (FIC indexes ranging from 0.14 to 0.5). Since both colistin and vancomycin are responsible for toxic effects at high concentrations [20], the possibility to use combination therapeutic approaches based on a reduced frequency of antibiotic administration and/or exposure to antibiotic may offer several advantages over conventional dosing schemes, as adverse side effects might be reduced.

However, the most potent synergism was observed for both ApoB derived peptides in combination with EDTA, with FIC indexes ranging from 0.089 to 0.4. It should be highlighted that, although in some cases FIC indexes very close to 0.5 make difficult to discriminate between synergistic and additive effects, no antagonistic interactions were observed between the peptides and the antimicrobials under test. Furthermore, combinations of ApoB derived peptides with

antibiotics and EDTA were found to have a strong antimicrobial activity also towards strains on which the peptides alone were found to be ineffective, such as both *S. aureus* strains and *P. aeruginosa* ATCC 27853, indicating that in drug combinations a reciprocal facilitation and potentiation of different mechanisms of action is realized.

Interestingly, ApoB derived peptides are also endowed with anti-biofilm activity. Microorganisms growing in a biofilm state are very resilient to the treatment by many antimicrobial agents. Indeed, biofilm infections are a significant problem in chronic and long-term infections, including those colonizing medical devices and implants [21]. Specific cationic HDPs have recently been described to possess multispecies anti-biofilm activity, which is independent of their activity against planktonic bacteria. ApoB derived peptides were found to be effective on biofilm formation, biofilm attachment, and were also found to strongly affect pre-formed biofilm. Interestingly, ApoB derived peptides anti-biofilm activity was detected even on bacterial strains not sensitive to peptide direct antimicrobial activity, such as *S. aureus* MRSA WKZ-2.

Moreover, it has to be highlighted that both $ApoB_L$ and $ApoB_S$ peptides were found exert immunomodulatory activities by significantly decreasing the release of pro-inflammatory IL-6 and NO in murine RAW 264.7 macrophages under LPS stimulation. Both ApoB derived peptides were found to efficiently act either when the cells were co-incubated with the peptide under test in the presence of LPS or when the cells were pre-treated with the peptide for 2 h and then incubated with LPS for further 24 h, thus indicating that both peptides were able to exert significant protective effects. However, it has to be noticed that, differently from $ApoB_L$ peptide, $ApoB_S$ was found to play anti-inflammatory activities, when co-incubated with LPS, only at the highest peptide concentration tested (20 μM), whereas both $ApoB_S$ concentrations under test (5 and 20 μM) were found to efficiently exert a protective effect. This might be due to the fact that ApoB derived peptides probably exert their immunomodulatory activity through different mechanisms, with $ApoB_L$ peptide mainly acting by binding to LPS and consequently interfering with its activity on target cells, and $ApoB_S$ peptide mainly acting on cell membrane and competing with LPS for the binding to specific cell sites. All these observations associated to their multifunctional properties open interesting perspectives to their therapeutic applications.

3.4 Experimental procedures

3.4.1. Bacterial strains and growth conditions

Eight bacterial strains were used in the present study, *i.e. E. coli* ATCC 25922, methicillin-resistant *Staphylococcus aureus* (MRSA WKZ-2), *Salmonella enteriditis* 706 RIVM, *Bacillus globigii* TNO BM013, *Bacillus licheniformis* ATTC 21424, *Staphylococcus aureus* ATTC 29213, *Pseudomonas aeruginosa* ATCC 27853, and *Pseudomonas aeruginosa* PAO1. All bacterial strains were grown in Muller Hinton Broth (MHB, Becton Dickinson Difco, Franklin Lakes, NJ) and on Tryptic Soy Agar (TSA; Oxoid Ltd., Hampshire, UK). In all the experiments, bacteria were inoculated and grown overnight in MHB at 37 °C. The next day, bacteria were transferred to a fresh MHB tube and grown to mid-logarithmic phase.

3.4.2. Synthetic peptides

CATH-2 peptide was obtained from CPC Scientific Inc. (Sunnyvale, USA), and LL-37 peptide was from Sigma Aldrich, Milan, Italy.

3.4.3. Measurement of IL-6 release

IL-6 levels were determined by ELISA assay (DuoSet ELISA kits, R&D Systems, Minneapolis, MN) following the manufacturer's instructions. Briefly, RAW 264.7 cells (5×10^4) were seeded into 96-well microtiter plates, and grown to semi-confluency. After 24 h, the culture medium was replaced with fresh medium containing the peptides under test (5 or 20 μM) in the presence or in the absence of LPS from *Salmonella Minnesota* (50 ng/mL, Sigma Aldrich, Milan, Italy) for 24 h at 37 °C. When the protective effect of peptides was evaluated, cells were pre-incubated with the peptides under test (5 or 20 μM) for 2 h at 37 °C. Following treatment, cells were washed three times with PBS prior to incubation with LPS (50 ng/mL) for further 24 h at 37 °C. In each case, at the end of incubation, the culture supernatants were collected, and centrifuged at 5,000 rpm for 3 min at room temperature, in order to remove cell debris. Samples were then analysed by reading absorbance values at 450 nm using 550 nm as a reference wavelength at an automatic plate reader (FLUOstar Omega, BMG LABTECH, Ortenberg, Germany).

3.4.4. Determination of NO production

To determine the levels of NO released by RAW 264.7 cells, a colorimetric assay based on the use of Griess reagent (Sigma Aldrich, Milan, Italy) was performed. The levels of nitrite (NO^{2-}) in cell supernatants were determined on the basis of a reference curve obtained by testing increasing amounts (from 1 to 50 μM) of sodium nitrite dissolved in water. Briefly, cell culture supernatants were mixed with equal volumes of 1% sulphanilamide dissolved in 2.5% phosphoric acid, and incubated for 5 min at room temperature. Samples were then diluted 1:1 (v/v) with 0.1% N-(1-naphthyl) ethylenediamine dihydrochloride, and incubated for further 5 min at room temperature. Absorbance values were then determined at 520 nm using an automatic plate reader (FLUOstar Omega, BMG LABTECH, Ortenberg, Germany).

3.4.5. Antimicrobial activity assay

The antimicrobial activity of ApoB derived peptides was tested towards eight bacterial strains, *i.e. E. coli* ATCC 25922, methicillin-resistant *Staphylococcus aureus* (MRSA WKZ-2), *Salmonella enteriditis* 706 RIVM, *Bacillus globigii* TNO BM013, *Bacillus licheniformis* ATCC 21424, *Staphylococcus aureus* ATCC 29213, *Pseudomonas aeruginosa* ATCC 27853, and *Pseudomonas aeruginosa* PAO1. In each case, bacteria were grown to mid-logarithmic phase in MHB at 37 °C. Cells were then diluted to $2x10^6$ CFU/mL in Nutrient Broth (Difco, Becton Dickinson, Franklin Lakes, NJ) containing increasing amounts of either $ApoB_L$ or $ApoB_S$ peptide (0,6-40 μM). In order to add the same volume of peptide to each sample, starting from a peptide stock solution, two-fold serial dilutions were sequentially carried out, accordingly to broth microdilution method [22]. Following over-night incubation, MIC_{100} values were determined as the lowest peptide concentration responsible for no visible bacterial growth.

3.4.6. Synergy evaluation

Synergism between ApoB derived peptides and antimicrobial agents was assessed by the so called "checkerboard" assay against *S. aureus* MRSA WKZ-2, *E. coli* ATCC 25922, *P. aeruginosa* ATCC 27853, *P. aeruginosa* PAO1, and *S. aureus* ATCC 29213. To this purpose, ApoB derived peptides were tested in combination with EDTA or antibiotics, such as ciprofloxacin, colistin, erythromycin, kanamycin sulfate, and vancomycin. All these antimicrobial agents were from Sigma Aldrich, Milan, Italy. Two-fold serial dilutions of each ApoB derived peptide and each antimicrobial agent were tested in combination on each strain tested. To do this, we tested peptide concentrations ranging from 0 to 20 μM. In the case of antibiotics and EDTA, experiments were preliminarily performed to define for each compound the appropriate concentrations to use depending on the specific bacterial strain under test. Compound concentrations tested on each strain are reported in **Table 4**. The fractional inhibitory concentration (FIC) index was calculated as follows: $FIC_A + FIC_B$, where FIC_A = MIC of drug A in combination/MIC of drug A alone, and FIC_B = MIC of drug B in combination/MIC of drug B alone. FIC indexes ≤ 0.5 were classified as synergism, whereas FIC indexes between 0.5 and 4 were associated to additive or "no interaction" effects [23]. Antagonism is usually associated to a FIC index > 4.

	S. aureus ATCC 29213	*S. aureus* MRSA WKZ-2	*P. aeruginosa* ATCC 27853	*P. aeruginosa* PAO1	*E. coli* ATCC 25922
Ciprofloxacin	0-0,5 μg/mL	0-1 μg/mL	0-2 μg/mL	0-1 μg/mL	0-0,03 μg/mL
Colistin	0-8 μg/mL	0-8 μg/mL	0-4 μg/mL	0-4 μg/mL	0-8 μg/mL
Erythromycin	0-4 μg/mL	0-4 μg/mL	0-16 μg/mL	0-128 μg/mL	0-128 μg/mL
Vancomycin	0-0,25 μg/mL	0-0,5 μg/mL	0-32 μg/mL	0-4 μg/mL	0-0,25 μg/mL
Kanamycin	0-0,5 μg/mL	0-0,125 μg/mL	0-64 μg/mL	0-8 μg/mL	0-0,125 μg/mL
EDTA	0-24,53 μg/mL	0-49,07 μg/mL	0-392,5 μg/mL	0-196,2 μg/mL	0-98,14 μg/mL

Table 4. Range of antimicrobial agents concentrations tested for combination therapy analyses. Based on specific bacterial strain susceptibility, different concentrations of each compound were used in combination with ApoB derived peptides (0- 20 μM) to evaluate synergistic effects.

3.4.7. Anti-biofilm activity

Anti-biofilm activity of ApoB derived peptides was tested on *S. aureus* MRSA WKZ-2, *E. coli* ATCC 25922, *P. aeruginosa* ATCC 27853, and *P. aeruginosa* PAO1 strains. Bacteria were grown over-night in MHB (Becton Dickinson Difco, Franklin Lakes, NJ), and then diluted to 1×10^8 CFU/mL in BM2 medium [24] containing increasing peptide concentrations (0 - 1 μM). Incubations with the peptides under test were carried out either for 4 h, in order to test peptide effects on biofilm attachment, or for 24 h, in order to test peptide effects on biofilm formation. When peptide effects on preformed biofilm were evaluated, bacterial cells were incubated for 24 h at 37 ˚C, and then treated with increasing concentrations (0 - 1 μM) of the peptides under test. In all the cases, at the end of the incubation, the crystal violet assay was performed. Samples optical absorbance values were determined at 630 nm by using a microtiter plate reader (FLUOstar Omega, BMG LABTECH, Germany). To determine the percentage of viable bacterial cells inside the biofilm structure, upon biofilm disruption with 0,1% Triton X-100 (Sigma Aldrich, Milan, Italy), bacterial cells were ten-fold diluted on solid TSA and incubated for 16 h at 37 °C. Once evaluated the number of colony forming units, bacterial cell survival was calculated as follows: $(CFU_{\text{in treated sample}}/CFU_{\text{in untreated sample}}) \times 100$.

3.4.8. Cytotoxicity assays

Cytotoxic effects of ApoB derived peptides on RAW 264.7 cells were determined by using the cell proliferator reagent WST-1(Roche Applied Science, Mannheim, Germany). To this purpose, RAW 264.7 cells were plated into 96-well plates at a density of 5×10^4 cells in 100 μL medium per well, and incubated over-night at 37 °C. Afterwards, cells were treated with increasing concentrations (0 - 20 μM) of the peptides under test for 24 h at 37 °C. Following incubation, peptide-containing medium was removed, and 100 μL of fresh medium containing 10% WST-1 reagent was added to each well. Following an incubation of 30 min at 37 °C in the dark, sample absorbance values were measured at 450 nm using 650 nm as a reference wavelength at a microtiter plate reader (FLUOstar Omega, BMG LABTECH, Germany).

3.4.9. Haemolytic activity

The release of haemoglobin from mouse erythrocytes was used as a measure for the haemolytic activity of ApoB derived peptides. To do this, EDTA anti-coagulated mouse blood was centrifuged for 10 min at 800 x g at 20 °C, in order to obtain red blood cells (RBCs), which were washed three times, and 200-fold diluted in PBS. Subsequently, 75 μL aliquots of RBCs were added to 75 μL peptide solutions (final concentration ranging from 0 to 20 μM) in 96-well microtiter plates, and the mixture was incubated for 1 h at 37 ◦C. Following the incubation, the plate was centrifuged for 10 min at 1,300 × g at 20 °C, and 100 μL supernatant of each well were transferred to a new 96-well plate. Absorbance values were determined at 405 nm by using an automatic plate reader (FLUOstar Omega, BMG LABTECH, Germany), and the percentage of haemolysis was calculated by comparison with the control samples containing no peptide (negative control) or 0.2% (v/v) Triton X-100 (positive control, complete lysis). Haemolysis (%) =

[($Abs_{405\ nm}$ peptide − $Abs_{405\ nm}$ negative control)/($Abs_{405\ nm}$ 0,2% Triton − $Abs_{405\ nm}$ negative control)] × 100.

3.4.10. Wound healing assay

Wound heling activity of $ApoB_L$ peptide was evaluated as previously described [25]. Human HaCaT keratinocytes were seeded into 12-well plates at a density of 6.3 x 10^5 cells/well in 1 mL medium per well. Following an incubation of 24 h at 37°C, cells were pre-treated with 3 µM mitomycin C for 30 minutes, in order to inhibit cell proliferation [26]. Cell monolayers were then wounded with a pipette tip to remove cells from a specific region of the monolayer. The culture medium was then removed and the cells were washed twice with PBS. Cells were then incubated with fresh culture medium containing increasing concentrations of $ApoB_L$ peptide (0 – 0.5 – 10 – 20 µM). Wound closure was then followed by multiple field time-lapse microscopy (TLM) experiments, using an inverted microscope (Zeiss Axiovert 200, Carl Zeiss, Germany) equipped with an incubator to control temperature, humidity and CO_2 percentage. Images were iteratively acquired in phase contrast with a CCD video camera (Hamamatsu Orca AG, Japan) by using a 10x objective. The microscope was also equipped with a motorized stage and focus control (Marzhauser, Germany) enabling automated positioning of the acquired samples. The workstation was controlled through a homemade software in Labview. Each cell sample was analysed in duplicate, and in any case at least two fields of view were selected. Since three independents experiments were carried out, from 4 to 12 independent fields of view were analysed for each sample. The delay between consecutive imaging of the same field of view was set to 15 min. The wound closure dynamics were quantified by using a homemade automated image analysis software, that allowed to measure the size of the wound area for each time point (A). For each field of view, determined values were normalized respect to the value of the wound area at time 0 (A_0), and plotted as function of time. After an initial lag phase, the wound area was found to decrease with a constant velocity [27]. By reporting A/A_0 values as a function of time, a linear decrease was observed for A/A_0 values lower than 0.8. For each sample, the lag time t_L was calculated as the time required to obtain an initial wound closure corresponding to A/A_0=0.8. Being R^2 typically higher than 0.98, the linear range of the curve was fitted, and the slope (-α) was considered a measure of the wound closure velocity. The values of wound closure velocity obtained for each field of view from three independent experiments were averaged (α), and normalized with respect to the value of the corresponding control sample (α_{contr}). For each peptide concentration tested, α/α_{contr} values obtained from three independent experiments were averaged and the standard error of the mean was calculated to account for reproducibility.

References

1. B.A. Kelly, I. Anti-infective activity of apolipoprotein domain derived peptides in vitro: identification of novel antimicrobial peptides related to apolipoprotein B with anti-HIV activity. BMC Immunol. 11 (2010) 13
2. C. Pierides, A. Immune responses elicited by apoB-100-derived peptides in mice. Immunol Res. 56 (2013) 96-108.
3. Pane K. Antimicrobial potency of cationic antimicrobial peptides can be predicted from their amino acid composition: application to the detection of "cryptic" antimicrobial peptides. Theorical Biologydoi: http://dx.doi.org/10.1016/j.jtbi.2017.02.012 (2017).
4. K. Pane. A new cryptic cationic antimicrobial peptide from human apolipoprotein E with antibacterial activity and immunomodulatory effects on human cells. FEBS J. 283 2115-2131 (2016).
5. A. van Dijk, M.H. Tersteeg-Zijderveld, J.L. Tjeerdsma-van Bokhoven, A.J. Jansman, E.J. Veldhuizen, H.P. Haagsman. Chicken heterophils are recruited to the site of Salmonella infection and release antibacterial mature Cathelicidin-2 upon stimulation with LPS. Mol Immunol 46 (2009) 1517-1526.
6. F.C. Odds. Synergy, antagonism, and what the chequerboard puts between them. J Antimicrob Chemother. 52 (2003) 1.
7. M. Vaara. Agents that increase the permeability of the outer membrane. Microbiol Rev. 56 (1992) 395–411.
8. D. Pletzer, S. R. Coleman, R.E.W. Hancock. Anti-biofilm peptides as a new weapon in antimicrobial warfare. Curr Opin Microbiol 33 (2016) 35-40.
9. X. Feng, K. Sambanthamoorthy, T. Palys, C. Paranavitana. The human antimicrobial peptide LL-37 and its fragments possess both antimicrobial and antibiofilm activities against multidrug-resistant Acinetobacter baumannii. Peptides 49 (2013) 131-137.
10. D. Takahashi, S.K. Shukla, O. Prakash, G. Zhang. Structural determinants of host defense peptides for antimicrobial activity and target cell selectivity. Biochimie 92 (2010) 1236-1241.
11. K.A. Brogden. Antimicrobial peptides: pore formers or metabolic inhibitors in bacteria? Nat Rev Microbiol 3 (2005) 238–250.
12. Y.J. Seo, K.T. Lee, J.R. Rho, J.H. Choi. Phorbaketal A, isolated from the marine sponge phorbas sp., exerts its anti-inflammatory effects via NF-kappaB inhibition and heme oxygenase-1 activation in lipopolysaccharide-stimulated macrophages. Mar Drugs 13 (2015) 7005–7019.
13. Gosslau, S. Li, C.T. Ho, K.Y. Chen, N.E. Rawson. The importance of natural product characterization in studies of their anti-inflammatory activity. Mol Nutr Food Res 55 (2011) 74–82.
14. C. Nathan. Points of control in inflammation. Nature 420 (2002) 846–852.
15. M.L. Mangoni, A.M. McDermott, M. Zasloff. Antimicrobial peptides and wound healing: biological and therapeutic considerations. Exp Dermatol 25 (2016) 167-173.
16. A. Tremel, A. Cai, N. Tirtaatmadja, B.D. Hughes, G.W. Stevens, K.A. Landman, A.J. O'Connor. Cell migration and proliferation during monolayer formation and wound healing. Chemical Engineering Science 64 (2009) 247-25.

17. O.L. Franco. Peptide promiscuity: an evolutionary concept for plant defense. FEBS Lett. 585 (2011) 995–1000.
18. R.E. Hancock. Alterations in outer membrane permeability. Annu Rev Microbiol. 38 (1984) 237–264.
19. Cirioni, O.; Silvestri, C.; Ghiselli, R.; Orlando, F.; Riva, A.; Mocchegiani, F.; Chiodi, L.;Castelletti, S.; Gabrielli, E.; Saba, V.; et al. Protective effects of the combination of alpha-helical antimicrobial peptides and rifampicin in three rat models of Pseudomonas aeruginosa infection. J. Antimicrob. Chemother. 2008, 62, 1332–1338.
20. H.M. Nguyen, C.J. Graber. Limitations of antibiotic options for invasive infections caused by methicillin-resistant *Staphylococcus aureus*: is combination therapy the answer? J Antimicrob Chemother. 65 (2010) 24–36.
21. D. Pletzer, S. R. Coleman, R.E.W. Hancock. Anti-biofilm peptides as a new weapon in antimicrobial warfare. Curr Opin Microbiol 33 (2016) 35-40.
22. Wiegand, K. Hilpert, R.E. Hancock. Agar and broth dilution methods to determine the minimal inhibitory concentration (MIC) of antimicrobial substances. Nat Protoc. 3(2008) 163-175.
23. F.C. Odds. Synergy, antagonism, and what the chequerboard puts between them. J Antimicrob Chemother. 52 (2003) 1.
24. J. Li, T. Kleintschek, A. Rieder, Y. Cheng, T. Baumbach, U. Obst, T. Schwartz, P.A. Levkin. Hydrophobic liquid-infused porous polymer surfaces for antibacterial applications. ACS Appl Mater Interfaces. 5 (2013) 6704-6711.
25. C.C. Liang, A.Y. Park, J.L. Guan. In vitro scratch assay: a convenient and inexpensive method for analysis of cell migration in vitro. Nat Protoc. 2 (2007) 329-333.
26. A. Di Grazia, F. Cappiello, A. Imanishi, A. Mastrofrancesco, M. Picardo, R. Paus, M.L. Mangoni. The Frog Skin-Derived Antimicrobial Peptide Esculentin-1a(1-21)NH2 Promotes the Migration of Human HaCaT Keratinocytes in an EGF Receptor-Dependent Manner: A Novel Promoter of Human Skin Wound Healing? PLoS One. 10 (2015) e0128663.
27. A.Q. Cai, K.A. Landman, B.D. Hughes. Multi-scale modeling of a wound-healing cell migration assay. J Theor Biol 245 (2007) 576-594.

Chapter 4

Novel bioactive peptides from PD-L1/2, a type 1 ribosome inactivating protein from *Phytolacca dioica* L. Broad evaluation of their antimicrobial properties and antibiofilm activities

4.1 Introduction

Higher plants are sedentary and lack the adaptive immune system that many animals deploy when challenged by microbial pathogens. Nevertheless, plants are not defenseless, and have developed a variety of mechanisms to protect themselves against microbial attack.
These include the production of proteins, secondary metabolites and reactive oxygen species that can inhibit the growth of microbial pathogens, the establishment of structural barriers such as lignin and polysaccharides that prevent penetration and colonization, and hypersensitivity responses that result in programmed cell death and isolate invading pathogens from sources of nutrients. Plants represent an extremely abundant and largely unexplored source of HDPs. The recent development of powerful high-throughput genomic techniques has disclosed the presence of large numbers, often even several hundreds of HDP-like genes in various plant genomes [1] indicating the importance of HDPs in the eukaryotes and particularly in plants.
The innate immune system is a generic defense response of both animals and plants to fend off invading microbes. In plants, it does not show the same degree of specificity as the adaptive immunity of vertebrates that evolves a highly specific response after initial exposure to a challenge, but, as well as in animals, innate immunity is triggered after recognition of conserved microbe-associated molecular patterns (MAMPs) by pattern recognition receptors.
HDPs can occur in all plant organs. In unstressed organs, HDPs are usually most abundant in the outer cell layer lining the organ, which is consistent with a role for the HDPs in constitutive host defense against microbial invaders attacking from the outside.

To note, as abundantly demonstrated, HDPs have the potential for use as anti-biofilm agents due to their different mechanisms, which include membrane-disrupting action, functional inhibition of proteins, binding with DNA, and detoxification of polysaccharides (lipopolysaccharide and lipoteichoic acid) and inhibiting molecules involved in biofilm formation induced via *quorum sensing*. Biofilms provide a survival advantage over planktonic or free-floating bacteria by enhancing nutrient trapping and colonization. Currently, biofilms are a widespread problem in hospitals and healthcare facilities. Indeed, the United States National Institutes of Health found that 80% of chronic infections are related to biofilms. Moreover, many studies have found that biofilms are associated with dental plaque, endocarditis, lung infection, and infection through medical devices. Bacterial cells are embedded into a matrix of extracellular polymeric substance, which is composed of extracellular DNA, proteins, lipids, and polysaccharides with various configurations. These components are very important targets for overcoming both biofilms and drug-resistant bacteria.

Specific databases with increasingly accessible information [2, 3] indicate that a number of HDPs were identified in proteins, known as HDP releasing proteins, not necessarily playing host defence activities. These proteins would release biologically active peptides upon proteolytic cleavage by bacterial and/or host proteases [4, 5]. A few of these bioactive peptides were found in cationic proteins (with an isoelectric point > 8.0), such as lysozyme [6], RNase A [7], histone H2A [8] and lactoferrin [9], all with high propensity to release unfolded peptides with a positive net charge.

In this framework, our research group identified, at first, an HDP in cationic PD-L4 enzyme, a type 1 ribosome inactivating protein (RIP) [10] from *Phytolacca dioica* L. [11], by a CNBr fragmentation approach performed on the native protein. RIPs are enzymes (3.2.2.22) identified in

plants, fungi, algae, and bacteria. They are endowed with N-glycosilase activity, which leads to the cleavage of a specific adenine residue at a conserved site of the 28S rRNA, with a consequent inhibition of protein synthesis [12]. They are classified as type 1 or 2 according to their structure. Type 1 RIPs are single-chain proteins, with a size of approximately 30 kDa and a basic pI, whereas dimeric type 2 RIPs consist of two peptide chains: an A chain of about 30 kDa, endowed with enzymatic activity, linked to a B chain of about 35 kDa, endowed with lectin activity and capable of binding to oligosaccharides containing galactose moieties [13]. Although the biological role of RIPs has not been completely elucidated, some reports indicate that they may be involved in host defence activities [14, 15].

To date, reports on HDPs derived from *Phytolacca dioica* L. are limited to our recent study [16] demonstrating that the identified peptide, named $PDL4_{40\text{-}65}$ exhibits structural and biological properties typical of host defence peptides.

In order to evaluate the presence of novel bioactive peptides in further RIP members, such as PD-L1/2, dioicin1 and dioicin2 [17, 18], here we used the previously described bioinformatics approach, in order to identify potential cryptic HDPs in protein precursors and to predict their strain specific antibacterial activity [19]. As a result of this screening, two very promising HDPs have been identified in the N-terminal region of PD-L1/2 (amino acid position Ile50-Ser80, **Fig. 1**) [20], which were here named IKY23 and IKY31. The present chapter focuses on the characterization of the antibacterial and anti-biofilm activities of these two novel PD-L1/2 derived peptides.

4.2 Results

4.2.1 Bioinformatics research in type 1 RIPs from *P. dioica*

The sequence of PD-L1/2 was analysed by using a previously described tool for the detection of cryptic HDPs [19]. The isometric plot, which correlates the predicted antimicrobial "absolute score" (AS) to all the possible peptides of length between 18 and 40 residues in the primary structure of PD-L1/2, shows two local maxima corresponding to peptides 50-79 (AS = 7.3-7.5) and 50-71 (AS = 6.8-7.0). These scores correspond approximately to predicted MIC values in the range 10-40 µM. On the basis of this analysis, we selected for the characterization peptides 50-73 and 50-80 (**Figure 1**), herein called IKY23 and IKY31, respectively. The small polar residues Asn72 and Ser80 were included at the C-termini of IKY23 and IKY31, respectively, in order to avoid that the negatively charged C-termini of the peptides were close to the antimicrobial region [21].

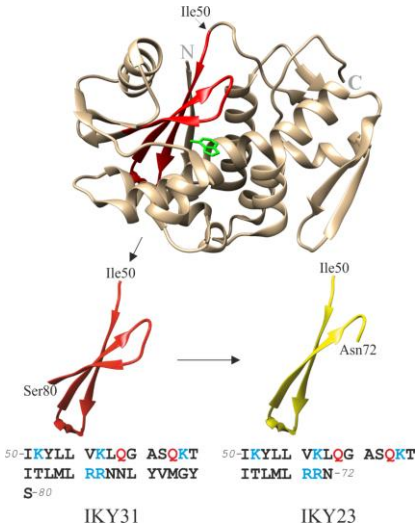

Figure 1. PD-L1/2 structure and PD-L1/2 derived peptides primary structures. **A**. Crystallographic structure of PD-L1/2 (PDB code: 3H5K). IKY31 and IKY23 are highlighted in red and yellow, respectively; **B**. Primary structures of both PD-L1/2 derived peptides. Cationic residues are in blue; glutamine and asparagine are in red.

4.2.2 Antibacterial activity

In order to evaluate the antibacterial activity of IKY23 and IKY31 peptides, antimicrobial assays were carried out on a panel of Gram-negative and Gram-positive bacterial strains, including *Escherichia coli* ATCC 25922 and *Enterococcus faecalis* ATCC 29212 (**Table 1**). Although PD-L1/2 derived peptides share a very similar amino acidic composition (**Fig. 1**), obtained MIC values highlighted that their antibacterial selectivity and potency are significantly different. Indeed, IKY23 exhibited a broad spectrum antimicrobial activity against both Gram-positive and Gram-negative bacteria, with MIC values similar to those obtained for control peptide (P)GKY20 [22] against *E. coli* (MIC =12.5 µM) and *S. aureus* (MIC = 6.25 µM) strains. In contrast, IKY31 displayed selective antibacterial activity against Gram-positive bacteria with MIC

values of 25 µM and 50 µM *versus S. aureus* and *E. faecalis*, respectively. Moreover, IKY31 was found to be ineffective against *K. pneumoniae* and *P. aeruginosa* strains, at least in our experimental conditions. It is worth noting that both bacterial strains are also strong biofilm producers. Bacteria living in biofilm growth mode are usually refractory to most conventional antibiotics, but they have been found to be sensitive to several HDPs, even at sub-MIC concentrations [23, 24]. Thus, we investigated PD-L1/2 derived peptides anti-biofilm properties against *K.pneumoniae* and *P.aeruginosa* strains.

Compound	**MIC**					
	E. coli	***K. pneumoniae***	***P. aeruginosa***	***S. aureus***	***E. faecalis***	***B. spizizenii***
IKY31	100	>100	>100	25	50	50
IKY23	12.5	50	50	6.25	25	50
(P)GKY20[a]	12.5	12.5	25	6.25	6.25	50
Polymyxin B[b]	1	1	1	>32	>32	>32
Vancomycin[b]	>32	>32	>32	1	>32	4
[a]**Values expressed in µM** [b]**Values expressed in µg/mL**						

Table 1. Antibacterial activity of PD-L1/2 derived peptides from *Phytolacca dioica* L. Assays were carried out by broth microdilution method in Nutrient Broth 0.5 X. MIC value shown are the highest values obtained from three independent experiments.

4.2.3 Anti-biofilm activity

To assess whether PD-L1/2 derived peptides affect bacterial biofilms, we first measured by crystal violet (CV) staining, the percentage of biofilm biomass formed in the absence or in the presence of increasing concentrations of each peptide (**Fig. 2**). We observed a dose-dependent reduction in biofilm biomass of *P. aeruginosa* and *K. pneumoniae* biofilms upon treatment with increasing concentrations of IKY31 (**Fig. 2A**) or IKY23 (**Fig. 2B**).

We also determined the minimum biofilm inhibitory concentration, *i.e.* peptide concentration determining 50% biofilm reduction ($MBIC_{50}$). We found that the $MBIC_{50}$ for IKY31 was about 5 µM against *P. aeruginosa* and about 0.6 µM against *K. pneumoniae* (**Fig. 2A**). Interestingly, it should be noted that peptide IKY31 exerted anti-biofilm activity even against bacterial strains that are not sensitive to peptide direct killing activity against planktonic cells (MIC >100 µM, **Table 1**). Using the same experimental set-up, peptide IKY23 was found to exert anti-biofilm activity, with $MBIC_{50}$ values of about 50 µM and about 0.8 µM against *P. aeruginosa* PAO1 and *K. pneumoniae*, respectively (**Fig. 2B**). It has been previously reported that different peptides exhibiting low bactericidal activity are strong anti-biofilm agents. This may be due to peptide self-aggregation, a phenomenon shown to contribute to anti-biofilm activity [25], or may alternatively be mediated by several mechanisms of action [26].

In order to further investigate the anti-biofilm properties of PD-L1/2 derived peptides, we also performed analyses using confocal microscopy. First, we analysed the effects of both PD-L1/2 derived peptides at sub-MIC concentrations (12.5 µM) on *K. pneumoniae* and *P. aeruginosa* biofilms. Incubations were carried out for 24 h at 37 °C in static conditions. Following incubation, chambers were double stained (Syto9/PI mix), in order to discriminate between live and dead biofilm cells. As shown in **Fig. 3A**, both peptides affected *K. pneumoniae* biofilm thickness. Indeed, the biofilm height of samples treated with IKY31 or IKY23 was reduced to about 16 µm and 22 µm, respectively, which was significantly lower than the value determined for the untreated sample (about 35 µm). Moreover, samples treated with IKY31 displayed a significant increase in cell death (**Fig.3A, middle panels**) together with reduced cell cohesion, which may be indicative of a disrupted extracellular matrix. On the other hand, treatment with peptide IKY23 led to decreased biofilm coverage (**Fig.3A, bottom panels**), although it did not dramatically reduce the number of adherent cells, which was found to be similar to that of the untreated control sample (**Fig.3A, top panels**). We also analysed the effect of both peptides against *P. aeruginosa* PAO1 biofilm formation (**Fig. 3B)**. In this case, only the longest PDL1/2 derived peptide induced cell death, as indicated by the higher percentage of PI positive cells (**Fig.3B, middle panels**) with respect to control sample (**Fig. 3B, top panels**). However, in this case, no obvious biofilm morphology alterations were recorded in the presence of peptide.

Altogether, these results indicate that both peptides significantly affect *K. pneumoniae* biofilm formation, in agreement with the crystal violet data obtained using the static microtiter plate assay. However, on the basis of our observations, it is possible to hypothesize that PD-L1/2 derived peptides exert their effects through different mechanisms of action. Collectively, the longest peptide (IKY31) seem to exert its anti-biofilm effects through an anti-adhesive mode of action, likely mediated by an alteration of the biofilm structural components (*e.g.*, those within the biofilm extracellular matrix). Since biofilm matrix components of *P. aeruginosa* PAO1 are well-characterized and, as described above, no remarkable biofilm morphology alterations were recorded when biofilms were grown under static conditions, we next investigated the anti-biofilm properties of PD-L1/2 derived peptides against *P. aeruginosa* PAO1 cells by using a more sensitive flow cell device apparatus. This system enables continuous monitoring of biofilm formation over time and thus constitutes an excellent platform for screening and identifying novel compounds endowed with biofilm detachment activity [27, 28]. PDL1/2 derived peptides were tested for their ability to eradicate 2-day-old pre-formed biofilm of the human pathogenic Gram-negative *P. aeruginosa* PAO1. As shown in **Fig. 4**, both peptides induced cell death when compared to the untreated control, as indicated by increased PI uptake into cells, which correlates with an altered membrane permeability. Interestingly, treatment with each peptide affected the biofilm mode of growth compared to the untreated control. Indeed, IKY23 substantially decreased adherent cells (**Fig. 4, middle panels**), whereas IKY31 (**Fig. 4, bottom panels**) reduced biofilm microcolonies, when compared to the untreated control (**Fig.4, top panels**).

These results suggest that the longest peptide (IKY31) might be able to interfere with cell-to-cell cohesion and aggregation, a key feature of biofilm growth. In order to evaluate the effect of PD-L1/2 derived peptides on structural biofilm features, we performed interaction studies with the exopolysaccharide alginate, an important component of the *P. aeruginosa* PAO1 extracellular biofilm matrix (see paragraph **4.3.3**).

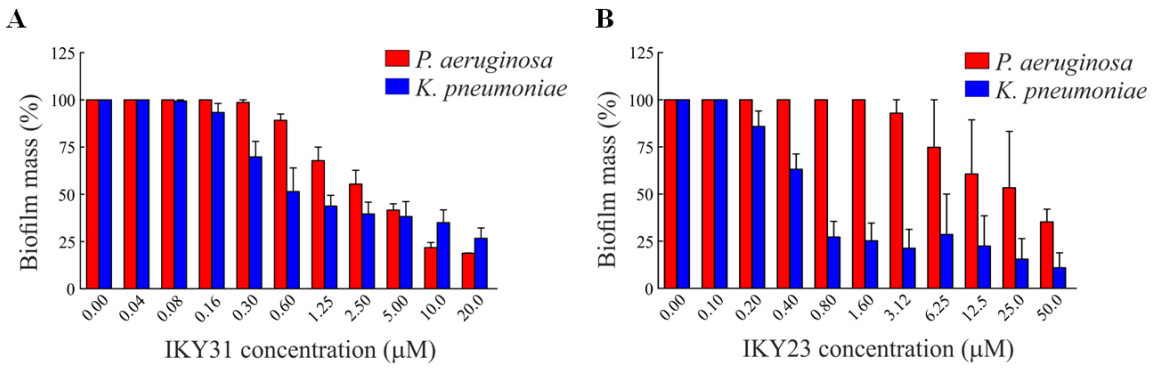

Figure 2. Biofilm biomass of wild-type *P. aeruginosa* PAO1 and *K. pneumoniae ATCC* 700603 upon treatment with PD-L1/2 derived peptides. Biofilms were grown at 37 °C for 48 h in the presence of increasing concentrations of IKY31 (**A**) or IKY23 (**B**), respectively. Biofilm growth was assessed by 0.1% crystal violet (w/v) staining and quantified at 595 nm. Data shown are the average values of experiments repeated twice independently ±SEM of biofilm mass percentage compared to biofilm mass growth in the absence of peptides.

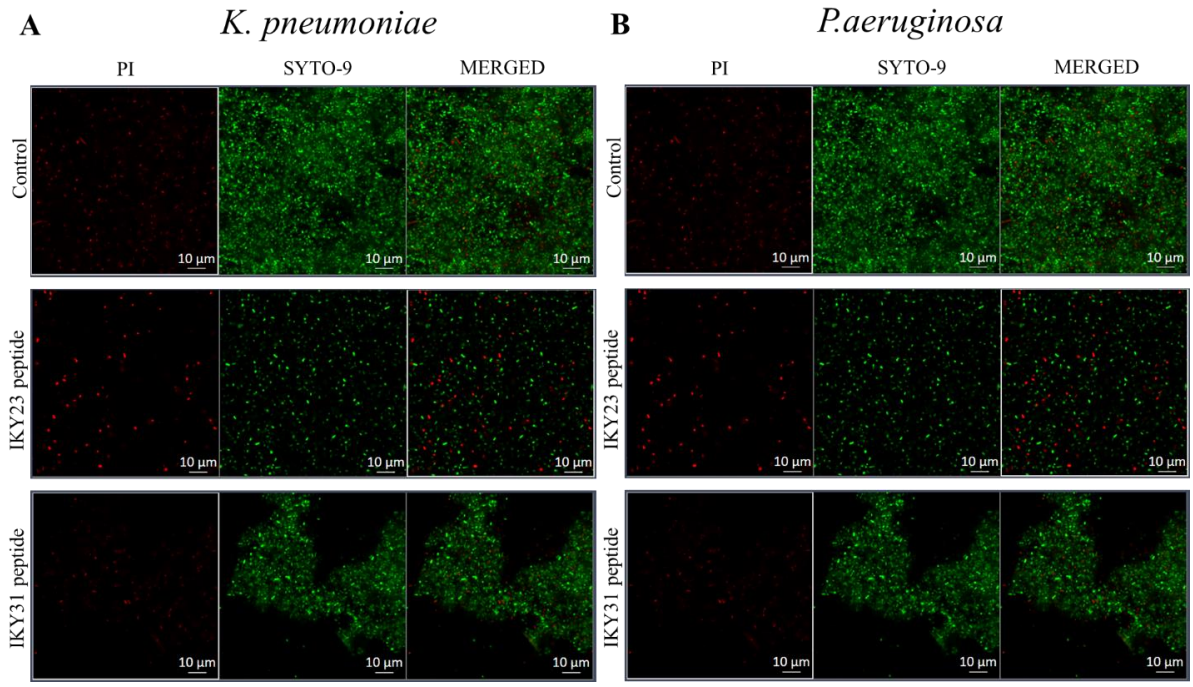

Figure 3. Analysis of the effect of PD-L1/2 derived peptides on static biofilm growth by CLSM imaging. A) *K. pneumoniae* ATCC 700603 and *P.aeruginosa* PAO1 wild type (B) untreated biofilm grown for 24 h in chambered coverglass slides (control) or in the presence of IKY31 (middle panels) or IKY23 (bottom panels). Biofilm cells were stained by using LIVE/DEAD BacLight bacterial viability kit (Molecular Probes, Eugene, OR) containing 1:1 ratio of Syto-9 (green fluorescence, all cells; center panel) and propidium iodide (PI; red fluorescence, dead cells; left panel). Images are 2D projections of biofilm structure obtained by confocal z-stack using Zen Lite 2.3 software. All images were taken under identical conditions. Scale bar correspond to 10 μm in all the cases.

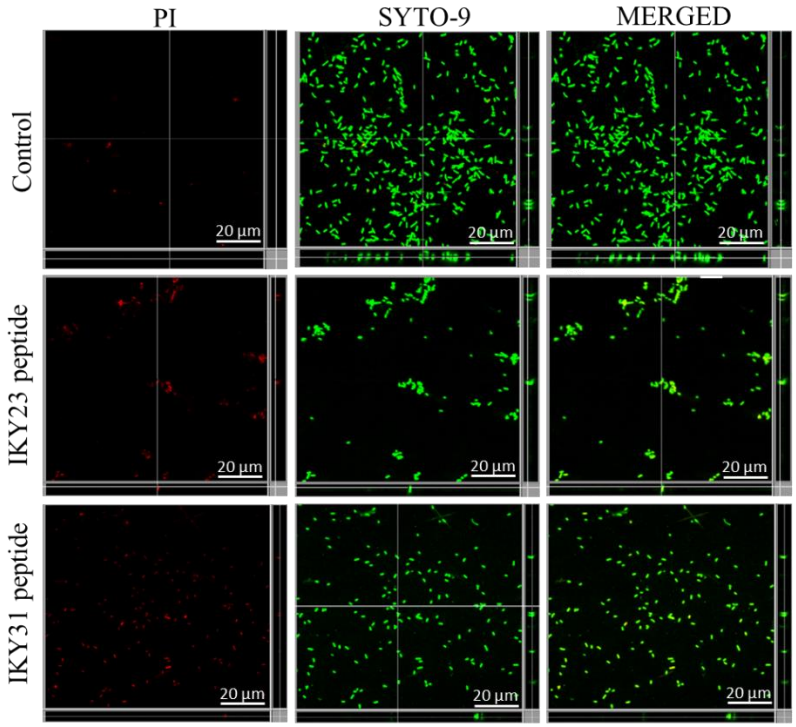

Figure 4. Anti-biofilm flow cell assays. Biofilm cells were stained by using a LIVE/DEAD BacLight bacterial viability kit (Molecular Probes, Eugene, OR) or Syto-9 alone prior to the microscopy experiments. A ratio of Syto-9 (green fluorescence, all cells; center panel) to propidium iodide (PI; red fluorescence, dead cells; left panel) of 1:1 was used. Microscopic analyses were performed by using a confocal laser-scanning microscope (Zeiss LSM 700 Laser Scanning Confocal), and three dimensional reconstructions were generated using the Imaris software package (Bitplane AG). Representative images out of two independent experiments are shown. Each panel shows reconstructions from the top in the large panel and sides in the right and bottom panels (xy, yz and xz dimensions). Scale bars correspond to 20 µm in all the cases.

4.2.4 Secondary structure determination

PD-L1/2 derived peptides conformation was characterized by circular dichroism (CD) spectroscopy. CD spectra were recorded in 10 mM sodium phosphate buffer pH 7.4, in the presence of increasing concentrations of TFE in phosphate buffer (10-30-50-70%) and in the presence of 20 mM SDS. TFE is commonly used to induce alpha-helical structure and to stabilize protein secondary structure, whereas SDS, being an anionic detergent, forms micelles in aqueous solution at appropriate concentrations, thus mimicking bacterial membranes.

Far-UV CD spectra recorded in phosphate buffer show negative peaks at ≈200 nm (**Fig. 5)**, indicating that IKY23 and IKY31 are largely unstructured in absence of any likely interactor. However, in the presence of increasing concentrations of TFE (from grey to black line), a conformational change occurred for both peptides, as evidenced by the appearance of new minima at around 208 nm and 222 nm, indicative of a typical helical structure.

The same conformation was induced also by 20 mM SDS (blue line) in the case of IKY31, whereas alpha helical content was found to be lower in the case of IKY23. This indicates that, upon interaction with membrane-mimicking agents, PD-L1/2 derived peptides are prone to assume an

alpha helical conformation, even if the effect was found to be less pronounced in the case of IKY23 peptide.

Since both peptides are endowed with antibacterial and antibiofilm activities, even if with differences in selectivity and potency, we also evaluated the effects on peptides secondary structure induced by LPS, a key molecule in Gram negative bacteria outer membrane, and alginate, is one of the main exopolysaccharides in PAO1 biofilm extracellular matrix [29].

As shown in **Fig. 5**, in the presence of 0.2 mg/mL of LPS (green line), CD spectra showed a strong negative band at ≈216 nm, indicative of a beta sheet conformation. This was observed in the case of both peptides, although the effect was less pronounced for IKY23. A similar pattern was observed for both peptides when dichroic spectra were recorded in the presence of 0.2 mg/mL alginate (red line). In this case, a negative band switches from ≈216 nm (green line) to a ≈ 220 nm (red line). Taken together, CD data indicate that IKY23 and IKY31 conformations are altered by environmental factors. This might explain their different effects towards planktonic and sessile cells.

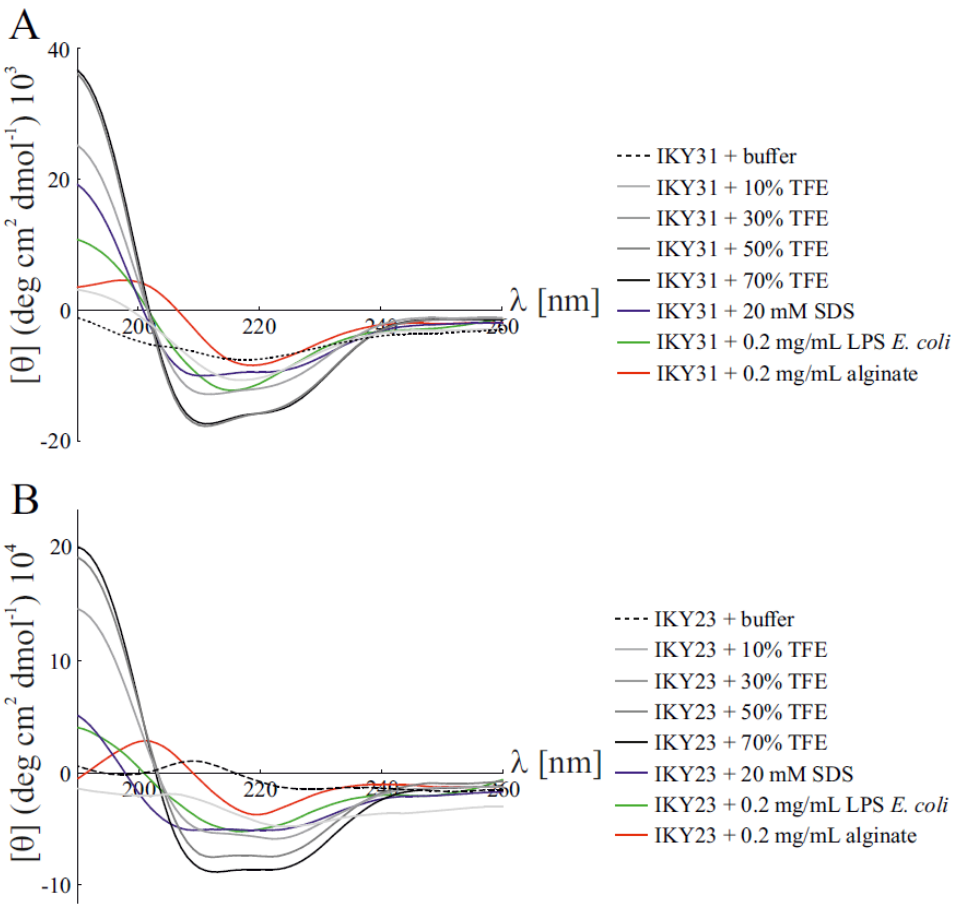

Figure 5. CD spectra of IKY23 (A) and IKY31 (B) under different conditions. Far-UV spectra (wavelength from 190 to 260 nm) were recorded in the presence of phosphate buffer (dashed line), increasing concentrations of TFE (grey line), 20 mM SDS (blue line), 0.2 mg/mL LPS (green line) and 0.2 mg/mL alginate (red line).

4.2.5 LPS binding assay

Analyses by circular dichroism indicated that both PD-L1/2 derived peptides are able to interact with Gram-negative lipopolysaccharide. Hence, binding to LPS might play a crucial role in peptides antibacterial and anti-biofilm activity, since IKY23 mostly inhibits *K. pneumoniae* and *P.aeruginosa* PAO1 planktonic cells growth, whereas IKY31 exerts a strong anti-biofilm activity on both strains. Although several mechanisms of action might mediate peptides effects, it has been widely reported that many HDPs act *via* LPS neutralization [30]. On the other hand, LPS play a crucial role in determining cell-to-cell interactions in biofilm matrices [31].
On the basis of these observations, we examined PD-L1/2 derived peptides ability to neutralize LPS. To this purpose, we used the *Limulus amebocyte* lysate assay, which allows detection of traces of free LPS. Free LPS from *Pseudomonas aeruginosa* P10 was used as a positive control. The same amount of LPS was incubated with IKY23 or IKY31 (25 μM) for 30 minutes at 37 °C. As shown in **Fig. 6**, in the presence of both peptides, a significant reduction of free LPS amount was detected. However, IKY23 seems to be slightly more efficient, in agreement with data indicating that planktonic Gram-negative bacterial cells are more susceptible to this peptide rather than to IKY31. On the other hand, in the case of IKY31 peptide, the ability to neutralize LPS could concur to its anti-biofilm activity.

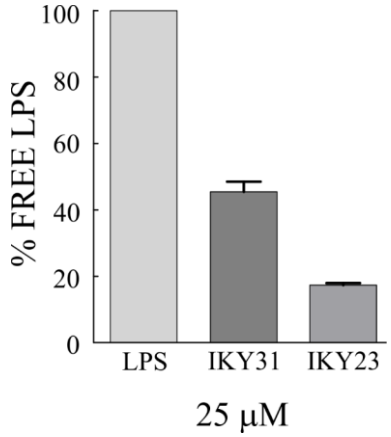

Figure 6. LAL assay to determine IKY23 and IKY31 binding to LPS. Commercial LPS from *Pseudomonas aeruginosa* P10 was used to induce a colorimetric reaction (grey bar). Each PD-L1/2 derived peptide (25 μM) was pre-incubated at 37° C with 12.5 ng/mL LPS for 30 minutes.

4.2.6 Cytotoxicity assays

Since HDPs are gaining increasing attention as promising antimicrobial compounds, it is fundamental to demonstrate their selectivity of action and to exclude any possible toxic effects on mammalian cells. PD-L1/2 derived peptides cytotoxicity was evaluated *in vitro* on human CaCo-2, HaCat and HeLa cell lines at three different incubation times (24, 48 and 72 h). As shown in **Fig. 7**, cytotoxicity of both peptides on CaCo2 or HaCat cells was negligible. Indeed, even at the highest concentration tested (100 μM), the percentage of viable cells was found to be higher than 90% even upon 72 h incubation. Similar results were obtained on HeLa cells as well (data not shown).

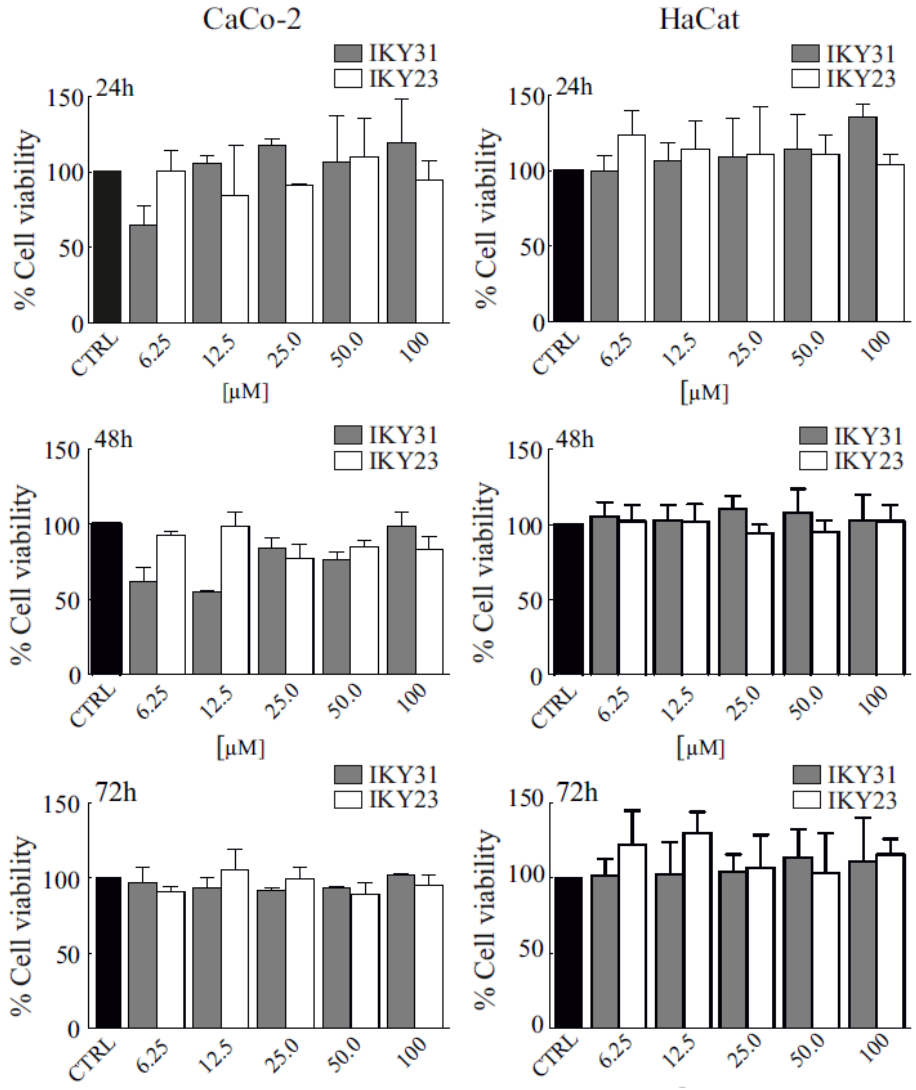

Figure 8. Effect of IKY23 and IKY31 peptides on eukaryotic cell viability. Cytotoxicity of PD-L1/2 derived peptides on CaCo2 and HaCaT cells was evaluated at three different incubation times (24, 48 and 72 h), and reported on the left and on the right columns, respectively. In all the experiments, the mean values ± SD from three independent experiments run in triplicate are shown.

4.3 Conclusions

Plants produce a diverse array of small proteins (less than 100 amino acid residues), most of which are cysteine-rich peptides (CRPs) that inhibit bacterial and fungal growth in vitro [32]. In plants, HDPs are mainly classified into cyclotides, defensins, thionins, lipid transfer proteins, snakins, and hevein-like vicilin-like and knottins. Plant hormones – gibberellins, ethylene, jasmonates, and salicylic acid, are among the physiological regulators that regulate the expression of HDPs. However, as widely reported in the literature, it is not to be ruled out that larger proteins that are not directly related to host defense can release, by proteolysis, small peptides with antibacterial activity.

Indeed, in a previous report, our group identified by chemical fragmentation, and characterized the first cryptic HDP hidden in PD-L4, a type 1 RIP from leaves of *P. dioica* [33]. Here, we identified, by using a recently described bioinformatic tool, a putative host defence region in the N-terminal domain of PD-L1/2, another member of the differently expressed pool of type 1 RIPs from *P. dioica*. Starting from this finding, two peptides contained in this region, here named IKY31 and IKY23, have been designed and synthesized, in order to structurally and functionally characterize them. Collected data indicate that both PD-L1/2 derived peptides exhibit antibacterial activities, even if with some differences. IKY23 exert its antibacterial activity with MIC values comparable to those of control peptide GKY20, whereas IKY31 seems to possess antimicrobial propensity only on planktonic Gram-positive bacteria. Since IKY31 is ineffective towards some Gram-negative bacteria, that are strong biofilm producers, it seemed interesting to verify if PD-L1/2 derived peptides showed the same antimicrobial trend highlighted on planktonic cells also on sessile bacteria forming biofilm. Interestingly, we provided evidences that IKY23 and IKY31 are able to induce a strong dose-dependent reduction in biofilm biomass with MBIC values lower than those obtained on planktonic cells.

Moreover, we found that PD-L1/2 derived peptides are also able to affect biofilm thickness and, in particular, the longest peptide (IKY31) seems to exert its anti-biofilm activity through an anti-adhesive mode of action, likely mediated by an alteration of the biofilm structural components. This suggests that IKY31 peptide might be able to interfere with cell-to-cell cohesion and aggregation, a fundamental event in biofilm expansion. Interestingly, on the basis of these observations, PD-L1/2 derived peptides may be classified as effective anti-biofilm agents, to be used as an efficient alternative to conventional antimicrobial agents, often ineffective on bacterial biofilm.

A key feature of membranolytic and anti-biofilm agents is their selectivity towards prokaryotic systems. To verify this, we performed experiments which stated that PD-L1/2 derived peptides specifically bind to prokaryotic membrane components and, at the same time, they are innocuous for eukaryotic cells. In agreement with the canonical properties of most HDPs, circular dichroism analyses indicated that these RIP derived peptides are unstructured in aqueous buffer, whereas they tend to assume a specific conformation in the presence of increasing concentrations of TFE and of a membrane mimicking agent, such as SDS. In addition, dichroic spectra also indicated that the conformation of both PD-L1/2 derived peptides is influenced by LPS and alginate, which might be indicative of a binding probably mediating the effects of the two peptides on sessile and planktonic bacteria.

Overall, the data herein collected also suggest the intriguing hypothesis that this consensus active region, also found in different members of type 1 RIPs, could play a rather important role in the host-pathogen relationship in plants. Indeed, during delicate physio-pathological processes, proteolytic events, induced by host and/or by plant, might promote the release of bioactive peptides, similar to IKY31 and IKY23, able to modulate the immune response.

As future perspective and application has been proposed, intriguingly, that transgenically produced HDP-plants will become a means showing that HDPs are able to mitigate host defense responses while providing durable resistance against pathogens. [34]

4.4 Experimental procedures

4.4.1 Bacterial strains

Bacterial strains used in this study were: *Escherichia coli* ATCC 25922, *Enterococcus faecalis* ATCC 29212 and *Klebsiella pneumoniae* ATCC 700603 (kindly provided by Dr. Eliana De Gregorio), wild-type *Pseudomonas aeruginosa* PAO1 (kindly provided by Dr. Donatella De Pascale) and *Staphylococcus aureus* ATCC 6538P (kindly provided by Prof. Mario Varcamonti).

4.4.2 Antimicrobial activity assay

The antimicrobial activity of PD-L1/2 derived peptides against planktonic bacteria was evaluated by broth microdilution method, performed as previously described for HDPs [35] with minor modifications. Peptides were dissolved in sterile water, and their concentration was determined by bicinchoninic acid colorimetric assay (Pierce™ BCA Protein Assay). Peptides were dispensed into aliquots (200 µM) and stored at -20°C until use. Antimicrobial assays were carried out in sterile 96-well polypropylene microtiter plates (Costar Corp., Cambridge, MA). Bacteria from an over-night culture were diluted in Nutrient broth (Difco, Becton Dickinson, Franklin Lakes, NJ) to a final concentration of 3-5 x 10^5 CFU/mL per well in the presence of two-fold serial dilutions of IKY23, IKY31, or (P)GKY20 peptide, respectively. (P)GKY20 peptide is a short cationic HDP derived from the C-terminus of human thrombin [36], here used as a positive control. In all the cases, two-fold serial dilutions of antibiotics (polymyxin B and vancomycin) were tested as control. Plates were incubated at 37 °C for 24 h. The MIC (Minimum Inhibitory Concentration) values were determined as the lowest concentrations of different compounds at which no visible bacterial growth was observed.

4.4.3 Microtiter plate biofilm assay

Biofilm formation was analyzed by using a static abiotic solid surface assay, as previously described [28]. To this end, stationary phase wild-type *Pseudomonas aeruginosa* PAO1 and *Klebsiella pneumoniae* ATCC700603 cells, obtained from an over-night culture, were diluted 1/100 in BM2 adjusted medium (62 mM potassium phosphate buffer, pH 7.0, 7 mM $(NH_4)_2SO_4$, 0.5 mM $MgSO_4$, 10 µM $FeSO_4$) containing 0.4% (wt/vol) glucose as a carbon source. Assays were carried out in sterile 96-well polypropylene microtiter plates (Costar Corp., Cambridge, MA) in the presence of different concentrations of PD-L1/2 derived peptides or antibiotics (polymyxin B and vancomycin). Samples in the absence of peptides were used as a positive control, whereas samples in the absence of bacteria were used as a negative control. Following incubation at 37 °C for 48 h, samples were gently washed with water, in order to remove planktonic cells, whereas biofilm biomass was stained with 0.1% crystal violet (Sigma Aldrich, Milan, Italy). Biofilm stained biomass was transferred into flat-bottom plystyrene 96-well plate and optical densities at 595 nm were measured using a microtiter plate reader (Synergy™ H4 Hybrid Microplate Reader, BioTek Instruments, Inc., Winooski, Vermont, USA). $MBIC_{50}$ values were determined as the lowest

concentration values determining 50% inhibition of biofilm formation with respect to the positive control.

4.4.4 Confocal microscopy (CLSM) analysis of static biofilm growth

Biofilms were grown into chambered coverglass slides (Nunc Lab-Tek, ThermoFisher Scientific, USA) in BM2 adjusted medium in static condition at 37 °C for 24 h. Bacterial cells from an over-night culture were diluted to about 2 x 10^9 CFU/mL and 2 x 10^8 CFU/mL for *K.pneumoniae* and *P.aeruginosa* PAO1, respectively, and seeded into wells of the chambers. After bacterial attachment for 4h at 37 °C, peptides were added to bacterial samples at a concentration of 12.5 μM and incubated for further 20 h. Upon incubation, non-adherent bacteria were removed by gently washing samples with sterile phosphate buffer. Viability of cells embedded into biofilm structure was determined by sample staining with LIVE/DEAD® BacLight™ Bacterial Viability kit (Molecular Probes ThermoFisher Scientific, USA), performed accordingly to manufacturer instructions. Biofilm images were captured by using a confocal laser scanning microscopy (Zeiss LSM 710, Zeiss, Germany) and a 63 X objective oil immersion system. Biofilm architecture was analysed by using the Zen Lite 2.3 software package. Each experiment was performed in triplicate. All images were taken under identical conditions.

4.4.5 Biofilm cultivation in flow chambers and microscopy

P.aeruginosa PAO1 biofilm was grown for 72 h in the absence or presence of each PD-L1/2 derived peptide (3 μmol/L) at 37 °C in flow chambers (channel dimensions of 1 by 4 by 40 mm) in BM2 minimal medium. Silicone tubing (inner diameter, 0.062 in.; outer diameter, 0.125 in.; wall thickness, 0.032 in.; VWR, Radnor, PA, USA) was used and the device was assembled and sterilized by pumping a 10% hypochlorite solution through the system for 5 min using a multichannel peristaltic pump. The system was then rinsed with sterile water and medium for 5 min for each channel. Flow chambers were inoculated by injecting 400 μL of wild-type *P.aeruginosa PAO1* over-night culture diluted to an OD_{600nm} of approximately 0.05. After inoculation, chambers were left without flow for 3 h, after which medium was pumped through the system at a constant rate of 2.4 mL/h. Bacteria were allowed to develop structured 2-day-old biofilms prior to peptide treatment for the following 22 h. Biofilm cells were stained using a LIVE/DEAD BacLight bacterial viability kit (Molecular Probes, Eugene, OR, USA) using a 1:1 ratio of Syto-9 (green fluorescence, all cells) to propidium iodide (PI; red fluorescence, dead cells). Microscopy analyses were carried out using a confocal laser scanning microscope (Zeiss LSM 700 Laser Scanning Confocal), and three-dimensional reconstructions were generated using the Imaris software package (Bitplane AG). Experiments were performed twice with identical results.

4.4.6 Circular dichroism analyses

Circular dichroism (CD) spectra of PD-L1/2 derived peptides were recorded with a J-810 spectropolarimeter equipped with a Peltier temperature control system (Model PTC- 423-S; Jasco Europe, Cremella, LC, Italy). Far-ultraviolet (far-UV) measurements (190–260 nm) were carried out at 25 °C using a 0.1 cm optical path length cell and a peptide concentration of 35 μm. CD spectra, recorded with a time constant of 4 s, a 2 nm bandwidth, and a scan rate of 10 $nm \cdot min^{-1}$ were signal-averaged over at least three scans. CD spectra were acquired in 10 mM sodium phosphate buffer pH 7.2 and in the presence of different concentrations of trifluoroethanol (TFE), 20 mM SDS, 0.2 mg/mL LPS from *Escherichia coli* 0111:B4 and 0.2 mg/mL alginate. Estimation of the secondary structure was carried out accordingly to the Variable Selection Method (CDSSTR) using DICHROWEB, as previously described [37].

4.4.7 Peptide binding to lipopolysaccharide (LAL assay)

The ability of PD-L1/2 derived peptides to neutralize LPS was determined by using the commercially available *Limulus amebocyte* lysate (LAL) assay (Pierce® LAL Chromogenic Endotoxin Quantitation Kit, ThermoFisher Scientific, Waltham, MA, USA) (Park *et al.*, 2009). Briefly, 25 μL of each peptide (25 μM) were added to 25 μl of 12.5 ng/mL *Pseudomonas aeruginosa* P10 LPS (Sigma Aldrich, Milan, Italy) for 30 min at 37 °C. Upon incubation, 50 μL of amebocyte lysate reagent were added to samples for 10 min. Absorbance values at 405 nm were measured 10 min after the addition of 100 μL of the chromogenic substrate, Ac-Ile-Glu-Ala-Arg-p-nitroanilide.

4.4.8 Cytotoxicity on mammalian cells

Cytotoxicity towards normal (HaCat) or tumor (HeLa and CaCo-2) cells was assessed by performing the 3-(4,5-dimethylthiazol-2-yl)-2,5 diphenyltetrazolium bromide (MTT) reduction inhibition assay [38]. Cytotoxicity experiments were performed at least four times independently. In all the cases, cells were grown for 24, 48 and 72 h in the absence or in the presence of increasing concentrations (0.6 to 100 μM) of each peptide. Cell survival values are expressed as percentage of viable cells with respect to control untreated samples.

References

1. Manners, J. M. (2007). Hidden weapons of microbial destruction in plant genomes. Genome Biol. 8, 225. doi: 10.1186/gb-2007-8-9-225
2. Wang, G. (2015) Improved methods for classification, prediction, and design of antimicrobial peptides. Methods in molecular biology (Clifton, N.J.), 1268, 43-66.
3. Wang, G., Li, X. and Wang, Z. (2016) APD3: the antimicrobial peptide database as a tool for research and education. Nucleic acids research, 44, D1087-1093.
4. Ganz, T. (2003) The role of antimicrobial peptides in innate immunity. Integrative and comparative biology, 43, 300-304.
5. Zanfardino, A., Pizzo, E., Di Maro, A., Varcamonti, M. and D'Alessio, G. (2010) The bactericidal action on Escherichia coli of ZF-RNase-3 is triggered by the suicidal action of the bacterium OmpT protease. FEBS J, 277, 1921-1928.
6. Mine, Y., Ma, F. and Lauriau, S. (2004) Antimicrobial peptides released by enzymatic hydrolysis of hen egg white lysozyme. J Agric Food Chem, 52, 1088-1094.
7. Torrent, M., Pulido, D., Valle, J., Nogues, M.V., Andreu, D. and Boix, E. (2013) Ribonucleases as a host-defence family: evidence of evolutionarily conserved antimicrobial activity at the N-terminus. The Biochemical journal, 456, 99-108.
8. Cho, J.H., Sung, B.H. and Kim, S.C. (2009) Buforins: histone H2A-derived antimicrobial peptides from toad stomach. Biochim Biophys Acta, 1788, 1564-1569.
9. Tomita, M., Takase, M., Wakabayashi, H. and Bellamy, W. (1994) Antimicrobial peptides of lactoferrin. Advances in Experimental Medicine and Biology, 357, 209-218.
10. Pizzo, E., Zanfardino, A., Di Giuseppe, A.M., Bosso, A., Landi, N., Ragucci, S., Varcamonti, M., Notomista, E. and Di Maro, A. (2015) A new active antimicrobial peptide from PD-L4, a type 1 ribosome inactivating protein of Phytolacca dioica L.: A new function of RIPs for plant defence? FEBS letters, 589, 2812-2818.
11. Di Maro, A., Valbonesi, P., Bolognesi, A., Stirpe, F., De Luca, P., Siniscalco Gigliano, G., Gaudio, L., Delli Bovi, P., Ferranti, P., Malorni, A. and Parente, A. (1999) Isolation and characterization of four type-1 ribosome-inactivating proteins, with polynucleotide:adenosine glycosidase activity, from leaves of Phytolacca dioica L. Planta, 208, 125-131.
12. Endo, Y., Mitsui, K., Motizuki, M. and Tsurugi, K. (1987) The mechanism of action of ricin and related toxic lectins on eukaryotic ribosomes. The site and the characteristics of the modification in 28 S ribosomal RNA caused by the toxins. The Journal of biological chemistry, 262, 5908-5912.
13. Barbieri, L., Battelli, M.G. and Stirpe, F. (1993) Ribosome-inactivating proteins from plants. Biochim Biophys Acta, 1154, 237-282.
14. Iglesias, R., Citores, L., Ragucci, S., Russo, R., Di Maro, A. and Ferreras, J.M. (2016) Biological and antipathogenic activities of ribosome-inactivating proteins from Phytolacca dioica L. Biochim Biophys Acta, 1860, 1256-1264.
15. Pizzo, E. and Di Maro, A. (2016) A new age for biomedical applications of Ribosome Inactivating Proteins (RIPs): from bioconjugate to nanoconstructs. Journal of biomedical science, 23, 54.
16. Pizzo, E., Zanfardino, A., Di Giuseppe, A.M., Bosso, A., Landi, N., Ragucci, S., Varcamonti, M., Notomista, E. and Di Maro, A. (2015) A new active antimicrobial peptide from PD-L4, a

type 1 ribosome inactivating protein of Phytolacca dioica L.: A new function of RIPs for plant defence? FEBS letters, 589, 2812-2818.
17. Parente, A., Berisio, R., Chambery, A. and Di Maro, A. (2010) Type 1 Ribosome-Inactivating Proteins from the Ombú Tree (Phytolacca dioica L.). In Toxic Plant Proteins (M., L.J. and Hartley, M.R. eds). Heidelberg, Germany: Springer, pp. 79-106.
18. Russo, R., Chambery, A., Severino, V., Parente, A. and Di Maro, A. (2015) Structural characterization of dioicin 1 from Phytolacca dioica L. gains novel insights into phylogenetic relationships of Phytolaccaceae type 1 RIPs. Biochemical and biophysical research communications, 463, 732-738.
19. Pane, K., Durante, L., Crescenzi, O., Cafaro, V., Pizzo, E., Varcamonti, M., Zanfardino, A., Izzo, V., Di Donato, A. and Notomista, E. (2016a) Antimicrobial Potency of Cationic Antimicrobial Peptides can be Predicted from their Amino Acid Composition: Application to the Detection of "Cryptic" Antimicrobial Peptides. Journal of Theoretical Biology.
20. Di Maro, A., Chambery, A., Carafa, V., Costantini, S., Colonna, G. and Parente, A. (2009) Structural characterization and comparative modeling of PD-Ls 1-3, type 1 ribosome-inactivating proteins from summer leaves of Phytolacca dioica L. Biochimie, 91, 352-363.
21. Gaglione, R., Dell'Olmo, E., Bosso, A., Chino, M., Pane, K., Ascione, F., Itri, F., Caserta, S., Amoresano, A., Lombardi, A., Haagsman, H.P., Piccoli, R., Pizzo, E., Veldhuizen, E.J., Notomista, E. and Arciello, A. (2017) Novel human bioactive peptides identified in Apolipoprotein B: Evaluation of their therapeutic potential. Biochem Pharmacol, 130, 34-50.
22. Pane, K., Durante, L., Pizzo, E., Varcamonti, M., Zanfardino, A., Sgambati, V., Di Maro, A., Carpentieri, A., Izzo, V., Di Donato, A., Cafaro, V. and Notomista, E. (2016b) Rational Design of a Carrier Protein for the Production of Recombinant Toxic Peptides in Escherichia coli. PLoS One, 11, e0146552.
23. Papareddy, P., Rydengård, V., Pasupuleti, M., Walse, B., Mörgelin, M., Chalupka, A., Malmsten, M. and Schmidtchen, A. (2010) Proteolysis of Human Thrombin Generates Novel Host Defense Peptides. PLoS Pathogens, 6, e1000857.
24. de la Fuente-Nunez, C., Korolik, V., Bains, M., Nguyen, U., Breidenstein, E.B., Horsman, S., Lewenza, S., Burrows, L. and Hancock, R.E. (2012) Inhibition of bacterial biofilm formation and swarming motility by a small synthetic cationic peptide. Antimicrob Agents Chemother, 56, 2696-2704.
25. Ansari, J.M., Abraham, N.M., Massaro, J., Murphy, K., Smith-Carpenter, J. and Fikrig, E. (2017) Anti-Biofilm Activity of a Self-Aggregating Peptide against Streptococcus mutans. Frontiers in microbiology, 8, 488.
26. Batoni, G., Maisetta, G. and Esin, S. (2016) Antimicrobial peptides and their interaction with biofilms of medically relevant bacteria. Biochim Biophys Acta, 1858, 1044-1060.
27. Bionda, N., Fleeman, R.M., de la Fuente-Nunez, C., Rodriguez, M.C., Reffuveille, F., Shaw, L.N., Pastar, I., Davis, S.C., Hancock, R.E. and Cudic, P. (2016) Identification of novel cyclic lipopeptides from a positional scanning combinatorial library with enhanced antibacterial and antibiofilm activities. Eur J Med Chem, 108, 354-363.
28. de la Fuente-Nunez, C., Cardoso, M.H., de Souza Candido, E., Franco, O.L. and Hancock, R.E. (2016) Synthetic antibiofilm peptides. Biochim Biophys Acta, 1858, 1061-1069.
29. Wei, Q. and Ma, L.Z. (2013) Biofilm matrix and its regulation in Pseudomonas aeruginosa. International journal of molecular sciences, 14, 20983-21005.

30. Skovbakke, S.L. and Franzyk, H. (2017) Anti-inflammatory Properties of Antimicrobial Peptides and Peptidomimetics: LPS and LTA Neutralization. Methods in molecular biology (Clifton, N.J.), 1548, 369-386.
31. Russo, D.M., Abdian, P.L., Posadas, D.M., Williams, A., Vozza, N., Giordano, W., Kannenberg, E., Downie, J.A. and Zorreguieta, A. (2015a) Lipopolysaccharide O-chain core region required for cellular cohesion and compaction of in vitro and root biofilms developed by Rhizobium leguminosarum. Applied and environmental microbiology, 81, 1013-1023.
32. Broekaert WF, Cammue BPA, DeBolle MFC, Thevissen K, DeSamblanx GW, Osborn RW: Antimicrobial peptides from plants. Crit Rev Plant Sci. 1997, 16: 297-323. 10.1080/713608148.
33. Pizzo E, Zanfardino A, Di Giuseppe AM, Bosso A, Landi N, Ragucci S, Varcamonti M, Notomista E, Di Maro A (2015) A new active antimicrobial peptide from PD-L4, a type 1 ribosome inactivating protein of Phytolacca dioica L.: a new function of RIPs for plant defence? FEBS Lett 589(19 Pt B):2812–2818. doi:10.1016/j.febslet.2015.08.018.
34. Ravinder K. Goyal, Autar K. Mattoo, Multitasking antimicrobial peptides in plant development and host defense against biotic/abiotic stress, In Plant Science, Volume 228, 2014, Pages 135-149, ISSN 0168-9452, https://doi.org/10.1016/j.plantsci.2014.05.012.
35. Wiegand, I., Hilpert, K. and Hancock, R.E. (2008) Agar and broth dilution methods to determine the minimal inhibitory concentration (MIC) of antimicrobial substances. Nat Protoc, 3, 163-175.
36. Papareddy, P., Rydengård, V., Pasupuleti, M., Walse, B., Mörgelin, M., Chalupka, A., Malmsten, M. and Schmidtchen, A. (2010) Proteolysis of Human Thrombin Generates Novel Host Defense Peptides. PLoS Pathogens, 6, e1000857.
37. Del Giudice, R., Arciello, A., Itri, F., Merlino, A., Monti, M., Buonanno, M., Penco, A., Canetti, D., Petruk, G., Monti, S.M., Relini, A., Pucci, P., Piccoli, R. and Monti, D.M. (2016) Protein conformational perturbations in hereditary amyloidosis: Differential impact of single point mutations in ApoAI amyloidogenic variants. Biochim Biophys Acta, 1860, 434-444.
38. Boukamp, P., Popp, S., Altmeyer, S., Hulsen, A., Fasching, C., Cremer, T. and Fusenig, N.E. (1997) Sustained nontumorigenic phenotype correlates with a largely stable chromosome content during long-term culture of the human keratinocyte line HaCaT. Genes Chromosomes Cancer, 19, 201-214.

Concluding remarks

Host defense peptides (HDPs) are important modulators in both mammalian and non-mammalian systems to prevent microbial colonization and tissue damage [1]. HDPs beneficial effects may encompass direct antimicrobial activity, binding to endotoxins, such as LPS or LTA, which reduce the detrimental pro-inflammatory response, and one or more direct effects on cellular behaviors, such as enhanced migration and proliferation. The majority of HDPs share common biochemical features, including relatively small size, cationicity and amphipathicity in membrane-mimicking environments. These features allow them to selectively interact with and damage bacterial membranes. Several proteins contain HDPs hidden inside their sequence called cryptic peptides [2, 3, 4].

Further, it is noteworthy that cryptic peptides were identified in larger proteins involved in not only host defense, but also sequences with completely different roles. Therefore, such functional cryptic peptides that are hidden in protein structures are named “cryptides” in general [5].

The cryptome consists of bioactive peptides generated by the proteolysis of precursor proteins. It is speculated that the cryptide repertoire increases the complexity of the proteome by an order of magnitude. Recently discovered cryptides are involved in the regulation of a diverse range of cellular processes including neuronal signaling, the inflammatory response, the adaptive immune response, and angiogenesis. They are derived from many well-studied proteins, including hemoglobin, cytochromes, laminins, and collagen [6, 7, 8, 9, 10].

Due to their potential as therapeutic agents, there has been an increasing interest in studying cryptides [11] as well as host defense peptides in particular.

HDPs, as a novel class of antimicrobial therapeutics, give hope to confining the rise of antibiotic resistances and to acting as promising novel weapons against microbial pathogens. Despite the success to date in antimicrobial development, the inexorable, ongoing emergence of resistance worldwide continues to spur the search for novel anti-infectives to replace and/or supplement conventional antibiotics. Human defensins, cathelicidin, and a significant number of diverse HDPs from bacteria, viruses, plants, vertebrates, and invertebrates all appear to have a universal multidimensional signature (i.e., a common three-dimensional structure) that defines antimicrobial activity. Manipulation of this chemical structure to create designer synthetic peptides represents a promising strategy for the development of HDPs as a new class of drugs to prevent and treat systemic and topical infections. Regarding to HDPs, there are several different potential strategies for their general therapeutic application: (1) as single anti-infective agents, (2) in combination with conventional antibiotics or antivirals to promote any additive or synergistic effects, (3) as immune stimulatory agents that enhance natural innate immunity, and (4) as endotoxin-neutralizing agents to prevent the potentially fatal complications associated with bacterial virulence factors that cause septic shock.

Unfortunately, of the potential pool of thousands of natural peptides and millions of synthetic peptide possibilities, relatively few have actually proceeded into clinical trials based on promising data from in vitro and animal studies. Despite a continuing optimism, the commercial success remains elusive. In 2004, a list of HDPs in clinical trials was published, and to date, none of the peptides described has obtained FDA (Food and Drug Administration) approval for their various clinical indications. Reasons of this lack could be found looking at some disadvantages of HDPs. In fact, although HDPs have considerable advantages for therapeutic applications, including broad-spectrum activity, rapid onset of activity, and relatively low possibility of

resistance emergence, they also have some limitations for drug development as low stability to pH changes and protease action as well as potential hemolytic properties. In order to overcome those obstacles, many methods have been proposed. For instances, introduction of unusual amino acids (mainly D-form amino acids) or modification of the terminal regions (acetylation or amidation) improved the stability of peptides by preserving them from proteolytic degradation. Also, the use of efficient drug delivery systems, such as liposome encapsulation, can be effective for the improvement of the stability and reduction of potential toxicity.

Moreover, since they are able to interact in some cases with eukaryotic cell membranes, as well, HDPs could be used as delivery vectors for several bioactive compounds. However, despite all of the benefits that have emerged with the development of HDPs, researchers aim to face several shortcomings and to enhance their antibacterial activity and mode of action by various modifications, leading to functionalized HDPs and HDP conjugates. In fact, HDPs can be functionalized to generate peptide conjugates, in which various substances are attached by different coupling strategies. The potential of such new HDP compositions was recently summarized by Brogden et al. [12]: for instance, antibiotics coupled to HDPs or HDP-like sequences, improving HDP activity by lipidation, decoration of particles and polymers with HDPs, conjugates out of HDPs and organometallic complexes.

References

1. M. Hemshekhar, V. Anaparti, N. Mookherjee, Functions of Cationic Host Defense Peptides in Immunity, Pharmaceuticals (Basel). Jul 4 (2016) 9(3).
2. C.V. Suschek, O. Schnorr, V. Kolb-Bachofen, The role of iNOS in chronic inflammatory processes in vivo: is it damage-promoting, protective, or active at all?, Curr Mol Med. Nov;4(7) (2003) 763-75.
3. J. Scheller, A. Chalaris, D. Schmidt-Arras, S. Rose-John, The pro- and anti-inflammatory properties of the cytokine interleukin-6, Biochim Biophys Acta. May;1813(5) (2011) 878-88.
4. E.J. Veldhuizen, V.A. Schneider, H. Agustiandari, A. van Dijk, J.L. Tjeerdsma-van Bokhoven, F.J. Bikker, H.P. Haagsman, Antimicrobial and immunomodulatory activities of PR-39 derived peptides, PLoS One. 9(4) (2014) e95939.
5. Cryptides: functional cryptic peptides hidden in protein structures. Ueki N, Someya K, Matsuo Y, Wakamatsu K, Mukai H.Biopolymers. 2007;88(2):190-8.
6. Autelitano DJ, Rajic A, Smith AI, Berndt MC, Ilag LL, Vadas M. The cryptome: a subset of the proteome, comprising cryptic peptides with distinct bioactivities. Drug Discov Today. 2006;11 (7–8):306–14. doi:10.1016/j.drudis.2006.02.003.
7. Pimenta DC, Lebrun I. Cryptides: buried secrets in proteins. Peptides. 2007;28(12):2403–10. doi:10.1016/j.peptides.2007.10.005.
8. Ueki N, Someya K, Matsuo Y, Wakamatsu K, Mukai H. Cryptides: functional cryptic peptides hidden in protein structures.Pept Sci. 2007;88(2):190–8.
9. Gelman JS, Sironi J, Castro LM, Ferro ES, Fricker LD. Hemopressins and other hemoglobin-derived peptides in mouse brain: comparison between brain, blood, and heart peptidome and regulation in Cpefat/fat mice. J Neurochem. 2010;113(4):871–80.
10. Gomes I, Dale C, Casten K, Geigner M, Gozzo F, Ferro E, et al. Hemoglobin-derived peptides as novel type of bioactive signaling molecules. AAPS J. 2010;12:658–69.
11. Analyzing the cryptome: uncovering secret sequences. Samir P, Link AJ. AAPS J. 2011 Jun;13(2):152-8. doi: 10.1208/s12248-011-9252-2. Epub 2011 Feb 16. Review.
12. Brogden N.K., Brogden K.A. Will new generations of modified antimicrobial peptides improve their potential as pharmaceuticals? Int. J. Antimicrob. Agents. 2011;38:217–225. doi: 10.1016/j.ijantimicag.2011.05.004.

APPENDIX

Abbreviations:

HDP: host defence peptides; **LPS**: lipopolysaccharide; **LTA**: lipoteichoic acid; **MIC**: Minimum inhibitory concentration; **SD**: standard deviation; **CD**: circular dichroism; **TFE**: trifluoroethanol; **IL-6**: interleukin 6; **NO**: nitric oxide; **CFU**: colony forming unit; **RBC**: Red blood cell; **HBTU**: 2-(1H-benzotriazole-1-yl)-1,1,3,3-tetramethyluronium hexafluorophosphate; **Oxyma**: cyano-hydroxyimino-acetic acid ethyl ester; **DIPEA**: N,N′-diisopropylethylamine; **TFA**: trifluoroacetic acid; **MeIm**: 4-methylimidazole; **MSNT** : 1-(Mesitylene-2-sulfonyl)-3-nitro-1,2,4-triazole; **DMF**: N,N-Dimethylformamide; **ACN**: Acetonitrile; **DCM**: dichloromethane; **Fmoc**: fluorenylmethyloxycarbonyl; **CATH-2**: cathelicidin-2; **TSA**: Tryptic Soy Agar; **AS**: absolute score; **MHB**: Muller Hinton broth; **NB**: Nutrient Broth; **MRSA**: methicillin-resistant *Staphylococcus aureus*; **VRE,** vancomycin-resistant enterococci; **AMPs**: Antimicrobial Peptides; **ApoE**: apolipoprotein E; **ApoB**: apolipoprotein B; **LDL**: low-density lipoprotein; **IL-10**: interleukin-10; **TSA**: Tryptic Soy Agar; **AS**: absolute score; **NB**: Nutrient Broth; **SDS**: sodium dodecyl sulfate; **FIC**: Fractional Inhibitory Concentration; **iNOS**: nitric oxide synthase; **CATH-2**: cathelidin-2; **PBS**: phosphate-buffered saline; **WH**: wound healing. **CNBr**: Cyanogen bromide; **Na/P**: Sodium phosphate buffer; **Tris•Cl**:Tris(hydroxymethyl)aminomethane-HCl buffer; **SEM**: Standard Error of the Mean; **LAL**: Limulus amebocyte lysate; **PI**: propidium iodide; **OD**: optical density.

List of Publications

Elio Pizzo, Rosario Oliva, Rita Morra, **Andrea Bosso**, Sara Ragucci, Luigi Petraccone, Pompea Del Vecchio, Antimo Di Maro. *Binding of a type 1 RIP and of its chimeric variant to phospholipid bilayers: evidence for a link between cytotoxicity and protein/membrane interactions.* Biochimica et Biophysica Acta (BBA) – Biomembranes, Volume 1859, Issue 10, October 2017, Pages 2106-2112. doi.org/10.1016/j.bbamem.2017.08.004.

A. Bosso, L. Pirone, R. Gaglione, K. Pane, A. Del Gatto, L. Zaccaro, S. Di Gaetano, D. Diana, R. Fattorusso, E. Pedone, V. Cafaro, H.P. Haagsman, A. van Dijk, M.R. Scheenstra, A. Zanfardino, O. Crescenzi, A. Arciello, M. Varcamonti, E.J.A. Veldhuizen, A. Di Donato, E. Notomista, E. Pizzo. *A new cryptic host defense peptide identified in human 11-hydroxysteroid dehydrogenase-1 β-like: from in silico identification to experimental evidence.* Biochim Biophys Acta. 2017 Apr 25. pii: S0304-4165(17)30134-4. doi: 10.1016/j.bbagen.2017.04.009.

Rosa Gaglione, Eliana Dell'Olmo, **Andrea Bosso**, Marco Chino, Katia Pane, Flora Ascione, Francesco Itri, Sergio Caserta, Angela Amoresano, Angelina Lombardi, Henk P. Haagsman, Renata Piccoli, Elio Pizzo, Edwin J.A. Veldhuizen, Eugenio Notomista, Angela Arciello. *Novel human bioactive peptides identified in Apolipoprotein B: Evaluation of their therapeutic potential.* Biochem Pharmacol. 2017 Apr 15;130:34-50. doi: 10.1016/j.bcp.2017.01.009. Epub 2017 Jan 25

Pizzo E, Zanfardino A, Di Giuseppe AM, **Bosso A**, Landi N, Ragucci S, Varcamonti M, Notomista E, Di Maro A. *A new active antimicrobial peptide from PD-L4, a type 1 ribosome inactivating protein of Phytolacca dioica L.: A new function of RIPs for plant defence?* FEBS Lett. 2015 Sep 14;589(19 Pt B):2812-8. doi: 10.1016/j.febslet.2015.08.018.

List of communications

Andrea Maria Guarino, Annaelena Troiano, Elio Pizzo, **Andrea Bosso**, Tiziana Angrisano, Alessandra Pollice,Viola Calabrò. *Y-box binding protein 1 from the inside-out: role in cellular stress and DNA damage response*. Celebrating 60 years of the Italian Association of Genetics 7-9 September 2017, Cortona (Arezzo, Italy).

Andrea Bosso, Rosa Gaglione, Katia Pane, Maaike Scheenstra, Angela Arciello, Edwin J.A. Veldhuizen, Eugenio Notomista, Elio Pizzo. *GVF27: a cryptic host defence peptide from a human putative dehydrogenase.* IMAP 2017, Peptide conferences. Copenhagen, Denmark August 25-27, 2017.

Rosa Gaglione, Eliana Dell'Olmo, **Andrea Bosso**, Katia Pane, Bartolomeo Della Ventura, Rocco Di Girolamo, Finzia Auriemma, Elio Pizzo, Renata Piccoli, Eugenio Notomista, Edwin J.A. Veldhuizen, Angela Arciello. *Human cryptic Host Defence Peptides identified in Apolipoprotein B: analysis of their antimicrobial, anti-biofilm and immunomodulatory properties.* IMAP 2017, Peptide conferences. Copenhagen, Denmark August 25-27, 2017.

A. Bosso, K. Pane, A. Avitabile, M. Verrillo, A. Del Gatto, L. Zaccaro, L. Pirone, S. Di Gaetano, R. Fattorusso, D. Diana, E. Pedone, V. Cafaro, E.J.A. Veldhuizen, E. Notomista, E. Pizzo. *Cryptic anti-microbial peptides in human secretory proteins: the case of H11β (235-261).* 15th the Naples Workshop on Bioactive Peptides. 23-25 June 2016

M. Verrillo, K. Pane, E. Pizzo, M. Varcamonti, A. Zanfardino, A. Amoresano, M. Siepi, **A. Bosso**, A. Di Donato, V. Cafaro, E. Notomosta. *Recombinant production and labelling of peptides with N-terminal cysteine residue.* 15th Naples Workshop on Bioactive Peptides. June 23-25, 2016, Naples Italy**.**

Katia Pane, **Andrea Bosso**, Rosa Gaglione, Angela Arciello, Valeria Cafaro, Elio Pizzo, Eugenio Notomista, Alberto Di Donato. *Novel antimicrobial weapons hidden in human secretoma*. ALTANT Conference 2016: Innate Host Defence and Infections | From basic science to applications 18-20 May 2016 – Utrecht – The Netherlands

Gaglione R., Pane K., Itri F., **Bosso A**., Cafaro V., Pizzo E., Piccoli R., Notomista E., Arciello A. *Novel cryptic cationic antimicrobial peptides from human ApoB.* ALTANT Conference 2016: Innate Host Defence and Infections | From basic science to applications 18-20 May 2016 – Utrecht – The Netherlands

Anna Zanfardino, Giovanni Gallo, Valeria Pistorio, Katia Pane, Michela Di Napoli, **Andrea Bosso**, Eugenio Notomista, Mario Varcamonti and Elio Pizzo. *Two new cryptic antimicrobial peptides identified in the human Apolipoprotein E*. FISV, 20-23 september 2016 Rome, Italy

A. Bosso. *'A new active antimicrobial peptide from PD-L4, a type 1 ribosome inactivating proteins of Phytolacca dioica L .: a new function of RIPs for plant defense?'* IMAP 2015 Peptide conferences, Peptide conferences, Burlington House Piccadilly London

K. Pane, V. Cafaro, A. Avitabile, **A. Bosso**, E. Pizzo, E. Notomista, A. Di Donato. *A novel carrier protein for AMPs production.* 5th Antimicrobial International Meeting on Antimicrobial Peptides, Burlington House 7th-8th September 2015.

A. Avitabile, V. Cafaro , K. Pane, **A. Bosso**, E. Pizzo , E. Notomista, A. Di Donato. *The activation peptide of human pepsinogen is an antimicrobial peptide.* 5th Antimicrobial International Meeting on Antimicrobial Peptides, Burlington House 7th-8th September 2015.

Elio Pizzo, Anna Zanfardino, Antonella MA Di Giuseppe, **Andrea Bosso**, Valeria Sgambati, Sara Ragucci, Nicola Landi, Antimo Di Maro. *A novel source of microbial agents: characterization of an antimicrobial peptide from PD-L4, a type 1 ribosome inactivating protein from Phytolacca dioica L*. 58° National Meeting of the Italian Society of Biochemistry and Molecular Biology, September 14-16, 2015. Urbino, Italy.